1-1-2012

The Egf-Ras-Erk Pathway and the Nkx-5/hmx Homeodomain Protein Mls-2 Promote Tube Development in the C.elegans Excretory System

Ishmail Abdus-Saboor
University of Pennsylvania, ishmail84@yahoo.com

The Egf-Ras-Erk Pathway and the Nkx-5/hmx Homeodomain Protein Mls-2 Promote Tube Development in the C.elegans Excretory System

Abstract
Tubular epithelial cells are one of the most abundant cell types in multicellular organisms. Tubular cells transport gases and liquids, and funnel harmful excretory waste from our bodies. It is clear that Receptor Tyrosine Kinase (RTK) signaling is essential for the formation of many tubular organs such as our kidneys and blood vessels. However, which steps in tube development require RTK signaling is less well understood. The C.elegans excretory system is a primitive renal system with just three essential cells (duct, pore, and canal cells), providing a simple yet dynamic system to study tube specification and morphogenesis. In the C.elegans excretory system, we demonstrated that the EGF-Ras-Erk signaling pathway specified the excretory duct tube versus the pore tube fate. In addition, EGF-Ras-Erk signaling influenced the positions that the duct and pore cells adopted within the tubular network. And finally, after position and fate determination, EGF-Ras-Erk signaling had a continued role in maintaining organ architecture of the duct tube. Goals for future research will be to determine how EGF-Ras-ERK signaling controls these genetically distinct steps during tube development.

In a separate project, I studied the Nkx5 homeodomain transcription factor, MLS-2, which was identified in a mutagenesis screen by a former graduate student in the lab. I discovered a role for MLS-2 in promoting proper cell shape of the duct and pore. mls-2 cooperated with the EGF-Ras-Erk pathway to turn on lin-48/Ovo during duct morphogenesis. I speculate that MLS-2 and other Nkx5 family members have conserved functions in promoting shape acquisition in cells that adopt complex morphologies similar to the duct and pore.

Degree Type
Dissertation

Degree Name
Doctor of Philosophy (PhD)

Graduate Group
Cell & Molecular Biology

First Advisor
Meera V. Sundaram

Keywords
elegans, homeodomain, MLS-2, Notch, Ras, tubulogenesis

Subject Categories
Developmental Biology

THE EGF-RAS-ERK PATHWAY AND THE NKX-5/HMX HOMEODOMAIN PROTEIN MLS-2 PROMOTE TUBE DEVELOPMENT IN THE *C.ELEGANS* EXCRETORY SYSTEM

Ishmail Abdus-Saboor

A DISSERTATION

in

Cell and Molecular Biology

Presented to the Faculties of the University of Pennsylvania

in

Partial Fulfillment of the Requirements for the

Degree of Doctor of Philosophy

2012

Supervisor of Dissertation

Meera V. Sundaram Ph.D., Associate Professor of Genetics

Graduate Group Chairperson

Daniel S. Kessler Ph.D., Associate Professor of Cell and Developmental Biology

Dissertation Committee:

Amin S. Ghabrial Ph.D., Assistant Professor of Cell and Developmental Biology
Steve DiNardo Ph.D., Professor of Cell and Developmental Biology
Klaus Kaestner Ph.D., Professor of Genetics
Daniel S. Kessler Ph.D., Associate Professor of Cell and Developmental Biology
David M. Raizen M.D., Ph.D., Assistant Professor of Neurology

Acknowledgements

I would like to begin by thanking my thesis advisor Meera Sundaram. Meera diligently guided me along my graduate career, and has helped me transition into thinking like an independent investigator. From having my ideas recognized at our weekly lab meetings, to one-on-one practice talks in her office, she has truly made the graduate experience a fulfilling endeavor.

I would like to thank all the members of my thesis committee: Amin S. Ghabrial, Steve DiNardo, Klaus Kaestner, Daniel S. Kessler, and David M. Raizen. They have not only been supportive during thesis meetings, but they have written me letters of recommendation for fellowships and postdocs, and also shared reagents (see Chapter Two acknowledgements).

I would also like to thank members of the Sundaram lab both past and present. Craig Stone began the MLS-2 project and helped me with it a great deal when I joined the lab. Kelly Howell helped me with technical assistance and made the lab a very pleasant place to work. Vincent Mancuso, my bay-mate for four years, was a great colleague and companion in the lab (see Chapter Two acknowledgements). Jean Parry, a talented postdoctoral fellow has been a great resource and companion, especially as the lab grew smaller in number. Also two former technicians, Kevin Cullison and Kate Palozola, were terrific to work with and very resourceful.

I would also like to thank members of the *C.elegans* community at UPenn, which has grown into a vibrant community with almost ten different labs. The worm community

has shared ideas and reagents, which have greatly enhanced my thesis research. Also members of the Department of Genetics have been very collegial and resourceful as well.

Lastly, I would like to thank a host of friends and family. Here at Penn I have made numerous lasting and important friendships from members of the E.E.Just Biomedical Society to members of the UPenn Muslim Student Association. I have been privileged to go to graduate school in the same city in which I was born and raised (Go Phils!) – so many family members and friends I have known throughout the years have been right here encouraging me along. I would like to especially thank my parents (and stepmother) and five younger siblings for their unconditional love and support. My mother continues to be the biggest cheerleader I have ever had, and it has meant the world. And lastly I would like to thank my lovely wife Fareedah and our two beautiful children for giving me great joy each day coming home from a long day with my worms.

ABSTRACT

THE EGF-RAS-ERK PATHWAY AND THE NKX-5/HMX HOMEODOMAIN PROTEIN MLS-2 PROMOTE TUBE DEVELOPMENT IN THE *C.ELEGANS* EXCRETORY SYSTEM

Ishmail Abdus-Saboor

Meera V. Sundaram

Tubular epithelial cells are one of the most abundant cell types in multicellular organisms. Tubular cells transport gases and liquids, and funnel harmful excretory waste from our bodies. It is clear that Receptor Tyrosine Kinase (RTK) signaling is essential for the formation of many tubular organs such as our kidneys and blood vessels. However, which steps in tube development require RTK signaling is less well understood. The *C.elegans* excretory system is a primitive renal system with just three essential cells (duct, pore, and canal cells), providing a simple yet dynamic system to study tube specification and morphogenesis. In the *C.elegans* excretory system, we demonstrated that the EGF-Ras-Erk signaling pathway specified the excretory duct tube versus the pore tube fate. In addition, EGF-Ras-Erk signaling influenced the positions that the duct and pore cells adopted within the tubular network. And finally, after position and fate determination, EGF-Ras-Erk signaling had a continued role in maintaining organ architecture of the duct tube. Goals for future research will be to determine how EGF-Ras-ERK signaling controls these genetically distinct steps during tube development.

In a separate project, I studied the Nkx5 homeodomain transcription factor, MLS-2, which was identified in a mutagenesis screen by a former graduate student in the lab. I

discovered a role for MLS-2 in promoting proper cell shape of the duct and pore. *mls-2* cooperated with the EGF-Ras-Erk pathway to turn on *lin-48/Ovo* during duct morphogenesis. I speculate that MLS-2 and other Nkx5 family members have conserved functions in promoting shape acquisition in cells that adopt complex morphologies similar to the duct and pore.

TABLE OF CONTENTS

LIST OF FIGURES

Chapter One

Chapter Two

Chapter Three

Chapter Four

Chapter Five

Chapter Six

Addendum

Chapter One:

INTRODUCTION

Overview

A fundamental question in developmental biology is how a single cell can give rise to an entire organism. For developmental geneticists, the questions more specifically asked are, "What genes and genetic pathways determine cellular identities?" Determining cellular identity or fate, was described almost fifty years ago elegantly by Conrad Waddington in his 'ball and hill' model of the epigenetic landscape. The 'ball and hill' model shows a ball representing a cell at the top of a hill with many valleys that each represent a distinct cell fate (Fig 1.1). When the ball is at the top of the hill, it has the ability to adopt multiple fates depending on which valley it descends upon. However, once the ball has rolled down the hill and landed in a valley, it cannot go back up the hill and choose a different valley, or cell fate. Though researchers can now take the ball back up the hill and reverse cells into a multi-potent, or stem-cell like fate, the basic 'ball and hill' model still holds true. Cells are guided down hills to distinct valleys by genetic pathways that specify unique cellular fates.

After a cell has passed the 'point of no return' and committed to a fate, additional genetic inputs are needed for the cell to reach its fully functional state. For example, in the case of a neuron, after fate specification many processes occur including dendrite arborization and axon elongation. Following morphogenesis, neurons form connections with neighboring cells by innervating target muscles or forming synapses with other neurons. The relationship between fate specification and morphogenesis of neurons and other cells, such as epithelial cells, is poorly understood.

Both vertebrate and invertebrate model organisms have been used to address the question of how cell fate specification and morphogenesis are coupled; many of the genes and genetic pathways have been identified using model organisms. With completed genome sequences of most model organisms, we now know that most genes are shared between organisms (Barr, 2003). Although we appreciate that signaling cascades such as the Receptor Tyrosine Kinase pathway are critical for numerous developmental processes including tubular organ formation, how signaling controls these processes, in many instances, is largely unknown. In the remainder of the introduction I will use tubular epithelial cells as a model and highlight what we know about specification and morphogenesis of these cells. I will end the introduction by describing the *C.elegans* excretory system, and thus demonstrating how a simple system of just three cells can provide insight into building a network of epithelial tubes.

Building a tube

Biological tubes are highly polarized cells that are responsible for transporting blood, excretory fluid, and essential gases. Tubes range in size from less than a micron in insect tracheal tubes to greater than 20 centimeters in the gut of an elephant (Lubarsky and Krasnow, 2003). Building a tube is an intricate process that requires several steps depending on the type of tube that is formed. Some tubes are formed by numerous cells making a single hollow lumen and forming a multicellular tube (Lubarsky and Krasnow, 2003). Other kinds of tubes can be unicellular, with just a single cell making a tube with a

hollow lumen (Lubarsky and Krasnow, 2003). All tubes generate a lumen apically, that serves as the location for the transport of fluid and gas. A number of models exist, both *in vitro* and *in vivo*, that explain how the lumen within a tube is formed (Andrew and Ewald, 2010; Lubarsky and Krasnow, 2003). In addition, tubes do not exist in isolation, but rather, they connect to neighboring tubular cells via junctional proteins that are conserved across species (Bryant and Mostov, 2008; Goldstein and Macara, 2007). The junctions that attach tubular cells together are remodeled to resist tension, to facilitate the exchange of cells into and out of the tubular network, and also to allow for cell elongation (Acloque et al., 2009; Baum and Georgiou, 2011; St Johnston and Sanson, 2011).

Types of tubes

Biological tubes are classified as either multicellular or unicellular, based on their cellular architecture (Fig 1.2). Multicellular tubes are the most common form of tubes found within vertebrate tubular organs (Lubarsky and Krasnow, 2003). A cross section through a multicellular tube reveals numerous cells connected by intercellular adherens junctions and forming a single hollow lumen (Lubarsky and Krasnow, 2003). The *Drosophila* trachea is arguably the most extensively studied model system for tube development. Large scale screens have been performed since the 1980s to reveal genes necessary to specify the trachea (Jurgens et al., 1984), while more recent screens have identified genes that promote tracheal morphogenesis (Ghabrial et al., 2011). The *Drosophila* trachea has been an attractive system because it contains a combination of both multicellular tubes in the dorsal trunk of the trachea, and unicellular tubes in the terminal cells of the trachea (Schottenfeld et al., 2010).

Unicellular tubes are sub-divided into two distinct classes and are found in a variety of organs across species. One type of unicellular tube has an autocellular adherens junction that seals the tube along its axis (Lubarsky and Krasnow, 2003). The other type of unicellular tube lacks an autocellular adherens junction and have thus been termed 'seamless'(Bar et al., 1984). Unicellular tubes are prevalent in the terminal ends of mammalian capillaries that transport blood into the brain and kidney (Bar et al., 1984). Interestingly, several *in vitro* and *in vivo* observations suggest that unicellular tubes may be the precursors to larger multicellular tubes (Blum et al., 2008; Folkman and Haudenschild, 1980; Kamei et al., 2006). The seamless unicellular tubes in *Drosophila* terminal cells form branches and connect to neighboring tissues to supply oxygen (Schottenfeld et al., 2010). All three cells of the *C.elegans* excretory system, described in detail below, are examples of unicellular tubes.

Tube Polarization and Lumen Formation

Tubes are highly polarized cells with an apical surface apposed to a hollow lumen and a basal surface contacting an underlying basement membrane and extracellular matrix (ECM) (Bryant and Mostov, 2008). Basal surfaces contain integrins, dystroglycans, and proteoglycans, which act as basal ECM receptors to link the epithelium to the underlying cytoskeleton (Bryant and Mostov, 2008). Apical surfaces are composed of heavily glycosolated transmembrane proteins such as zona-pellucida proteins, that can reorganize the apical organization of cells during morphogenesis (Plaza et al., 2010). Some apical epithelial surfaces are specialized for various types of absorption and secretion (Bryant and Mostov, 2008). For example, the duct and pore

tubes in the *C.elegans* excretory system secrete collagen apically into the lumen (Nelson and Riddle, 1984), while chitin is secreted apically into the lumen of the *Drosophila* trachea (Devine et al., 2005). Most studies of epithelial integrity have focused on the role of the basal ECM (Berrier and Yamada, 2007). However, recent studies from our lab have shown that leucine-repeat proteins that localize to the apical ECM can affect the integrity of the underlying cell-cell junctions between tubular epithelial cells (Mancuso et al., 2012).

Epithelial cells form tubes from existing polarized tissue by either wrapping or budding (Figure 1.3 A,B) (Andrew and Ewald, 2010; Lubarsky and Krasnow, 2003). Both wrapping and budding are driven by apical constriction, a cell shape change that leads to invagination of the apical side of an epithelium (Sawyer et al., 2010). With wrapping, the newly formed tube folds inward and eventually separates from the original epithelium by a fusion mechanism (Andrew and Ewald, 2010). One example of a tube that forms by wrapping from pre-existing polarized tissue is the vertebrate neural tube primordium during a process called primary neurulation (Schoenwolf and Smith, 1990). During vertebrate primary neurulation, hingepoint cells in the neuroepithelium apically constrict to cause bending that leads to wrapping of the neural tube (Sawyer et al., 2010). Two of the three cells of the *C.elegans* excretory system (duct and pore) also form by wrapping – not from a polarized epithelium, but from non-polarized precursor cells (described below).

An example of a fusion step following wrapping is found in two unicellular epithelial tubes of the *C.elegans* digestive tract, named pm8 and vpi1 (Albertson and

Thomson, 1976; Rasmussen et al., 2008). pm8 is the terminal most cell in the *C.elegans* foregut, and vpi1 attaches to pm8 as the foremost cell in the valve, which connects the foregut to the intestine. Both pm8 and vpi1 form by wrapping from an initially polarized epithelium (Albertson and Thomson, 1976; Rasmussen et al., 2008). pm8 expresses the fusogen protein *aff-1* in a Notch dependent manner, while vpi1 expresses a different fusogen named *eff-1*(Rasmussen et al., 2008). EFF-1 and AFF-1 are fusogen proteins found in *C.elegans* that can fuse heterologous cells and also promote viral insertion when expressed on the surface of viruses (Avinoam et al., 2011; Podbilewicz et al., 2006; Sapir et al., 2007). Following wrapping pm8 and vpi1 both have an autocellular junction which is then fused via *aff-1* in pm8 and *eff-1* in vpi1(Rasmussen et al., 2008). Interestingly, because both cells express a different fusogen they do not fuse to each other. The duct cell of the *C.elegans* excretory system forms by a similar wrapping and fusion process (Stone et al., 2009)(see below).

The second method of epithelial tube formation from a pre-existing epithelium is budding. Epithelial cells that invaginate and bud from an existing epithelium remain contiguous with the original epithelium (Andrew and Ewald, 2010). The *Drosophila* trachea forms from pre-existing polarized tissue budding off of an existing parental branch to form an epithelial sac (Brodu and Casanova, 2006; Metzger and Krasnow, 1999). Just hours later after the initial invagination, primary and secondary branches bud and migrate out from the epithelial sacs (Ghabrial et al., 2003). During larval development hundreds of terminal branches will extend from the secondary branches to provide oxygen to neighboring tissues (Ghabrial et al., 2003).

Epithelial cells form tubes from non-polarized precursors by two related hollowing mechanisms (Andrew and Ewald, 2010; Lubarsky and Krasnow, 2003). Cord hollowing occurs when multiple cells polarize and form lumen at sites of apical membrane contact. The lumena from multiple cells then coalescence into a single lumen. (Andrew and Ewald, 2010; Lubarsky and Krasnow, 2003) (Fig 1.3 C). Examples of tubes that form by cord hollowing are found during formation of the zebrafish gut (Bagnat et al., 2007) and during secondary neurulation in the chick and mouse embryo (Schoenwolf, 1984; Schoenwolf and Delongo, 1980). Related to cord hollowing is the process of cell hollowing whereby small vesicles coalescence to form a lumen within a single cell (Andrew and Ewald, 2010; Lubarsky and Krasnow, 2003) (Fig 1.3 D). During cord hollowing the lumen is initially formed extracellularly by fusion of vesicles with the plasma membrane, while in cell hollowing the fusion of vesicles occurs within the cell (Andrew and Ewald, 2010; Lubarsky and Krasnow, 2003).

Cavitation is the third way to generate a polarized tube from non-polarized cells (Andrew and Ewald, 2010; Lubarsky and Krasnow, 2003). Cavitation occurs when the cells on the periphery of an epithelium initiate *de novo* polarization, while the cells in the interior undergo apoptosis to create a hollow lumen (Andrew and Ewald, 2010; Lubarsky and Krasnow, 2003) (Fig 1.3 E). The apoptosis of the interior cells does not appear to initiate polarization, but rather promotes clearance and maintenance of the interior lumen (Andrew and Ewald, 2010; Lubarsky and Krasnow, 2003)(Debnath et al., 2002, Martín-Belmonte et al., 2008). Examples of tube formation by cavitation can be found during mammalian salivary gland development (Borghese, 1950; Melnick and Jaskoll, 2000).

Tube elongation

Several strategies exist that facilitate the elongation of tubular epithelial cells including cell rearrangements, cell division, cell recruitment, and changes in cell shape (Andrew and Ewald, 2010). Cell division and cell recruitment invoke the addition of cells to the elongating tube, while cell rearrangement and cell shape change do not change the number of cells in the tube, but rather the architecture of the cells. The Drosophila trachea elongates after the initial invagination by changes in cell shape accompanied by cell migration (Andrew and Ewald, 2010). At stage 11, the first indications of tracheal invagination can be observed with the apical marker PKC (Brodu and Casanova, 2006). As the cells begin to invaginate, the cells at the apical surface change shape by pinching towards the newly formed apical surface (Brodu and Casanova, 2006). By mid stage 11, the trachea tube has elongated and concomitant with the cell shape changes is a movement of the cells from the dorsal side to form a new layer of cells below the epidermal surface (Brodu and Casanova, 2006). The invagination with accompanied cell shape changes in the Drosophila trachea requires Epidermal Growth Factor Receptor (EGFR) signaling (Brodu and Casanova, 2006; Cela and Llimargas, 2006; Nishimura et al., 2007; Samakovlis et al., 1996). *C.elegans* excretory tube development also involves changes in cell shape, without cell division (see below).

Receptor Tyrosine Kinase (RTK) signaling specifies tube fates

Congenital anomalies of the kidney and urinary tract (CAKUT) are amongst the most common human birth defects (Song and Yosypiv, 2011). With aberrant RTK signaling often associated with cases of CAKUT (Song and Yosypiv, 2011), a better understanding of how RTK signaling promotes tube development in the kidney and other tubular organs is critical for human health. RTK signaling promotes tubulogenesis in numerous tubular organs, from the mammalian kidney to the protonephridial tubules of the planarian flatworm (Costantini, 2010; Rink et al., 2011). RTK stimulation can even drive the assembly of MDCK cells into tubes in three-dimensional matrix gels (Pollack et al., 1998). In addition, RTKs are involved in numerous development processes including proliferation, survival, and migration (Blume-Jensen and Hunter, 2001; Schlessinger, 2000). While targets of RTK signaling during cell proliferation are known, such as the HMG box protein Cic (Tseng et al., 2007), the downstream effectors of RTK signaling involved in tube development are largely unknown.

RTK signaling consists of ligands binding to dimerized RTK receptors, which then undergo autophosphorylation on specific tyrosine residues. Following autophosphorylation, RTKs interact with adaptor proteins that activate guanine nucleotide exchange factors that exchange GDP for GTP on the Ras GTPase at the plasma membrane. Ras activation initiates an intracellular kinase cascade that results in the terminal kinase in the pathway translocating to the nucleus to mediate transcription (see Fig 1.4 for example of an RTK pathway). One of the most appreciated roles for RTK signaling during tube development is to specify ‘leader’ or tip cells, versus ‘follower’ or stalk cells.

GDNF signaling in the mammalian kidney

The kidney is a collection of cells including blood vessels, thousands of nephrons, and a collective duct system that transports urine from nephrons to the bladder (Costantini, 2010). Interactions between epithelial cells and surrounding mesenchymal cells are critical for proper patterning of the kidney. Development of the kidney is initiated when the Wolfian Duct (WD) forms from the intermediate mesoderm (Costantini and Shakya, 2006). Subsequently, the Ureteric Bud (UB), a component of the immature kidney will grow out from one specific region of the WD (Costantini and Shakya, 2006). The UB is not a part of the mature kidney, but gives rise to components that are, including the epithelium of the collecting ducts, calyces, pelvis, and the ureter (Costantini, 2010). Under control from signals from the surrounding mesenchyme, the UB epithelium will continue to branch to give rise to a highly branched and mature kidney (Costantini and Shakya, 2006). What controls the initial outgrowth of the UB has been an area of intense research over the past ten years. Studies mainly from the Costantini lab have shown that the TGF-b family member, glial cell-line-derived neurotrophic factor (GDNF) specifies which cells will grow out from the WD to form the UB tube.

The growth factor GDNF binds to the RTK Ret during UB development. In both *Ret* and *GDNF* -/- mice, the UB fails to form (Moore et al., 1996; Schuchardt et al., 1994). In an elegant chimeric assay, the Costantini lab implanted GFP labeled *Ret* -/- ES cells (green) into a wild type blastocyst with wild type cells labeled with CFP (blue). At the beginning of UB outgrowth around E9.5 green and blue cells were equally distributed

across the WB. However, one day later at E10.5 as the UB tube grew out from the WB, only blue wild type cells incorporated the tip cells of the UB, while the green *Ret* -/- cells followed and made the stalk cells of the UB. When *Ret* -/- cells were implanted into a blastocyst of *Ret* hypomorph cells, the *Ret* -/- cells could sometimes adopt a tip cell fate (Chi et al., 2009). Together these data showed that the cells that express the highest amount of the Ret RTK were more competent to respond to the GDNF ligand and out-compete other cells to adopt a tip cell fate. Thus RTK signaling promotes the tip versus stalk cell fate in the developing kidney. The tip cell is of great importance in generating a functional kidney, as future branches will extend from the tip cells.

How does signaling through Ret RTK specify the tip versus stalk cell fate? Two *Ets* transcription factors *etv-4* and *etv-5* are targets of Ret signaling that appear to contribute to the tip cell decision (Kuure et al., 2010b). *etv-4* and *etv-5* have similar expression patterns as Ret, they can be up-regulated by providing exogenous Ret, and *etv-4*, *etv-5* -/- mice lack kidneys (Lu et al., 2009). The Costantini lab once again performed chimeric studies with GFP labeled *etv-4,etv-5* -/- ES cells (green) and implanted them into a CFP labeled wild type blastocyst (blue). At early embryonic stages the WD had an equal distribution of green and blue cells. However, as the UB grew from the WB at E10.5, the blue wild type cells out-competed the trailing *etv-4,etv-5* -/- cells to encompass the tip domain similar to *Ret* -/- cells (Chi et al., 2009; Kuure et al., 2010b). These data combined with previous studies suggest that the Ret RTK pathway promotes fate specification in the developing kidney by turning on two Ets family transcription factors.

FGF signaling in the *Drosophila* trachea

The *Drosophila* trachea begins formation by invaginating from an already polarized epithelium at early stage 11(Ghabrial et al., 2003). The Fibroblast Growth Factor (FGF) *Branchless* signals from outside of the trachea to activate the FGFR *Breathless* to pattern the trachea with numerous branched tubes (Ghabrial et al., 2003; Klambt et al., 1992; Lee et al., 1996; Shishido et al., 1993; Sutherland et al., 1996). After responding to the *Breathless* growth factor and migrating, tip cells of the trachea pull the rest of the cells in the branch along (Sutherland et al., 1996). Analogous to observations made in the developing kidney, FGFR signaling in the developing *Drosophila* trachea biases which cells will be specified as leading tip cells.

In 2006, in elegant mosaic screen was performed by Amin Ghabrial, Mark Krasnow, and others in which they recovered mutants that were able to occupy every tracheal position except the terminal tip cell position (Ghabrial and Krasnow, 2006). Six of the mutations, either missense or nonsense mutations, all mapped to the *breathless* FGFR (Ghabrial and Krasnow, 2006). In a separate screen a weak loss-of-function allele of *breathless* was identified that allowed flies to grow up unlike the null alleles of *breathless* (Ghabrial and Krasnow, 2006). Even though the weak allele of *breathless* retained some breathless activity, the *breathless* hypomorphic cells were always outcompeted for the tip cell fate by cells with higher levels of *breathless* (Ghabrial and Krasnow, 2006). Therefore the cells with the highest *Breathless* activity were specified as tip cells, while the cells with lower *Breathless* activity were specified as follower or stalk cells. Additionally, the Krasnow lab was able to demonstrate that lateral inhibition

mediated by Notch signaling occurs during tip cell migration (Ghabrial and Krasnow, 2006). After high *Breathless* signaling specifies the tip cell fate, the tip cell signals via Notch to the trailing cells to reinforce their tip cell fate, and assure that the follower cells do not try to take their position.

VEGF signaling during angiogenesis

Angiogenesis, the process of growing new blood vessels, is an essential process during mammalian development. Angiogenesis is the sprouting of new capillaries from pre-existing endothelial blood vessels (Ferrara et al., 2003), and not the initial formation of blood vessels, which is known as vasculogenesis. Over $4billion USD have been invested into research and medications that either promote or restrain angiogenesis, making angiogenesis one of the most funded areas of medical research (DeWitt, 2005). Since its discovery in the early 1980s, the vascular endothelial growth factor (VEGF) has emerged as the most important regulator of angiogenesis (Ferrara et al., 2003). Targeted deletion of one or both alleles of *VEGF-A* in mice results in E11 embryonic lethality and a failure to induce angiogenesis (Carmeliet et al., 1996). VEGF is a potent stimulator of new blood vessel formation. However, only a subset of tip cells respond to the VEGF cue to form a new tube from the parental vessel (Eilken and Adams, 2010).

Tip cell versus stalk cell fate specification during angiogenesis is similar to the two previous examples discussed in the kidney and trachea. Neighboring endothelial cells initially express the Notch ligand DII4 at similar levels (Eilken and Adams, 2010). Upon stimulation by VEGF, one cell preferentially expresses the Notch ligand DII4 at higher

levels than its neighbor (Eilken and Adams, 2010). The neighbor with high Notch ligand expression will turn on the Notch pathway in its neighbor (Eilken and Adams, 2010). In the neighbor with the Notch pathway activated, VEGFR2 and VEGFR3 will be downregulated (Hellstrom et al., 2007; Suchting et al., 2007; Tammela et al., 2008), thus establishing a bias with one neighbor having higher VEGF levels than the other and adopting a tip cell fate. VEGF signaling specifies the tip cell versus stalk cell during angiogenesis after Notch signaling creates a bias to determine which cell will be more competent to respond to VEGF.

Roles for genes downstream of RTK signaling after tip cell fate specification

Genes that act downstream of RTK signaling, as either targets or parallel effectors, can also promote tip cell differentiation and tubular branching. In the mammalian kidney GDNF/RET signaling specifies the tip cell fate of the ureteric bud and promotes ureteric branching (Costantini, 2010). A combined loss of the highly similar transcription factors, *Sox8* and *Sox9*, results in ureteric branching defects similar to GDNF-/- mice (Reginensi et al., 2011). *Sox-8/9* do not promote RET signaling, nor are they targets of RET signaling (Reginensi et al., 2011). However, expression of key GDNF/RET target genes that are turned on in the tip cell, including the Ets factors *etv-4* and *etv-5*, are not maintained in a *Sox-8/9* mutant background (Reginensi et al., 2011). Thus, tip cell identity is not maintained in a *Sox-8/9* background, leading to later defects in ureteric branching. The GDNF/RET and *Sox-8/9* cooperation on target genes such as *etv-4/5* promotes branching downstream of tip cell specification.

Actin depolymerizing factors (ADFs) are also required downstream of GDNF/RET during ureteric branching. A combined loss of the ADFs cofilin1 (Cfl1) and destrin (Dstn) results in arrested ureteric branching in the mouse kidney (Kuure et al., 2010a). Loss of these ADFs results in an abnormal accumulation of F-actin and irregular cell shapes of the ureteric bud epithelial cells (Kuure et al., 2010a). Interestingly, expression of these two ADFs is not controlled by RET signaling and adding exogenous GDNF cannot rescue the branching defects (Kuure et al., 2010a). Thus, Cfl1 and Dstn likely act in parallel to GDNF to promote ureteric branching through direct regulation of the actin cytoskeleton.

In the Drosophila trachea, the Ets factor *pointed* is a downstream effector in the FGFR signaling pathway. While cells mutant for the *breathless* FGFR are never specified as tip cells, *pointed* -/- cells can occupy the tip cell position, suggesting that breathless promotes initial tip cell specification independent of *pointed* (Ghabrial and Krasnow, 2006). However, when *pointed* -/- cells adopt the tip cell position, the tip cell is not able to differentiate as a tip cell (Ghabrial and Krasnow, 2006). It is not clear how genetically separable tip cell specification versus position are in the trachea. These data do suggest that some aspects of tip cell differentiation, downstream of fate specification, are controlled by *breathless* and *pointed*. After tip cell specification and differentiation, the trachea undergoes substantial branching. Both *breathless* and *pointed* promote branch migration thru transcriptional regulation of the Dpp pathway effectors, *Knirps* and *Knirps-related* (Myat et al., 2005). Thus, FGFR signaling promotes some aspects of differentiation after tip cell specification, thru the Ets transcription factor *pointed*.

Drosophila serum response factor, or *pruned*, also acts downstream of FGFR signaling during tracheal branching morphogenesis (Gervais and Casanova, 2011). In *pruned* mutants, elongation of terminal branches is blocked, but terminal cells are still specified (Gervais and Casanova, 2011). FGFR signaling induces *pruned* expression, suggesting that FGFR mediated regulation of *pruned* drives terminal cell elongation. However, overexpressing the FGF ligand *branchless* produces normal terminal branch differentiation in the absence of *pruned* (Gervais and Casanova, 2011). Conversely, overexpressing pruned cannot drive terminal branch differentiation in the absence of FGFR signaling (Gervais and Casanova, 2011). The model that has emerged is that tip cell specification is independent of *pruned*, and *pruned* is utilized by the FGFR pathway but not absolutely required for branching elongation and progression.

In these three examples from distinct tubular organs (kidney, blood vessels, trachea), it is clear that RTK signaling has a very early role in specifying the leading tip cells of a newly forming tube. RTK signaling can also promote later aspects of tube development in collaboration with other genes. Understanding more about the later roles of RTK signaling in tubulogenesis and how signaling promotes these steps is an area of ongoing research.

The Nkx5/HMX family of transcription factors

The Nkx5/HMX gene family is present throughout the animal kingdom, ranging from fruit flies to humans. In fact the first family member, *TgHbox5*, was identified in sea

urchins (Wang et al., 1990). Most members of the Nkx5/HMX family are expressed in the developing central nervous system and sensory organs (Gongal et al., 2011; Martinez and Davidson, 1997; Wang et al., 2000). Consistent with nervous system expression, mice and humans with loss-of-function mutations in Nkx5/HMX genes display nervous system related abnormalities (Schorderet et al., 2008; Wang et al., 2004). However, only a few targets have been identified for Nkx5/HMX family members, leaving the precise function of this family of transcription factors elusive.

Family present in wide range of species

Members of the Nkx5/HMX gene family can be found in sea urchins, fruit flies, mice, rats, chicks, worms, zebrafish, and humans (Fig 1.5) (Adamska et al., 2000; Adamska et al., 2001; Bober et al., 1994; Deitcher et al., 1994; Herbrand et al., 1998; Martinez and Davidson, 1997; Rinkwitzbrandt et al., 1995; Shaw et al., 2003; Stadler et al., 1995; Stadler et al., 1992; Stadler and Solursh, 1994; Wang et al., 1990; Wang et al., 2000; Yoshiura et al., 1998). The founding member of the family, *TgHbox5,* was shown to have at best ~60% identity with the homeodomain from other homeodomain proteins (Wang et al., 2000), while all members of the Nkx5/HMX family have a nearly identical homeodomain sequence. Early investigations revealed that family members from human, mouse, and chick had similar expression profiles during development in the central and peripheral nervous system (Bober et al., 1994; Rinkwitzbrandt et al., 1995; Stadler et al., 1995; Stadler and Solursh, 1994; Wang et al., 1998; Yoshiura et al., 1998). The reported phenotypes of Nkx5/HMX family members to date are predominantly nervous system related, consistent with the expression patterns of most family members.

Lessons learned from HMX genes in vertebrates

With a lack of targets or known binding partners of Nkx5/HMX family members, the precise function of the family remains obscure. However, phenotypic analysis of *hmx-1* and *hmx-2;hmx-3* double mutants from vertebrate models has provided some insight. *Hmx-1* or *dumbo* mutant mice have a ventrolateral displacement of the ears, which may be caused by malformation of the gonial or squamous temporal bones which are both in close proximity to the external ear (Munroe et al., 2009). Humans with mutations in *HMX1* have similar defects as *hmx-1* mice, with deformations and aplasia in the external ear (Schorderet et al., 2008). It has been speculated that polymorphisms in *HMX1* may lead to variable external ear phenotypes (Munroe et al., 2009). However, it remains unclear how *HMX1* could be promoting normal placement of the ears.

In mice at E11.5, Hmx2 and Hmx3 are all expressed in the entire vestibular portion of the otic vesicle (Wang et al., 2004). The pear-shaped otic vesicle is a highly specialized sensory organ that elongates and divides into a dorsal vestibular region and a ventral cochlear region (Fekete, 1999). *hmx-2;hmx-3* double null mice present with a variety of defects, including a complete loss of the auditory/otic vesicle (Wang et al., 2004). It is not clear if the loss of the otic vesicle in *hmx-2/3* null mice is a fate specification defect or a differentiation defect. The Drosophila HMX gene, which is expressed in the fly nervous system, can completely rescue the otic vesicle phenotype of *hmx-2/3* null mice, suggesting that family members across species have highly conserved functions (Wang et al., 2004).

Interestingly, a combined knockdown of *hmx-2* and *hmx-3* in zebrafish leads to similar ocular differentiation defects observed in *hmx-2/3* null mice (Feng and Xu, 2010). Also subsets of hmx-2/3 zebrafish morphants have small and misshapen ventral ganglia. In the zebrafish anterior otic vesicle a feedback loop exist whereby FGF signaling turns on expression of *hmx-2/3*, and subsequently *hmx-2/3* is required to maintain expression of FGF ligands (Feng and Xu, 2010). *hmx-2/3* is also required to turn on the transcription factor Pax-5 for further development of zebrafish sensory hair cells (Feng and Xu, 2010). This is one of only a few examples showing the Nkx5/HMX family to act in transcriptional activation. However, *pax-5* morphants are largely wild type, and expression of Pax-5 RNA cannot rescue *hmx2/3* morphants (Feng and Xu, 2010). Therefore additional targets must exist that explain the mouse and zebrafish ocular defects. The role of *C.elegans* MLS-2 in the excretory system (described in Chapter Three) may provide valuable insight into the mechanism of action of the HMX/Nkx5 gene family in vertebrates.

MLS-2, a *C.elegans* Nkx5/HMX family member

The first reported role for MLS-2 in *C.elegans* was during post-embryonic development of the non-essential M lineage (Jiang et al., 2005). In the M lineage, MLS-2 is important for cell fate specification and cell proliferation. MLS-2 promotes expression of the *C.elegans* MyoD protein HLH-1 during coelomocyte fate specification in the M lineage (Jiang et al., 2005). In addition, MLS-2 requires the cell cycle regulator CYE-1 for its role in cell proliferation in the M lineage (Jiang et al., 2005).

Most members of the Nkx5/HMX family have the HMX motif [A/S]A[E/D]LEAA[N/S] located immediately downstream of the homeodomain (Wang and Lufkin, 2005; Yoshiura et al., 1998). However, MLS-2 and its closest relative, the chick SOHo1 protein lack the HMX motif (Deitcher et al., 1994). The significance of MLS-2 lacking the HMX motif is unclear, as no role has been assigned for the HMX motif.

Like other Nkx5/HMX family members, MLS-2 has roles in nervous system development. MLS-2 is expressed predominantly in neurons and glial cells (see Chapter Three), and MLS-2 is required for differentiation and morphogenesis of the AWC chemosensory neurons and the CEP sheath glial cells (Kim et al., 2010; Yoshimura et al., 2008). The AWC left and right neurons are a pair of amphid sensory neurons required to chemotax to volatile odors (Bargmann et al., 1993). The AWC neurons have an elaborate shape with elongated cilia that are buried within a sheath and are not directly exposed to the outside environment like other chemosensory neurons in *C.elegans* (Ward et al., 1975). CEH-36 promotes AWC identity (Lanjuin et al., 2003), and MLS-2 turns on expression of CEH-36 in the AWC neuron (Kim et al., 2010). The AWC neuron is not converted to an alternate fate in *mls-2* mutants and most AWC specific genes are not expressed due to loss of CEH-36 expression (Kim et al., 2010). MLS-2 is also expressed in the CEP sheath glial cell (Yoshimura et al., 2008). The CEP sheath glial cells envelope the *C.elegans* nerve ring, which is considered the worm's brain, and sends processes to some synaptic sites in the brain (Ward et al., 1975). *mls-2* disrupts ventral glia cell differentiation and terminal markers for the ventral CEP sheath glial fate are not

expressed in *mls-2* mutants (Yoshimura et al., 2008). Thus *mls-2* promotes differentiation of these two elongated cell types, the AWC neuron and the CEP sheath glia cell. However, the targets that act downstream of MLS-2 besides other transcription factors, to promote morphogenesis, are unknown.

The *C.elegans* excretory system

The *C.elegans* excretory system is a simple model to investigate how a tubular epithelial network is made and maintained. The excretory system is the worm's primitive renal-like system and is required for fluid waste expulsion (Buechner, 2002; Nelson et al., 1983; Nelson and Riddle, 1984). All of the cells of the excretory system (the canal, duct, and pore cells) are unicellular tubes that connect in tandem via apico-lateral junctions (Fig 1.6). The canal cell is the largest cell in the worm and appears to collect fluid waste (Buechner, 2002). The canal cell is a large H-shaped cell with its nucleus at the anterior of the worm and four hollow canals that extend down the lateral side of the worm (Buechner, 2002). The duct and pore cells are smaller epithelial tubes that connect the canal cell to the outside environment. The duct and pore cells are lineal homologs and are initially equivalent precursor cells (Sulston et al., 1983). Several hours after fertilization all three cells have adopted distinct fates and formed into tubular epithelial cells from non-epithelial precursor cells.

The canal and duct are required for survival of the worm, and animals that lack either of these cells die during the first larval stage with a fluid filled rod-like phenotype

(Nelson and Riddle, 1984). In addition, mutants with physiological defects in the excretory system also die during the first larval stage with the rod-like phenotype (Liegeois et al., 2007). Over the years, our lab has performed forward and reverse genetic screens to find new genes involved in excretory system development, using the rod-like lethal phenotype as an easy 'read-out' for new mutants. For example, the lab has identified genes involved in fate specification of the duct cell (Abdus-Saboor et al., 2011; Howard and Sundaram, 2002)(Abdus-Saboor et al. 2012, submitted), lumen connectivity between the duct and pore cells (Stone et al., 2009), and maintenance of junction connectivity between the duct and pore (Mancuso et al., 2012). The forward mutagenesis screens performed by the lab have not been saturated; therefore more genes are likely to be discovered from future screens.

Simple yet dynamic tubular network

Unlike complex multicellular tubes that may contain hundreds of cells, the *C.elegans* excretory system only contains three main cells, allowing visualization of tube development with single cell resolution. Despite the simplicity in the number of cells, the excretory system undergoes similar processes that more complex tubular organs undergo such as mesenchymal-to-epithelial transition or MET. The cells of the excretory system are polarized like other tubular epithelial cells. However, at the early pre-enclosure embryonic stage the duct and pore cells are mesenchymal-like with no associated junctions. At the pre-enclosure stage, the duct precursor cell is on the left side of the embryo, while the pore precursor is on the right side (Sulston et al., 1983). Several hours later by the 1.5-fold stage of embryogenesis, the precursors have migrated to the ventral

midline and stacked on top of each other (Stone et al., 2009; Sulston et al., 1983). Also by the 1.5-fold stage both the duct and pore have formed junctions with themselves and neighboring cells (discussed in further detail in Chapter Two). The signal(s) that initiates the MET of the duct and pore is unknown.

Tubulogenesis can also be reversible; that is tubular epithelial cells can undergo an epithelial-to-mesenchymal transition, or EMT, and withdraw from the tube. Approximately seven hours after the embryo hatches, the G1 pore cell withdraws from the excretory system (Jean Parry, personal communication; Sulston et al., 1983). As the G1 pore migrates away from the excretory system, it goes back into the cell cycle and divides to give rise to two neurons (Sulston et al., 1983). A neighboring epithelial cell, named G2 moves in and replaces the embryonic G2 pore (Sulston et al., 1983). During the 'pore swap', the duct must release its junction from the G1 pore and form new junctions with the G2 pore. The 'G1-to-G2 pore swap' is a remarkable example of neuronal specification, and also of single cell EMT. The factors which promote or restrain the G1 pore EMT remain to be identified.

Three tubes with three distinct ways to form a lumen

The cells of the excretory system are unicellular tubes that generate a lumen by either wrapping or hollowing. Shortly after birth of the canal cell during early embryogenesis, a lumen begins to form in the canal cell (Buechner, 2002). Previous reports suggested that small vacuoles appear in the canal cell body and coalesce, forming an apical lumen within the canal (Buechner, 2002). However, studies from our lab

suggest that canal lumen formation begins at the canal-duct junction, and presumably continues via an inward growth mechanism (Stone et al., 2009). At this time a thick material can be visualized in the immature canal cell lumen by electron microscopy (images at www.wormatlas.org). By the time the embryo hatches the previous electron dense material in the canal is replaced by a new electron dense material (Buechner, 2002). The new electron dense material in the canal at hatch is likely related to the canal beginning to function as an osmoregulatory organ (Buechner, 2002).

In 1999 Matthew Buechner performed a screen where he identified 12 mutants (*exc1-9*, *let-4*, *let-653*, and *sma-1*) with large fluid-filled cysts accumulating in the canal cell lumen (Buechner et al., 1999). Interestingly, most of the canal cystic mutants are not organismal lethal. Since the initial screen, work from the Buechner lab and others have shown that the *exc* genes encode ion channels and their regulators (Berry et al., 2003; Hisamoto et al.,2008; Liegeois et al., 2007), cytoskeletal proteins (Gao et al., 2001; Gobel et al., 2004; Praitis et al., 2005; Suzuki et al., 2001; Tong and Buechner, 2008), and an RNA-transport protein *exc-7* (Fujita et al., 2003). *exc-7* (ELAV) binds and transports *sma-1* (β-spectrin) mRNA, which is then transported along the canals (Tong and Buechner, 2008; Fujita et al., 2003). An unknown mechanical sensor activates *exc-9* (CRIP), and *exc-9* activates *exc-4*(CLIC) and *exc-5* (Berry, 2003; Tong and Buechner, 2008). Recently it has been shown that *exc-5*, a homologue of the FGD family of mammalian exchange factors, mediates passage of early endosomes to recycling endosomes apically via the CDC-42 GTPase, to maintain a normal canal lumen (Mattingly and Buechner, 2011). Importantly, these models are based mainly on genetic

arguments and await further verification from complementary biochemical approaches.

The duct and pore tubes form a lumen by wrapping, instead of hollowing like the canal cell. The pore cell forms a lumen by wrapping around itself and forming an autocellular junction, which can be observed by the AJM-1::GFP apical junction marker or by electron microscopy (Stone et al., 2009). The duct also forms a lumen by wrapping, followed by a secondary self-fusion event like the one described above in the *C.elegans* digestive tract (Rasmussen et al., 2008; Stone et al., 2009). AJM-1::GFP does not label the duct cell. However, in an *aff-1* mutant background, the duct cell autocellular junction can now be visualized with AJM-1::GFP (Stone et al., 2009). AFF-1 is a molecule involved in homotypic fusion (Sapir et al., 2007), and the duct cell presumably expresses *aff-1*. Therefore, when *aff-1* is not present the duct cell cannot fuse its autocellular junction. Self-fusion of the duct cell after wrapping does not appear to be an essential function, as the majority of *aff-1* mutants are viable. One hypothesis is that the duct fuses its autocellular junction because it will remain in the tubular network, while the G1 pore cell does not fuse its autocellular junction to facilitate an easy break down of the junction and subsequent withdraw of the G1 pore from the excretory system.

Three cells that adopt complex morphologies

Mid-way through embryogenesis at the 1.5-fold stage, electron microscopy shows the cells of the excretory system stacked in block-like orientations (Stone et al., 2009) (Fig 1.6). However, between 1.5-fold and hatch, which is approximately seven hours, many morphogenic and cell shape changes occur. The canal cell requires Notch signaling in its grandparent cell ABplpapp to be specified (Lambie and Kimble, 1991b; Moskowitz

and Rothman, 1996). However, no direct roles for Notch signaling in the morphogenesis of the canal have been identified. By the time the worm hatches, the hollow canals will have elongated to a length of half of the worm's body (Buechner, 2002). As the worm continues to grow, so does the canal cell, with the canals extending to the nose of the worm at the anterior, and past the anus near the tail at the posterior of the worm (Buechner, 2002).

Outgrowth of the canals has been compared to neuronal outgrowth because similar genes are involved in both processes (Hedgecock et al., 1997; Antebi et al., 1997). Canal tips appear to be guided during canal extension just like neuronal growth cones are guided during outgrowth (Buechner, 2002). For example, mutants of *unc-5* (netrin) and its receptor *unc-6*, both have shortened mispositioned canals that fail to extend normally (Hedgecock et al., 1990). Instead of the canals extending alongside the lateral epidermis, in *unc-5* and *unc-6* the shortened canals extend alongside the ventral epidermis (Hedgecock et al., 1990). Also CEH-6, a POU homeodomain transcription factor, is expressed in the canal cell and promotes canal morphogenesis (Burglin and Ruvkun 2001). The canal cell is specified in *ceh-6* mutants, but the resultant canals have defects in morphogenesis. The targets of CEH-6 that promote canal morphogenesis are unknown (Burglin and Ruvkun, 2001).

Like the canal, the duct undergoes numerous morphogenic processes, including elongation after fate specification. Previous studies suggested that the duct versus pore fate decision is specified by *let-60*/Ras (Sulston et al., 1983; Yochem et al., 1997). To what extent EGF-Ras-Erk signaling controlled morphogenesis of the duct was unclear. Interestingly, Notch mutants, like *let-60*/Ras mutants also lack a duct cell (Lambie and

Kimble 1991). A missing duct cell in Notch mutants could be a secondary consequence of lacking a canal cell, or Notch signaling may have a cell autonomous role in the duct (addressed in Chapter Two).

During the period between 1.5-fold and hatch, the duct elongates extensively and adopts a unique asymmetric shape (Fig 1.6). The region of the duct that connects to the pore is narrow in diameter similar to an axonal extension. The duct expresses the transcription factor LIN-48, an ortholog of Drosophila shavenbaby/ovo that influences duct position and/or length (Wang and Chamberlin, 2002). However, *lin-48* mutants do not arrest with excretory system lethality, suggesting that the duct cell has normal function. In addition, the previous analysis performed on *lin-48* mutants measured the distance between the terminal pharyngeal bulb and the pore, which is a low resolution and indirect measure of duct shape (the panel of markers that exist to study the shape of the duct were not available when the original *lin-48* studies were performed). Nonetheless, the original *lin-48* studies suggested that other factors exist that contribute to the morphogenesis of the duct.

The morphogenesis of the pore in some ways is more remarkable than the duct and canal, because two different cells will function as the pore throughout the worm's life. The G1 pore appears to be the default fate after the duct is specified. The G2 pore fate is specified by Notch signaling (Greenwald et al., 1983). However, there is no evidence that implicate Notch signaling in morphogenesis of the G2 pore after fate specification. Both the G1 and G2 pore have regular, conical shapes, without extensive elongation. However, the G2 pore is slightly taller in height than the G1 pore - this

increase in height likely corresponds to the increased size of the worm between embryonic and larval stages.

Project Summary

The three cells of the excretory system form tubes by different mechanisms and ultimately adopt unique shapes. Examples of both MET and EMT are observed in this relatively simple model. Both Ras and Notch signaling have been implicated in excretory system development for years. However, which steps in tube development require signaling had not been clarified. In Chapter 2, I demonstrate that Ras has genetically separable roles in excretory system development. Surprisingly, I found that Ras had a continued role in maintaining organ architecture of the duct tube. In Chapter 3, I describe a forward mutagenesis screen performed by Craig Stone, a former graduate student in the lab, to identify new genes involved in excretory system development. I show that one gene identified in the screen, an Nkx5/HMX homeodomain transcription factor named *mls-2*, promotes shape acquisition of the duct and pore, while acting genetically in parallel to Ras signaling. Chapter 4 demonstrates an attempt to identify the core cytoskeletal subunits involved in promoting morphogenesis of excretory system cells. A surprising genetic interaction was revealed between *mls-2* and cytoskeletal genes in early embryos. Finally, in Chapter 5 I describe an RNAi enhancer screen I performed to identify *mls-2* redundant factors. This screen identified a chromatin remodeling factor

that genetically interacts with both *mls-2* and the EGF-Ras-ERK pathway, presumably during duct development.

In summary, our results provide insight into which steps require Receptor Tyrosine Kinase signaling during tube formation. Our data also show which type of gene can act downstream or parallel to Receptor Tyrosine Kinase signaling to promote morphogenesis of elongated cells.

Figure Legends

Figure 1.1. Conrad Wallington's epigenetic landscape. Model of a ball at the top of a hill representing a cell. Each valley represents a distinct cell fate. [Figure taken from Conrad Wallington's *Epigenetic Landscape*].

Figure 1.2. The three types of tubes. (A) Multicellular tube showing basal and apical surfaces with junctions between the cells. (B) Unicellular tube with autocellular junction going down the seam of the tube. (C) Unicellular tube without an autocellular junction, also known as 'seamless' [Figure taken from (Lubarsky and Krasnow, 2003)].

Figure 1.3. Building a lumen and polarizing a tube. (A) Building a tube by wrapping from an already polarized epithelium. The new tube is discontinuous from the old epithelium. (B) Building a tube by budding from an already polarized epithelium. The new tube maintains connection with the parental epithelium. (C) Building a tube by hollowing a cord. The lumen forms when multiple cells fuse their lumena together. (D)

Building a tube by cell hollowing. The lumens form within the cell when small vesicles fuse. (E) Building a tube by cavitation. The lumen forms within a tube by programmed cell death [Figure taken from (Andrew and Ewald, 2010)].

Figure 1.4. The EGF-Ras-ERK signaling pathway. Diagram of Epidermal Growth Factor signaling cascade from EGF ligand to downstream effectors LIN-1 and EOR-1. *C.elegans* and also mammalian names shown where applicable. The yellow rectangle represents the cytoplasm, and the white circle represents the nucleus. Dashed arrow shows MPK-1 likely has other substrates that have not been identified. LIN-1 shown in red acts as a repressor, but when phosphorylated by MPK-1, we hypothesize that LIN-1 then acts as an activator. LIN-1 is redundant with EOR-1 and EOR-2(not shown).

Figure 1.5. A phylogenetic tree of the HMX family. Sequence analysis performed with Clustal W showing the highly similar homeodomain of MLS-2 and HMX genes from other species [Figure taken from (Jiang et al., 2005)].

Figure 1.6. Timeline of *C.elegans* Excretory System development. (A) Schematics of excretory canal cell (red, ABplpappaap), duct (yellow, ABplpaaaapa), G1(blue, ABprpaaaapa) at different developmental stages, based on (Sulston et al., 1983), prior electron microscopy (Stone et al., 2009), and work described in Chapter Two. Dark black lines, apical junctions; dotted line, duct auto-fusion; arrow, pore autocellular junction; arrowhead, duct-canal cell intercellular junction; bracket, duct cell body. Colored circled represent relative positions of the three cells in the live worm. Not shown are the non-essential excretory gland cells, which also connect to the duct-canal junction (Nelson et

al., 1983; Nelson and Riddle, 1984). (B) Adult canal cell marked with *vha-1p*::GFP. Note that the canal cell elongates extensively. (C,D) L1 larvae. (C) AJM-1::GFP marks pore autocellular junction and duct-canal junction. The duct no longer has an autocellular junction. (D) *dct-5p*::mcherry marks the cytoplasm of the duct and G1 pore.

Figure 1.1

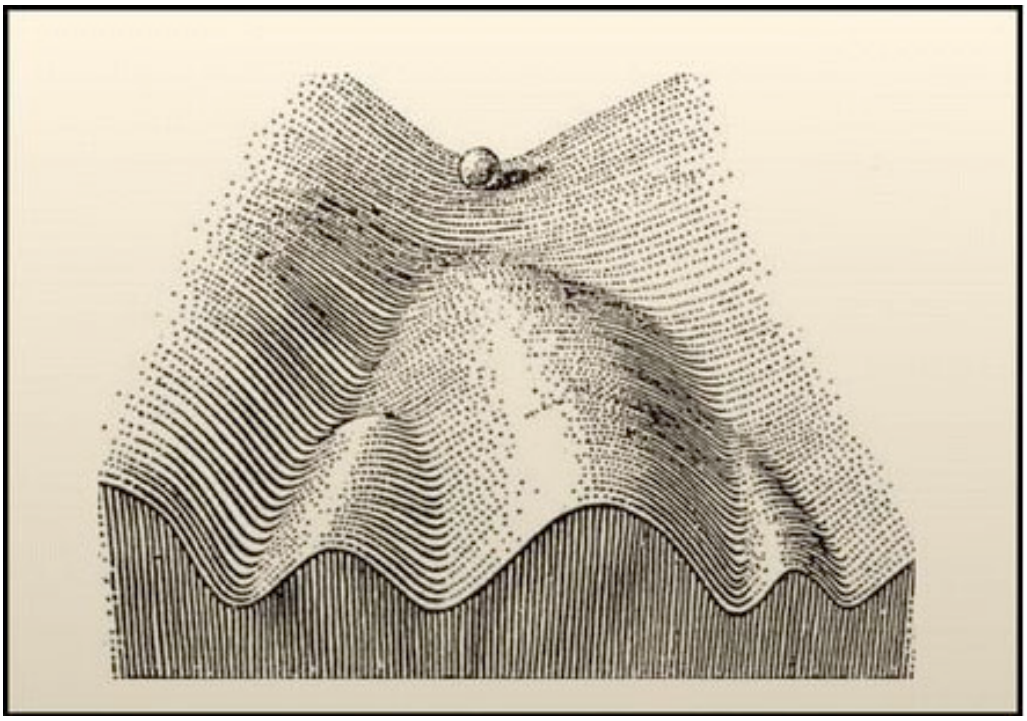

Figure 1.2

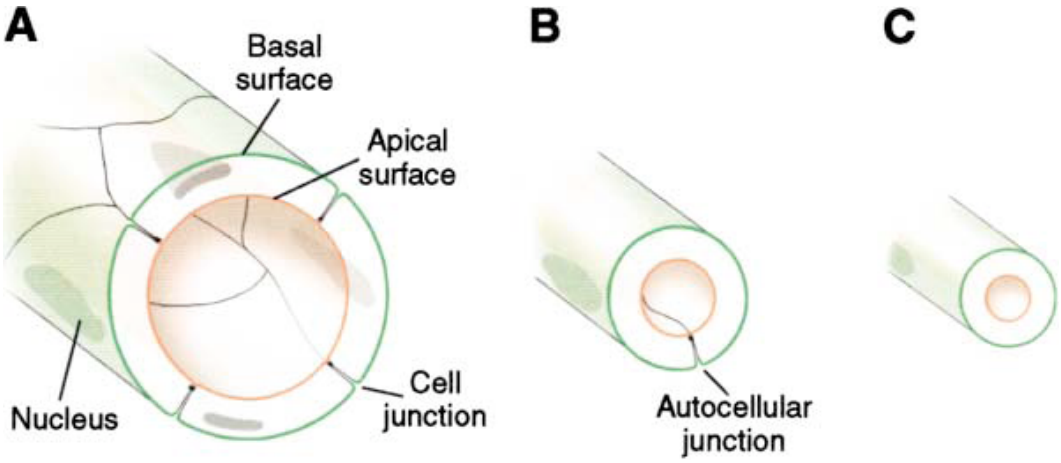
A
Basal surface
Apical surface
Nucleus
Cell junction
B
Autocellular junction
C

Figure 1.3

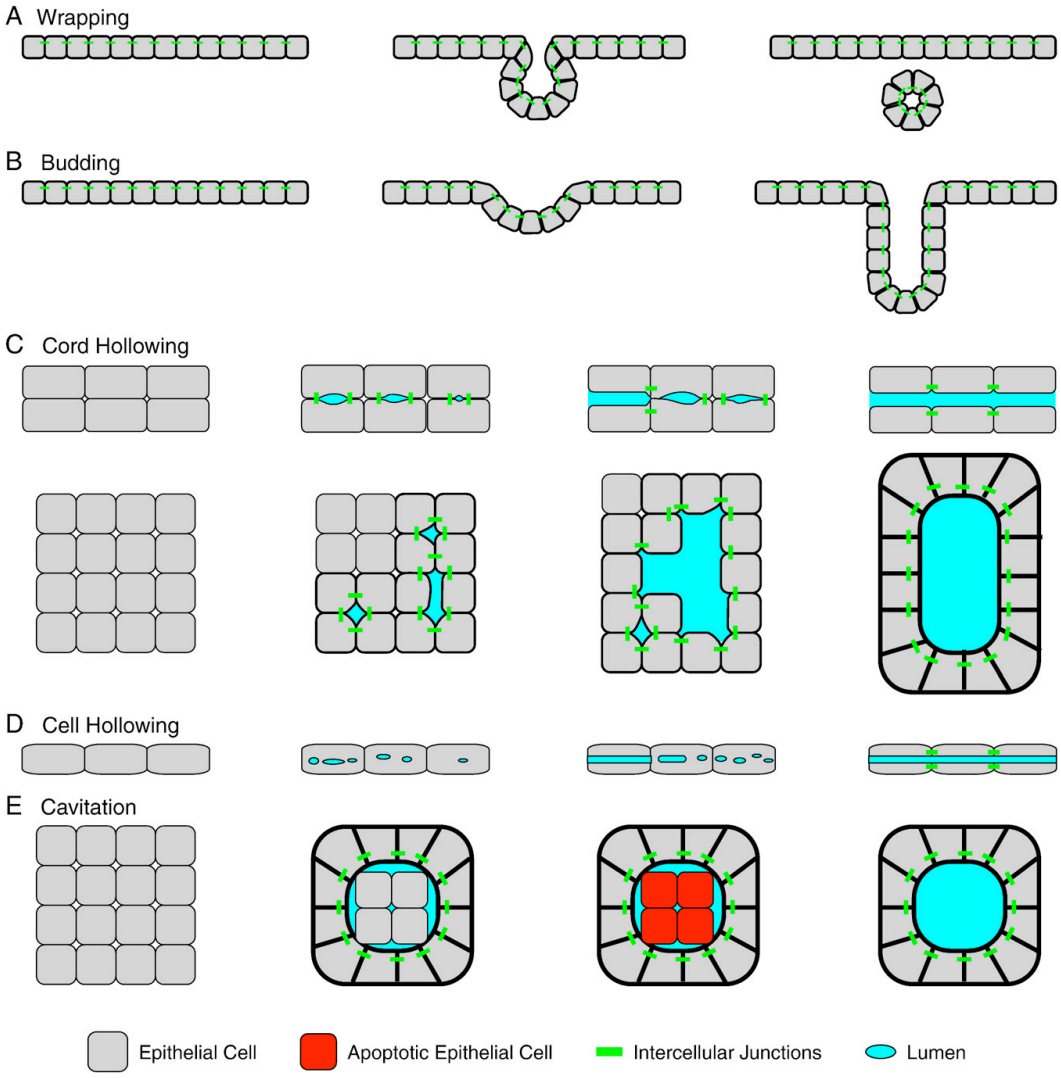
A Wrapping
B Budding
C Cord Hollowing
D Cell Hollowing
E Cavitation
Epithelial Cell
Apoptotic Epithelial Cell
Intercellular Junctions
Lumen

Figure 1.4

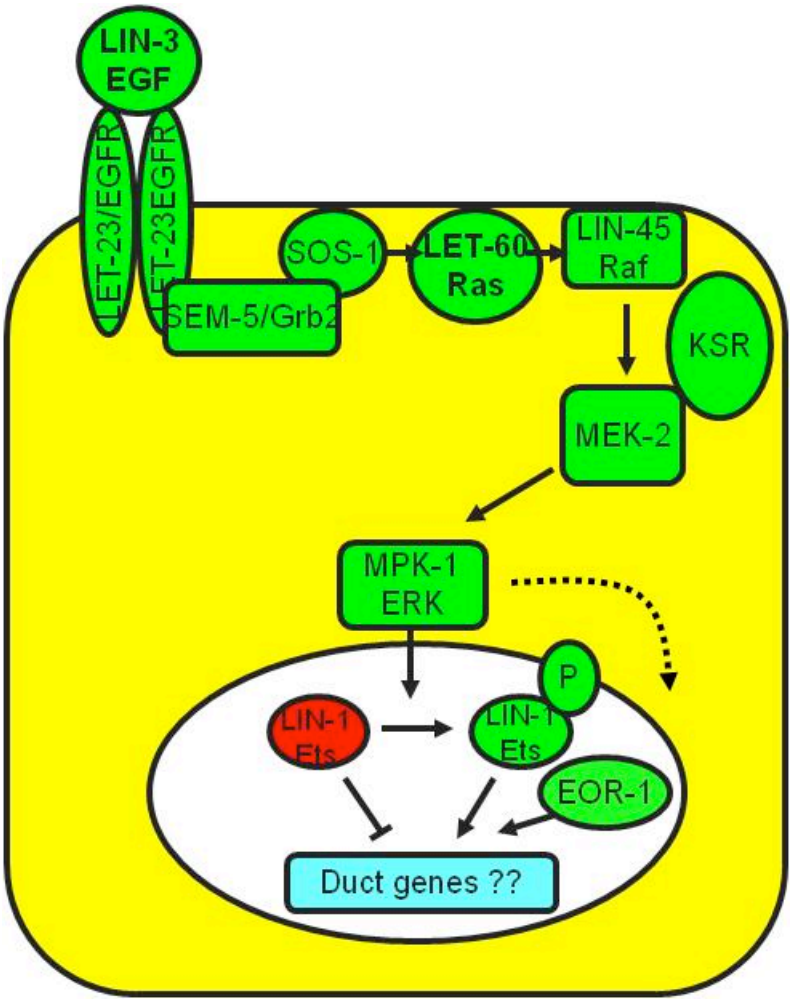
LIN-3
EGF
LET-23/EGFR
LET-23EGFR
SOS-1
LET-60
Ras
LIN-45
Raf
SEM-5/Grb2
KSR
MEK-2
MPK-1
ERK
P
LIN-1
Ets
LIN-1
Ets
EOR-1
Duct genes ??

Figure 1.5

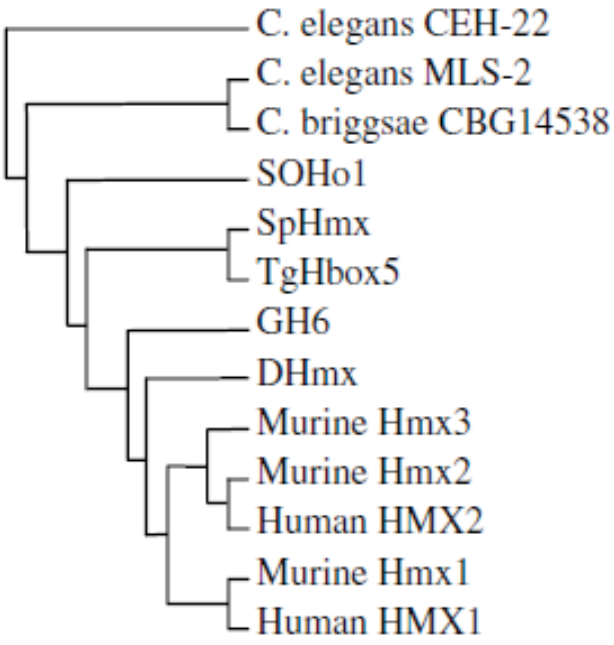
C. elegans CEH-22
C. elegans MLS-2
C. briggsae CBG14538
SOHo1
SpHmx
TgHbox5
GH6
DHmx
Murine Hmx3
Murine Hmx2
Human HMX2
Murine Hmx1
Human HMX1

Figure 1.6

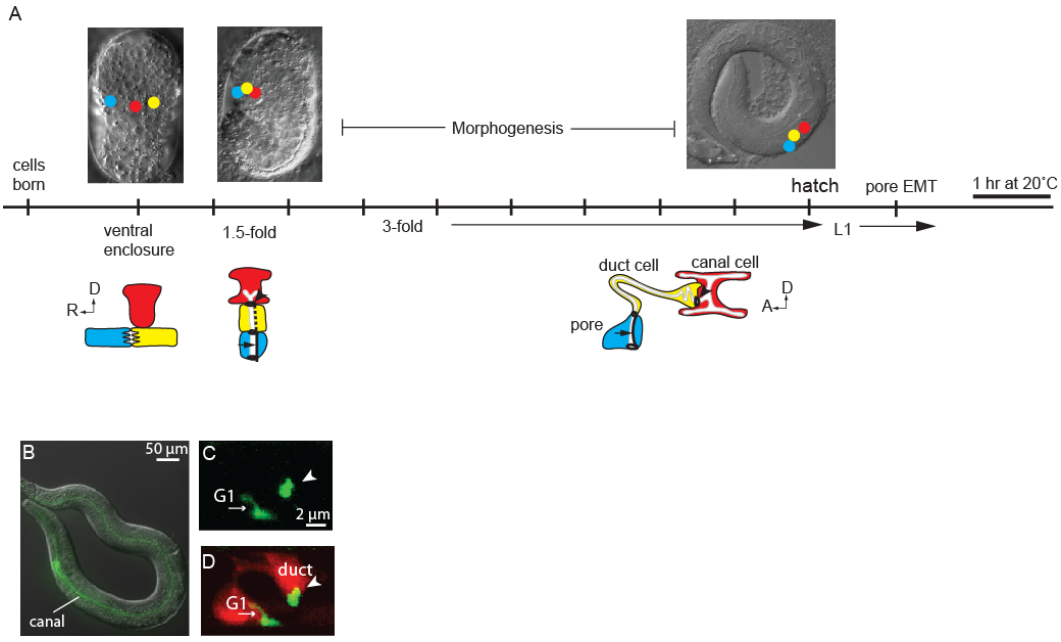
A
Morphogenesis
cells born
ventral enclosure
1.5-fold
3-fold
hatch
pore EMT
1 hr at 20°C
L1
D
R
duct cell
canal cell
pore
D
A
B
50 µm
canal
C
G1
2 µm
D
duct
G1

Chapter Two:

NOTCH AND RAS PROMOTE SEQUENTIAL STEPS OF EXCRETORY TUBE DEVELOPMENT IN *C. ELEGANS**

*This chapter was published as **Ishmail Abdus-Saboor***, Vincent P. Mancuso*, John I. Murray, Katherine Palozola, Carolyn Norris, David H. Hall, Kelly Howell, Kai Huang and Meera V. Sundaram. Development **138**, 3545-3555 (2011). Note: some additions to the text are contained in this chapter.

SUMMARY

Receptor Tyrosine Kinases and Notch are critical for tube formation and branching morphogenesis in many systems, but the specific cellular processes that require signaling are poorly understood. Here we describe sequential roles for Notch and Epidermal Growth Factor (EGF)-Ras-ERK signaling in the development of epithelial tube cells in the *C. elegans* excretory (renal-like) organ. This simple organ consists of three tandemly connected unicellular tubes, the excretory canal cell, duct and G1 pore. *lin-12* and *glp-1*/*Notch* are required to generate the canal cell, which is a source of LIN-3/EGF ligand and physically attaches to the duct during *de novo* epithelialization and tubulogenesis. Canal cell asymmetry and *let-60/Ras* signaling influence which of two equivalent precursors will attach to the canal cell. Ras then specifies duct identity, inducing auto-fusion and a permanent epithelial character; the remaining precursor becomes the G1 pore, which eventually loses epithelial character and withdraws from the organ to become a neuroblast. Ras continues to promote subsequent aspects of duct morphogenesis and differentiation, and acts primarily through Raf-ERK and the transcriptional effectors LIN-1/Ets and EOR-1. These results reveal multiple genetically-separable roles for Ras signaling in tube development, as well as similarities to Ras-mediated control of branching morphogenesis in more complex organs, including the mammalian kidney. The relative simplicity of the excretory system makes it an attractive model for addressing basic questions about how cells gain or lose epithelial character and organize into tubular networks.

INTRODUCTION

Many organs, such as the mammalian kidney and the vasculature, consist of complex networks of tubules that develop from clusters of initially unpolarized mesenchymal cells (Dressler, 2009; Hogan and Kolodziej, 2002; Lubarsky and Krasnow, 2003). The processes by which these cells polarize, form epithelial or endothelial junctions, and then organize into complex tubular shapes are only beginning to be elucidated. In many cases, signaling pathways involving Receptor Tyrosine Kinases (RTKs) and Ras are critical for formation and patterning of the tubular network. For example, during branching morphogenesis of the ureteric bud in the kidney, signaling by the Ret RTK promotes tip cell identity and specifies the location of new branches (Chi et al., 2009; Shakya et al., 2005b). Similarly, during sprouting angiogenesis, signaling by vascular endothelial growth factor receptors promotes tip cell identity (Phng and Gerhardt, 2009). Absence of RTK signaling results in renal or vascular agenesis. Although the importance of RTK pathways in controlling tube development is clear, the specific cellular behaviors that require signaling, and the downstream mechanisms that control them, are not well understood.

Tubulogenesis can be reversible, as cells can withdraw from an existing tube and give rise to different cell types. For example, venous endothelial cells in the mouse de-differentiate and divide to give rise to new coronary arteries, capillaries and veins as part of their normal developmental program (Red-Horse et al., 2010). Epithelial-to-mesenchymal transition (EMT) or endothelial-to-mesenchymal transition (EndMT) are central features of injury-induced fibrosis in the kidney and heart (Kalluri and Neilson,

2003; Zeisberg et al., 2007) and underlie the metastatic properties of many tumor cells (Kalluri and Weinberg, 2009). Tubes that form by *de novo* polarization may be particularly prone to EMT, but the mechanisms that promote or restrain such behaviors remain poorly understood.

The *C. elegans* excretory system is a simple example of an epithelial tube network. The excretory system is the worm's renal-like system and is required for fluid waste expulsion (Nelson et al., 1983; Nelson and Riddle, 1984). It consists of three tandemly arranged unicellular tubes: the large canal cell (which runs the length of the body and appears to collect waste fluid), and the smaller duct and pore cells (which connect the canal cell to the outside environment) (Fig. 2.1). While the canal cell and duct tubes are permanent throughout the life of the animal, the G1 pore eventually withdraws from the excretory system to become a neuroblast, at which time a neighboring epidermal cell (G2) replaces G1 as the excretory pore tube (Stone et al., 2009; Sulston et al., 1983). Thus the excretory system provides a simple, genetically tractable system for studying the dynamic control of epithelial junctions, cell shape and cell identity.

The progenitors of the excretory duct and G1 pore tubes are left/right lineal homologs that appear to compete for the duct fate (Sulston et al., 1983). In wild-type animals, the left cell always becomes the duct and adopts the most canal cell-proximal position, while the right cell always becomes G1 and adopts a more distal position. However, ablation of the mother of the presumptive duct causes the presumptive G1 to adopt a duct-like position and morphology, showing that both cells have the capacity to

become a duct and suggesting some lateral inhibitory mechanism that prevents both from doing so. Both *let-60*/Ras and *lin-12 glp-1*/Notch mutants lack an excretory duct, implicating Ras and Notch in the duct vs. G1 pore fate decision or some other aspect of duct development (Lambie and Kimble, 1991a; Yochem et al., 1997).

Here we show that Notch and Epidermal Growth Factor (EGF)-Ras-ERK act sequentially during excretory tube development. We identify multiple, genetically separable requirements for signaling in controlling tube cell position, identity, shape and function. Finally, we establish the excretory duct and G1 pore system as a model for investigating many basic cell biological processes associated with tube development and EMT-coupled cell fate plasticity.

RESULTS

Excretory tube development involves *de novo* formation and remodeling of epithelial junctions

Excretory tube development occurs in three broad phases (migration/tubulogenesis, morphogenesis/differentiation, and G1 withdrawal/remodeling) (Fig. 1A) (Berry et al., 2003; Buechner, 2002; Stone et al., 2009; Sulston et al., 1983). To visualize the excretory duct and G1 pore during these phases, we used lineage-specific markers in combination with epithelial apical junction markers AJM-1 (Koppen et al., 2001b) and DLG-1/Discs Large (Bossinger et al., 2001)(Fig. 2.1). GFP::MLS-2 marks all ABpl/rpaaa descendants (including the duct and G1) plus additional lineages during ventral enclosure (Yoshimura et al., 2008) (J.I.M., unpublished data) (Fig. 2.1B-C,E),

while *dct-5p*::mCherry marks the duct, G1 and some other epithelial cells during L1 (this work, Fig. 2.1J-K). We also analyzed a ventral enclosure embryo by transmission electron microscopy (TEM) of serial sections (Fig. 2.1D) and traced the canal, duct, and G1 pore lineages through ventral enclosure from 3D confocal movies of eight histone::mCherry-expressing embryos (Materials and Methods).

The canal cell, duct and G1 pore progenitors are born in disparate locations of the embryo. During ventral enclosure (Fig. 2.1B-E), the duct (left) and G1 pore (right) progenitors migrate toward the canal cell, which is located slightly left of the ventral midline. The duct progenitor has a shorter distance to migrate, and it appears to reach the canal cell first (Fig. 2.1C). TEM of an embryo at ventral enclosure shows the duct progenitor and the canal cell closely apposed, while the G1 progenitor is excluded from the canal cell by the duct and other intervening cell bodies (Fig. 2.1D). In 6/8 3D confocal movies, the duct nucleus arrives adjacent to the canal cell about 5-10 minutes before G1. At this time, 1-2 nuclei still separate the canal from G1; the most consistent of these is RIS, a right-derived neuron whose left homolog is related to the canal cell and undergoes programmed cell death. In 2/8 movies, the duct and G1 nuclei arrive near the canal cell at approximately the same time, so it is not possible to determine which cell contacts the canal cell first in the absence of a membrane or cytoplasmic label. After the duct reaches the canal cell, they begin to ingress, while G1 moves to a ventral position between the G2 and W epidermal cells (Fig. 2.1E). Together, these observations suggest that asymmetry of the canal cell and its lineal relatives might contribute to asymmetry in duct and G1 pore behavior.

The cells initially lack epithelial junctions (Fig. 2.1B, D), but after they contact each other, they form epithelial junctions and undergo tubulogenesis (Fig. 2.1F). As described previously (Stone et al., 2009), the duct and G1 pore cells wrap up into tube shapes and form autocellular junctions. G1 retains this autocellular junction, but the duct cell rapidly auto-fuses, becoming a seamless toroid. The canal cell forms lumen intracellularly at the site of the duct-canal cell intercellular junction. By the 1.5 fold stage, the canal cell, duct and pore form a simple block-like stack of tandemly connected unicellular tubes with a continuous lumen and prominent epithelial junctions (Fig. 2.1A,F).

Further morphogenesis occurs during the latter part of embryogenesis, such that by the first larval stage, the excretory duct (Fig. 2.1G-J) and canal cell (Fig. 2.1L) have distinctive elongated shapes. The cells also begin expressing unique differentiation markers, such as the *lin-48*/Ovo transcription factor in the duct (Fig. 2.1I) (Johnson et al., 2001).

G1 withdrawal and G2 entry occur in the first larval stage, after the excretory system has already begun to function. At this time, G1 migrates dorsally and loses its epithelial junctions while a neighboring epidermal cell, G2, forms an autocellular junction and replaces it as the pore (Fig. 2.1K) (Sulston et al., 1983; Stone et al., 2009). G2 subsequently divides in L2 to generate a neuronal daughter (G2.a) and an epithelial daughter (G2.p) that replaces it as the permanent pore tube (Sulston and Horvitz, 1977). Throughout this time the duct process must remodel its ventral junction to connect to its new partners.

let-60/Ras is both necessary and sufficient for duct vs. G1 pore fate specification

let-60/Ras is required cell autonomously within the excretory duct cell for proper excretory system function and organismal viability and was previously proposed to promote the duct vs. G1 pore fate (Yochem et al., 1997). To test this model, we used AJM-1::GFP and *lin-48p*::GFP markers to examine *let-60 ras* mutants (Fig. 2.2).

Most *let-60(sy101sy127lf)* null mutants, obtained from heterozygous mothers, have two pore-shaped cells with autocellular junctions and no *lin-48p*::GFP (Fig. 2.2B-C,K-L), consistent with a duct-to-G1 pore cell fate transformation. Although the mutants lack a duct-like cell, the overall arrangement of the excretory system resembles that of wild-type animals: two cells are arranged in tandem, with one contacting the canal cell and the other contacting the ventral epidermis. Thus, initial migration, stacking and tubulogenesis appear normal, but auto-fusion does not occur and duct-specific differentiation markers are not expressed.

let-60(sy101sy127lf) mutants die as late L1 larvae with a rigid, fluid-filled appearance termed “rod-like lethality”. Fluid first accumulates near or within the two pore-like tubes (Fig. 2.2C'). Notably, the timing of fluid accumulation in mid-L1 coincides with the normal timing of pore remodeling and is often associated with large junctional rings or discontinuities (Fig. 2.2C). Since withdrawal from the excretory system is a normal feature of G1 pore identity, withdrawal of both pore-like cells may explain the inviability.

let-60(n1046gf) hypermorphic mutants have two duct-like nuclei expressing *lin-48p*::GFP and no autocellular junctions (Fig. 2.2D,K-L), consistent with a G1 pore-to-duct cell fate transformation. The two duct cells fuse to form a binucleate cell, as would be predicted for two adjacent cells expressing the fusogen *aff-1*, which is required for duct auto-fusion (Stone et al., 2009) and generally sufficient for fusion of adjacent cells (Sapir et al., 2007). Removal of *aff-1* in a *let-60(gf)* background restored both intercellular and autocellular junctions (data not shown). The binucleate duct cell attaches to the ventral epidermis, allowing for fluid excretion, and is permanent throughout the life of the animal.

We conclude that Ras signaling is both necessary and sufficient to promote duct vs. G1 pore identity, and that identity can be uncoupled from cell position. Notably, however, some *let-60* null mutants still possess a cell with at least partial duct-like character (Fig. 2.2K-L). Evidence below suggests that this is due to maternally-provided *let-60* activity; maternal activity cannot be completely removed in our experiments because of the requirements for *let-60* and other pathway components in germline development (Church et al., 1995).

let-60/Ras functions within the canonical EGF-Ras-ERK pathway to promote the duct fate

Animals mutant for *lin-3*/EGF or various other components of the canonical EGF-Ras-ERK pathway all display a rod-like lethal phenotype associated with excretory

system failure (Ferguson and Horvitz, 1985; Sundaram, 2006). We examined mutants for *lin-3/EGF* and *lin-1/Ets*, which lie at the beginning and end of this pathway, respectively (Beitel et al., 1995b; Hill and Sternberg, 1992). *lin-3(lf)* and *lin-1(gf)* mutants appear similar to *let-60(lf)* mutants, and *lin-3* overexpression and *lin-1(lf)* mutants appear similar to *let-60(gf)* mutants (Fig. 2.2E-H,K-L). Furthermore, a variety of other Ras pathway mutants examined (including hypomorphic alleles of *let-23/EGFR* and *lin-45/Raf*) also show evidence of duct-to-pore fate transformations (Fig. 2.2K-L). Finally, *eor-1* and *sur-2* are nuclear factors that act redundantly downstream of MPK-1/ERK (Howard and Sundaram, 2002); *eor-1* also appears to act redundantly with a cryptic positive function of *lin-1*/Ets (Howard and Sundaram, 2002). We found that *eor-1; sur-2(RNAi)* and *lin-1 eor-1* double mutants frequently have two pore-like cells (Fig. 2.2I-L). These data are consistent with the entire canonical pathway promoting duct vs. G1 pore identity.

During this analysis, we noted that some mutants with reduced signaling had paradoxical "0 G1"-like junction patterns, without concomitant duct fate duplication, or had excretory failure despite apparently normal junction patterns and fates (Fig. 2.2K-L). These observations suggested that Ras signaling plays roles beyond cell fate specification (see below).

The excretory canal cell expresses *lin-3*/EGF

Since the mutant analyses above suggest that signaling by LIN-3/EGF through LET-23/EGFR is responsible for LET-60/Ras activation in the duct, we asked where

these proteins are expressed. Consistent with the fact that both cells can respond to LIN-3 to adopt the duct fate, a functional LET-23::GFP reporter, *gaIs27* (Simske et al., 1996), is expressed in both presumptive duct and G1 pore cells during ventral enclosure (Fig. 3A). To examine *lin-3* expression, we used a *lin-3* promoter::GFP reporter (*syIs107*) that contains ~2.5 kb of upstream regulatory sequence as well as the first *lin-3* intron (Hwang and Sternberg, 2004). Most notably, *lin-3p*::GFP is strongly expressed in the excretory canal cell, beginning soon after canal cell birth and continuing into early larval development (Fig. 2.3B, D). *lin-3p*::GFP is also expressed in a variety of other cells that are further away from the presumptive duct and G1 pore. These data suggested that the canal cell might be a relevant source of the duct-inducing signal, a model that fits with the observation that the left member of the equivalence group, which is closest to the canal cell, is the cell that normally adopts the duct fate.

Ras signaling promotes cell stacking and a canal cell-proximal position

EGF-Ras signaling could promote duct vs. G1 pore cell fate specification independently of cell stacking and tubulogenesis, or signaling could also control initial cell positioning. The latter possibility was suggested by results of a prior mosaic analysis, in which a *let-60(+)* presumptive G1 cell could outcompete a *let-60(-)* presumptive duct cell for the more dorsal, canal cell-proximal position and take on the duct fate (Yochem et al., 1997).

Consistent with a model in which both cells compete for the canal cell-proximal position, animals homozygous for a partial loss-of-function allele, *let-60(n2021),* display a variable phenotype in which the presumptive duct and G1 cells often adopt adjacent positions rather than stacking on top of each other (Fig. 2.4C-D). In many of these cases, a single duct-like cell reaches from the ventral epidermis to the canal cell, while the second cell is mispositioned to the side and appears non-tubular, giving a "1 duct, 0 G1" phenotype (Fig. 2.4G-H). In other cases, a single pore-like (un-induced) cell reaches from the ventral epidermis to the canal cell, giving a "0 duct, 1 G1" phenotype (Fig. 2.4I-J). Similar defects are seen in other hypomorphic mutants and in *lin-1; eor-1* double mutants (Fig. 2.2K and data not shown). We conclude that Ras signaling influences duct and G1 pore stacking.

Notably, the adjacent phenotype is observed only occasionally in *let-60* or *lin-3* null mutants obtained from heterozygous mothers (Fig. 2.2K, Fig. 2.4K). This is due in part to maternal rescue, since most *let-60(n2021rf)* mutants obtained from heterozygous mothers also have normal cell stacking, in contrast to those obtained from homozygous mutant mothers (Fig. 2.4K). Nevertheless, progeny from *let-60(sy101sy127lf)/let-60(n2021rf)* mothers have a lower frequency of adjacent cells than those from *let-60(n2021rf)* mothers (Fig. 2.4K). Therefore, the adjacent phenotype may reflect problems in resolving cell competition under circumstances where Ras signaling is sub-optimal but not absent (see Discussion).

The canal cell is required for stacking and tubulogenesis of the duct and G1 pore

To test if LIN-3/EGF expression by the canal cell is required for duct fate specification or cell stacking, we first removed the canal cell (or its mother) physically by laser ablation. In the absence of the canal cell, most animals still had a *lin-48p::GFP*+ cell (Table 1), indicating that other sources of LIN-3 are sufficient to induce at least some features of duct identity. However, duct morphology was abnormal and the G1 pore autocellular junction was missing (Fig. 2.5L-M), suggesting that stacking had been disrupted.

We next examined the effects of removing the canal cell genetically using Notch mutants. Mutants lacking both *C. elegans* Notch receptors, LIN-12 and GLP-1, the DSL ligand LAG-2 or the CSL transcription factor LAG-1 have a constellation of defects referred to as the "Lag" (*lin-12* and *glp-1*) phenotype (Lambie and Kimble, 1991a). *lag* mutants lack an excretory canal cell due to a lineage transformation affecting the canal cell's great-grandmother ABplpapp (Lambie and Kimble, 1991a; Moskowitz and Rothman, 1996). As in canal cell-ablated animals, *lag* mutants often possess a morphologically abnormal *lin-48p::GFP*+ cell, and lack a G1 pore autocellular junction (Table 2.1, Fig. 2.5). A ventral perspective revealed that the presumptive duct and G1 pore cells adopt adjacent ventral positions in the epidermis (Fig. 2.5B,C). Thus *lag* mutants resemble *let-60/Ras* partial loss-of-function mutants.

Several lines of evidence suggest that the *lag* duct and G1 pore stacking defects are a secondary consequence of canal cell absence. First, canal cell ablation in wild-type

embryos can phenocopy *lag* mutants. Second, a functional LIN-12::GFP reporter *(arIs41)* is not detectably expressed in the duct or G1 pore progenitors during ventral enclosure (Fig. 2.3E), nor is a LIN-12- and GLP-1-responsive reporter, *ref-1p*::GFP (data not shown); thus Notch signaling is unlikely to impact directly on duct and G1 pore fate specification or tubulogenesis. Third, *lin-12* hypermorphic mutants, which have a single canal cell, have normal duct and G1 pore morphology (Table 2.1, Fig. 2.5M). Finally, examination of *lin-12* null mutants or *lag-2(q420)* hypomorphic mutants, in which absence of the canal cell is variable, revealed a strong correlation between absence of the canal cell and failure of the duct and G1 pore to stack and undergo tubulogenesis (Fig. 2.5 D-E,G-H,M).

Together, the ablation and Notch mutant data support a model in which the canal cell facilitates duct and G1 pore stacking and tubulogenesis. The canal cell likely provides physical support to the duct and G1 pore as it adheres to the duct during these processes. Stacking and tubulogenesis appear independent of canal cell-expressed *lin-3/EGF*, since these processes are intact in *lin-3* zygotic null mutants, despite defects in cell fate specification (Fig. 2.2K-L). Duct fate specification also appears partially independent of canal cell-expressed *lin-3*/EGF, stacking and tubulogenesis, since it is only mildly affected by canal cell absence (Table 2.1). Nevertheless, since the canal cell does express *lin-3*/EGF, and partial reduction of *let-60*/Ras can mimic canal cell absence, localized LIN-3/EGF expression by the canal cell may help orient relative duct and G1 pore positions during stacking and bias which cell ultimately adopts the duct fate (see Discussion).

Continued signaling through SOS-1 and Ras is required for duct differentiation

To determine if there was a role for EGF-Ras signaling in the duct cell after the duct cell had been specified and adopted a canal proximal position, we tested the temporal requirement for EGF-Ras signaling with a *sos-1* temperature sensitive mutant. The *cs41* lesion of *sos-1* affects the CDC25-related Ras GEF domain of SOS-1, rendering SOS-1 unable to exchange GTP on Ras and lead to its activation (Rocheleau et al., 2002). When *sos-1(cs41)* worms were grown at the standard growing temperature for *C.elegans* which is 20°C, the mutants appeared essentially wild-type (Rocheleau et al., 2002)(Fig 2.6A). However when *sos-1(cs41)* worms were raised at 25°C they all arrested with excretory system abnormalities (Rocheleau et al., 2002) (Fig 2.6A). Importantly, the lethal excretory system abnormalities of *sos-1(cs41)* were almost completely rescued by hyper-activating the EGF-Ras pathway with a *let-60(n1046)* gain-of-function mutant (Rocheleau et al., 2002) or a hypomorphic allele of the Ras downstream effector gene *lin-1* (Fig 2.6A). The suppression of *sos-1(cs41)* lethal defects by *let-60(n1046 gf)* and *lin-1(e1275)* indicated that the lethal abnormalities were caused by a failure in Ras-ERK mediated signaling. Since *let-60 ras* is required only in the duct cell (and not in the G1 or G2 pore or canal cell) for proper excretory function and viability (Yochem et al., 1997), we further infer that any excretory abnormalities of *sos-1(ts)* animals reflect requirements for Ras-ERK signaling in the developing duct cell.

When *sos-1(ts)* mutants were shifted from the permissive temperature and raised to the non-permissive temperature early in development before the 1.5-fold stage of embryogenesis, most worms failed to express the *lin-48p::GFP* duct fate marker (Fig 2.6B). Consistent with this result, *sos-1(ts)* worms shifted prior to the 1.5-fold stage of embryogenesis also failed to undergo auto-fusion of the duct cell, resulting in two pore-like cells with autocellular junctions (AJs) (Fig 2.6C). Thus early upshifs of *sos-1(ts)* mutants recapitulated the *let-60/Ras* zygotic null phenotype of a duct-to-pore fate transformation (Fig 2.2). *sos-1(ts)* mutants upshifted after the 1.5-fold stage of embryogenesis expressed *lin-48p*::GFP and auto-fused the duct cell, suggesting that these two aspects of duct fate specification have been completed by the 1.5-fold stage of embryogenesis (Fig 2.6B,C). In addition, the earliest maternal upshifts could occasionally generate adjacent cells (data not shown), as seen in *let-60*(*n2021*) hypomorphs (Fig 2.4), which further supports a role for EGF-Ras signaling in cell stacking.

When *sos-1(ts)* mutants were shifted from the non-permissive temperature and lowered back to the permissive temperature, most animals were normal for excretory morphology, as long as they were shifted before the bean stage of embryogenesis (Fig. 2.6C). When *sos-1(ts)* mutants were downshifted after the bean stage of embryogenesis, an increasing proportion of larvae displayed defects in duct auto-fusion (Fig 2.6C). However, these defects in duct auto-fusion were observed less frequently than in the un-shifted control worms (Fig 2.6C), demonstrating that restoring SOS-1 activity late can still promote at least one aspect of duct identity. These results are consistent with the model that Ras signaling and cell fate specification occur around the 1.5-fold stage of

embryogenesis as the presumptive duct and G1 pore cells approach the canal cell and undergo tubulogenesis.

Unexpectedly, the *sos-1*(*ts*) temperature-sensitive period for lethal excretory defects extended from the bean stage into the L1 larval stage (Fig. 2.6D). *sos-1(ts)* mutants upshifted from the permissive to the restrictive temperature displayed excretory lethality until the first larval stage (Fig 2.6D). The ~50% lethality of *sos-1(ts)* mutants shifted at the L2 stage of larval development was not due to excretory related lethality, but rather these worms died with a scrawny phenotype characteristic of *egl-15*/FGFR mutants (DeVore et al., 1995; Roubin et al., 1999). SOS-1 is also downstream of the FGF receptor in *C.elegans*, however only EGF signaling promotes duct development and not FGF signaling. We also verified that the *sos-1(ts)* mutants that died from the FGF related scrawny phenotype had a normal duct cell (data not shown). *sos-1(ts)* mutants downshifted from the restrictive to the permissive temperature displayed excretory lethality beginning around the bean stage (Fig 2.6D). Together, the upshift and downshift data demonstrate that the temperature senstive period (TSP) of SOS-1 and the critical window of Ras signaling extends from the bean stage to the L1 stage of development.

We next visualized the excretory system with AJM-1::GFP and *lin-48p*::GFP in *sos-1(ts)* mutants that died during late upshifts. At least 70% of animals upshifted at the 1.5-fold, twofold, threefold or early L1 stages (n>20 each) accumulated fluid either within the excretory tubules or near the canal-duct junction, despite an initially normal junction and *lin-48p*::GFP marker pattern (Fig 2.6E,F). Therefore the duct cell can express a terminal fate marker and fuse its auto-junction, but when SOS-1 and Ras

signaling are subsequently reduced, fluid can still escape from the excretory system leading to defects in organ architecture.

A cell that fails to establish duct identity early is generally incapable of supporting proper excretory function even when *sos-1* activity is restored at later time-points. However, even when early markers of duct identity are properly established, continued signaling is required to execute and/or maintain the duct fate. Although additional studies including transmission electron microscopy might be needed to understand the cellular basis of these later defects, we conclude that SOS-1 and Ras, and most likely the entire EGF-Ras-ERK pathway, play additional roles in duct morphogenesis and differentiation.

G1 pore withdrawal can still occur in the absence of G2

When the G1 pore withdraws from the excretory system during L1, a neighboring epidermal cell, G2, moves in to replace it as the pore (Stone et al., 2009; Sulston et al., 1983) (Fig. 2.1J; Fig. 2.7A-C,M). By examining Ras and Notch pathway mutants, we were able to address a basic question about the G1-G2 remodeling event: is communication between G1 and G2 important to trigger G1's withdrawal and/or G2's entry into the excretory system?

As described above, *let-60(n1046gf)* mutants invariably lack a G1 pore and have a binucleate duct cell attached directly to the ventral epidermis. In 16% (11/67) of such mutants, G2 still moves in and gives rise to a morphologically normal larval pore cell; in

the remainder, G2 (or G2p) wraps around the base of the duct but does not form a pore of normal height (Fig. 2.7 D-F,M). Thus, G2 entry does not require a "come here" signal from the G1 pore, but its morphogenesis and ability to insert between the duct and epidermis may be facilitated by the act of G1 withdrawal.

To test the requirements for G2, we used *lin-12*/Notch single mutants, which affect the G2 vs. W neuroblast cell fates (Greenwald et al., 1983). *lin-12(d)* hypermorphic mutants have two G2 cells, and one of these forms a normal larval pore while the other wraps around its ventral base (Fig. 2.7J-L,M). Conversely, *lin-12(0)* loss-of-function mutants lack a G2 cell. In such mutants, G1 still withdraws from the excretory system during mid-L1, and the duct then attaches directly to the ventral epidermis (Fig. 2.7G-I,M). Thus, G1 withdrawal does not require a "go away" signal from G2.

DISCUSSION

We've shown that Notch signaling and Ras signaling function sequentially to control tube development in the *C. elegans* excretory system. Notch signaling is required to generate the canal cell, which is a central organizer of duct and G1 pore development, serving both as a source of LIN-3/EGF ligand (which contributes to Ras activation) and as a physical attachment site for the duct (which is important for cell stacking and tubulogenesis). Ras signaling influences cell positions, specifies duct vs. G1 pore identity, and promotes subsequent aspects of duct morphogenesis and differentiation. Below we propose a model for duct and G1 pore development and discuss similarities and

differences between development of the excretory system and development of more complex tube networks.

A biased competition model for excretory duct vs. G1 pore fate specification

All excretory tubes are examples of left-right asymmetries in what is a mostly bilaterally symmetric embryo (Pohl and Bao, 2010; Sulston et al., 1983). Notch signaling on the left side of the embryo is required for the earliest of these asymmetries, generation of the excretory canal cell (Lambie and Kimble, 1991a; Moskowitz and Rothman, 1996). We propose that Notch-dependent asymmetry of the canal cell leads to the Ras-dependent asymmetry of the excretory duct and G1 pore.

According to this biased competition model, the presumptive duct and G1 pore cells are initially equivalent. As these cells migrate toward the canal cell during ventral enclosure, the left cell has an advantage due to the left-biased asymmetric position of the canal cell; this bias may be strengthened by the presence of cells on the right side whose left relatives undergo cell death. The left cell therefore reaches and adheres to the canal cell first, and also receives earlier or quantitatively more LIN-3/EGF signal. LIN-3/EGF signaling stimulates LET-60/Ras to promote duct identity and strengthen adhesion with the canal cell. Signaling may also trigger production of an unknown lateral inhibitory signal that prevents the presumptive G1 from also responding to LIN-3/EGF. Steric hindrance or differences in relative Ras vs. inhibitory signaling levels cause the presumptive G1 to take a more ventral position. Polarization and initial tubulogenesis

appear independent of Ras signaling; however, after both cells wrap up into tube shapes, continued LIN-3/EGF signaling from the canal cell (and elsewhere) promotes duct vs. G1 pore identity and later aspects of duct morphogenesis and differentiation into a functional tube.

Two aspects of this model can explain the stacking defects of *let-60*/Ras hypomorphs, in which depletion of both maternal and zygotic *let-60/Ras* compromises (but does not eliminate) the earliest steps of signaling. First, the presumptive duct, upon reaching the canal cell, may not adhere to it strongly. Second, the presumptive duct may not express the proposed inhibitory signal in a timely manner. Under conditions where Ras signaling is reduced but not absent, this would allow the presumptive G1 pore to respond to LIN-3/EGF and compete for a canal-cell proximal position. Failure of either cell to adhere to the canal cell (as in *lin-12 glp-1*/Notch mutants), or failure to resolve competition between the two cells such that both adhere, could lead to the observed adjacent positions.

Lateral inhibition is a central feature of RTK-mediated branching morphogenesis in several tubular organs (Chi et al., 2009; Ghabrial and Krasnow, 2006) and lateral inhibition of Ras-dependent processes is frequently mediated by Notch signaling (Chen and Greenwald, 2004; Sundaram, 2005). However, we find no evidence that Notch signaling directly influences excretory duct vs. G1 pore cell fates. Differences in cell adhesion and steric hindrance may be sufficient to explain the stacking process, but they are unlikely to explain how only a single duct-like (*lin-48p*::GFP+) cell is specified from

the two adjacent precursors in a *lin-12 glp-1*/Notch mutant (Table 2.1). Therefore, an unknown signaling pathway may be used to mediate lateral inhibition of the duct fate.

Downstream consequences of EGF-Ras-ERK signaling in the excretory duct

In addition to influencing cell positions, EGF-Ras-ERK signaling is both necessary and sufficient for several aspects of duct vs. G1 pore identity, including duct-specific patterns of gene expression, auto-fusion, and a permanent epithelial identity. This latter difference in duct epithelial permanence vs. G1 withdrawal may ultimately explain the lethality of the duct-to-G1 pore fate change in *let-60 ras* null mutants. G1 withdrawal does not depend on cues from the replacement cell G2, but instead appears to be an intrinsically programmed characteristic of the duct and G1 progenitors that is repressed by Ras signaling. Ras may inhibit withdrawal in part by stimulating *aff-1*-dependent auto-fusion to permanently remove the duct autocellular junction and prevent its later unwrapping; however, Ras must have additional effects since the duct cell still remains permanent in most *aff-1* mutants despite a failure of auto-fusion (Stone et al., 2009).

sos-1(ts) temperature-shift experiments suggest that Ras signaling continues to be required after initial fate specification for development of a fully functional duct tube. After its auto-fusion to form a toroid, the duct elongates, changes shape, and elaborates a complex lumen (Stone et al., 2009). The junctions between the duct and its neighboring tubes must be maintained and may undergo further maturation to establish barrier functions and prevent excretory fluid leakage. Finally, the duct-pore junction must be

remodeled as G1 withdraws and G2 enters. The continued requirement for *sos-1* as these events are occurring suggests that Ras signaling may directly promote such morphogenetic and differentiation processes.

Most or all of the responses to Ras signaling in the excretory duct appear to be transcriptionally-mediated. *sos-1(ts)* defects can be rescued by loss of the LIN-1/Ets transcription factor, which is regulated by MPK-1 ERK phosphorylation (Jacobs et al., 1998) and acts as a repressor of the duct fate. *sos-1(ts)* defects also can be mimicked by combinatorial loss of LIN-1 and another downstream transcription factor, EOR-1 (a BTB-zinc finger protein) (Howard and Sundaram, 2002; Howell et al., 2010), revealing a second (but redundant) activity of LIN-1/Ets in promoting the duct fate. A challenge for future work will be to connect these transcriptional effectors to downstream targets that control the various cell biological processes of duct auto-fusion, morphogenesis, and epithelial maintenance.

Similarities and differences between the excretory system and more complex tube networks

C. elegans excretory tubes are topologically quite different from epithelial tubes in other renal systems in that they are each only one cell in diameter. However, similar unicellular tubes have been described in other organ systems, including the Drosophila trachea (Ghabrial et al., 2003) and the mammalian microvasculature (Bar et al., 1984).

Furthermore, in vitro studies suggest that unicellular tubes may be developmental precursors to some larger bore tubes in the vasculature (Iruela-Arispe and Davis, 2009).

Despite their topological differences, *C. elegans* excretory tubes and larger multicellular tubes must undergo many similar cell biological processes. For example, initially unpolarized cells must transition to an epithelial state, define an appropriate apical domain, form new junctions, and build a lumen; the difference is that excretory tubes define an intracellular rather than an extracellular lumen. Furthermore, distinct tube types must join to form a continuous conduit. The maturing tubes must be structurally strong to withstand internal pressure from their contents, yet flexible enough to elongate and grow as organismal size or physiological demands increase. Finally, some epithelial tube cells, like the G1 pore, retain the developmental potential to adopt different fates (Jarriault et al., 2008; Kalluri and Weinberg, 2009; Mani et al., 2008; Red-Horse et al., 2010; Weaver and Krasnow, 2008). Given the simplicity of the *C. elegans* excretory system and its amenability to genetic manipulations, further studies in this system should give insights into basic cellular mechanisms involved in these common steps of tubular organ development.

MATERIALS AND METHODS

Strains and alleles

N2 var. Bristol was the wild-type strain. Unless otherwise indicated, all strains were grown at 20˚C under standard conditions (Brenner, 1974) and all mutant alleles are

described in (Riddle et al., 1997). *I: lag-1(q385), lag-2(q411), lag-2(q420). II: let-23(sy97). III: lin-12(n137), lin-12(n137n720), lin-12 (n941), glp-1(q46), glp-1(q231). IV: eor-1(cs28)* (Rocheleau et al., 2002), *let-60(sy101sy127), let-60(n1046), let-60(n2021), lin-1(e1275), lin-1(n304)* (Beitel et al., 1995b), *lin-1(n1761)* (Jacobs et al., 1998), *lin-3(n1059), lin-45(n2018). V: sos-1(cs41)* (Rocheleau et al., 2002). *X: lin-15(n765), sem-5(n2019).* Transgenes used are: *arIs12 (lin-12 intra)* (Struhl et al., 1993), *arIs41* (LIN-12::GFP) (Levitan and Greenwald, 1998), *gaIs27* (LET-23::GFP) (Simske et al., 1996), *jcIs1* (AJM-1::GFP) (Koppen et al., 2001b), *saIs14* (*lin-48p*::GFP) (Johnson et al., 2001), *syIs107* (*lin-3p*::GFP) (Hwang and Sternberg, 2004), *wIs78* (AJM-1::GFP) (Koh and Rothman, 2001), *xnIs17* (DLG-1::GFP) (Totong et al., 2007), *vha-1p*::GFP (Oka et al., 1997), *zuIs143* (*ref-1p*::GFP) (Neves and Priess, 2005). *qnEx59 (dct-5p*::mcherry) was provided by Julia and David Raizen and contains 845 bp of the *dct-5* 5' region. *csIs55* (GFP::MLS-2) was generated from a pYJ59-containing array (Jiang et al., 2005) by gamma-irradiation-induced integration. *csEx146* (*lin-48p*::mcherry) contains 4.8 kb of the *lin-48* 5' region and mcherry in vector pPD49.26 (Fire et al., 1990). *lin-3* overexpression was achieved with an integrated *lin-3p*::LIN-3::GFP transgene provided by Min Han.

Marker Analysis and Imaging

Images were captured by differential interference contrast (DIC) and epi-fluorescence microscopy using a Zeiss Axioskop and Hamamatsu C5985 camera, or by confocal

microscopy using a Leica SP5. Images were processed for brightness and contrast using Photoshop or ImageJ. Some AJM-1::GFP images were inverted for clarity.

For electron microscopy, embryos were mounted on an agarose pad and observed under light microscopy to identify timepoints for fixation. A laser was used to place 3-4 holes in the eggshell, allowing the embryo to be aldehyde fixed while on the pad (see more details at www.wormatlas.org/laserhole.htm). The fixed embryo was postfixed with osmium tetroxide, potassium ferrocyanide, and tannic acid, and then post-stained with uranyl acetate before embedding in plastic resin. Transverse serial thin sections were collected on slot grids and photographed on a Philips CM10 electron microscope. The G1 and duct cells were identified within a series of 600 serial thin sections on the basis of their positions relative to the canal cell and to the G2 and W epidermal cells (Fig. S1) and by comparison to known nuclear positions in time-lapse confocal movies.

To visualize the duct and pore progenitor migration paths and timing, we generated 3D confocal movies of strains UP2051 (pie-1::mCherry::HIS-58::pie-1utr; his-72pro::HIS-24::mCherry::let-858utr; GFP::MLS-2) and RW10890 (pie-1::mCherry::HIS-58::pie-1utr; his-72pro::HIS-24::mCherry::let-858utr; PAL-1::GFP) as previously described (Murray et al., 2006) on a Leica TCS SP5 resonance-scanning confocal microscope with 0.5 micron z slice spacing and 1.5 minute time point spacing. Temperature was 22.5˚C. We used a hybrid blob-slice model and StarryNite (Bao et al., 2006; Santella et al., 2010) for automated lineage tracing and curated the duct, pore and canal lineages (ABplpaa and ABprpaa) through ventral enclosure (approx. 275 minutes) with AceTree (Boyle et al., 2006).

Ablations

Laser ablations were performed with a Micropoint Laser Ablation system (Photonic Instruments, St. Charles, IL) mounted to a Leica DM5500B or Zeiss Axiophot microscope. The canal cell mother (ABplpappaa) was identified using *zuIs143* (*ref-1p*::GFP) (Neves and Priess, 2005). Successful ablation was confirmed by the absence of the canal cell as assessed by DIC and either *vha-1p*::GFP or AJM-1::GFP patterns.

Immunostaining

Embryos were permeabilized by freeze-cracking and fixed in methanol as described (Duerr et al., 1999) and incubated with primary antibodies overnight at 4°C and with secondary antibodies for 2hrs at room temperature. The following antibodies were used: preadsorbed rat anti-MLS-2 (CUMCR6; 1:400) (Jiang et al., 2005) goat polyclonal anti-GFP (Rockland; 1:50), rabbit polyclonal anti-DLG-1 (1:50 to 1:100) (Segbert et al., 2004). All secondary antibodies were from Jackson ImmunoResearch Laboratories and were used at a dilution of 1:50 to 1:200.

Temperature Shifts

For upshifts, *sos-1(ts)* mutants were shifted from 20°C to 25°C at the stage indicated. For downshifts, *sos-1(ts)* L4 larvae were placed at 25°C and their progeny were shifted to

20°C at the stage indicated. We staged embryos by number of hours after egg-lay (see Table 2.2). Marker expression was scored at 3-fold or early L1. Worms that failed to reach the L4 stage within 4 days after shift were scored as lethal.

Acknowledgements

All of the data presented in this chapter was published with great collaboration from Vincent P. Mancuso, John I. Murray, Katherine Palozola, Carolyn Norris, David H. Hall, Kelly Howell, Kai Huang and Meera V. Sundaram (individual contributions are mentioned under corresponding figure legends). I am thankful to Stuart Kim for generously providing the LET-23::GFP translational reporter *gaIs27*. I am also thankful to Jun Liu for generously providing us with the MLS-2::GFP translational reporter. I am thankful to Meera Sundaram for great assistance in preparing the manuscript. I would also like to thank Matthew Buechner, Helen Chamberlin, Iva Greenwald, Min Han, Jeff Hardin, Jim Priess, David Raizen, Paul Sternberg and the Caenorhabditis Genetics Center (University of Minnesota, USA) for providing strains; Craig Stone and Helin Shiah for generating reporters; and Iva Greenwald and John Yochem for helpful discussion and comments on the manuscript. The Transmission Electron Microscopy of embryo morphogenesis was originally carried out in collaboration with Ed Hedgecock.

Figure Legends

Figure 2.1. Timeline of excretory system development. (A) Schematics of excretory canal cell (red, ABplpappaap), duct (yellow, ABplpaaaapa), G1(blue, ABprpaaaapa), G2 (green, ABplapaapa) and W (green, ABprapaapa) at different developmental stages, based on (Sulston et al., 1983), prior electron microscopy (Stone et al., 2009) and this work. Dark black lines, apical junctions; dotted line, duct auto-fusion; arrow, pore autocellular junction; arrowhead, duct-canal cell intercellular junction; bracket, duct cell body. Not shown are the non-essential excretory gland cells, which also connect to the duct-canal junction (Nelson et al., 1983; Nelson and Riddle, 1984). (B-E) Progressively older ventral enclosure stage embryos. (B-C,E) Ventral views. GFP::MLS-2 marks the presumptive duct and G1 pore nuclei. DLG-1::GFP marks epidermal cell junctions in B and E, which are confocal projections. (B) The presumptive duct and G1 initially lack junctions. (C) The presumptive duct is closer to the canal cell than is the presumptive G1. (D) TEM of a wild-type embryo at a similar stage to C, with cells pseudo-colored as in A. Transverse anterior view. The presumptive duct and G1 have met at the ventral midline. The duct makes extensive contact with the canal cell, while G1 is excluded. No epithelial junctions or lumen are detectable. (E) G1 moves ventrally. The asterisk indicates the site of future G1 pore opening between G2 and W epidermal cells. (F-L) Left lateral views. (F) 1.5-fold stage embryo immunostained for DLG-1, showing newly formed autocellular junctions (inset) just before duct auto-fusion. (G-K) L1 larvae. The box in G indicates the region magnified in H. AJM-1::GFP marks junctions. The duct no longer has an autocellular junction. (I) *lin-48p*::mcherry marks the duct. (J) *dct-5p*::mcherry marks the duct and G1 pore in early L1 and (K) the duct and G1 in late L1 after G1 withdrawal and G2 entry. (L) Adult canal cell marked with *vha-1p*::GFP. Note that the canal cell

elongates extensively. David Hall and Carolyn Norris generated analyzed the transmission electron microscopy images of the immature excretory system, and Meera Sundaram did most of the analysis. John I. Murray did the lineage analysis of the GFP::MLS-2 strain.

Figure 2.2. *let-60/Ras* promotes the duct versus G1 pore fate. (A-J) AJM-1::GFP (left column) and *lin-48p*::GFP or (C') *dct-5p*::mCherry (middle column) expression in L1 larvae of the indicated genotypes. Lateral views, with schematic interpretations (right column) and symbols as in Fig. 1. Colors represent lineal identity, not fate. Mutants with reduced signaling usually have two pore-like cells with autocellular junctions, but as fluid (carat) accumulates during L1 (C), large junctional rings (asterisk) are common. In (C'), white arrows indicate two stacked pore-like cells. Mutants with increased signaling have a seamless binucleate duct that connects to the ventral epidermis. (K-L) Quantification of marker phenotypes. Note that some mutants with '0 G1' have defects in cell stacking and tubulogenesis rather than in cell fate specification (see Fig. 4). Scale bar: 2μm. . Kai Huang, Katherine Palozola, Kelly Howell, and Meera Sundaram built and analyzed several of the strains.

Figure 2.3. *lin-3*/EGF, *let-23*/EGFR and *lin-12*/Notch reporter expression in the excretory system. (A-C) LET-23::GFP is expressed in the presumptive duct and G1 pore at ventral enclosure (A) and in the duct (bracket) at 3-fold (C). (B-D) *lin-3p*::GFP is expressed in the canal cell from ventral enclosure (B) through L1 (D). (E) LIN-12::GFP is expressed in the presumptive G2 and W but not in the presumptive duct or pore at

ventral enclosure. In A, C and E, embryos were co-stained with anti- GFP and either anti-MLS-2 or anti-DLG-1 to mark the duct and G1 pore (*n*>10 each). Scale bars: 5µm. John I. Murray did the lineage analysis of the GFP::MLS-2 strain.

Figure 2.4. *let-60/Ras* hypomorphs reveal defects in cell competition and stacking. (A,B,E,F) Wild-type. (C,D,G-J) *let-60*(*n2021rf*). (A,C)AJM-1::GFP in threefold embryos, ventral view. Lines indicate ventral junctions between the presumptive G1 or duct and the epidermis. (E,G,I,K) AJM-1::GFP and *dct-5p*::mCherry in early L1s, lateral view. Asterisks indicate ventral cells with neither duct-like nor pore-like morphology. In *let-60*(*n2021rf*) mutants, the presumptive duct and G1 adopt adjacent positions in the epidermis (C,D) and one cell usually reaches from the ventral epidermis to the canal cell (G-J). The lineal identity of this cell is unknown and may be variable. (K) Quantification of adjacent defects in early L1 larvae from heterozygous versus homozygous mutant mothers. Animals with no G1 pore autocellular junction or with a single autocellular junction that stretched from the ventral epidermis to the canal junction were scored as 'adjacent'. Meera Sundaram built these strains and did some of the analysis.

Figure 2.5. The canal cell is required for duct and G1 pore stacking and tubulogenesis. (A-I,L) AJM-1::GFP. D,G,H also contain *lin-48p*::GFP. (J,K) Schematic diagrams. (A-C)Early threefold embryos, ventral view. (D-F) Early L1s, ventral view. (G-L) Early L1s, lateral view. In wild-type (A), the G1 pore contacts G2 and W in the ventral epidermis. In *lag-1*(*RNAi*) (B) or *lin-12*(*n941*) *glp-1*(*q46*) double mutants (C,F,I), the presumptive duct and G1 pore (lines) both contact the epidermis and lack autocellular junctions. In *lag-2*(*q420rf*) mutants (D,E,G,H), the presence of a canal cell (D,G)

correlates with normal duct and G1 pore morphology. *aff-1*(*tm2214*) (E) has no impact on the *lag-2*(*q420rf*) phenotype. (L) Ablation of the canal cell mother eliminates the G1 pore autocellular junction. (M) Quantification of junction phenotypes in early L1 larvae. Animals with no G1 pore autocellular junction were scored as 'adjacent'. Scale bar: 2µm. Vincent Mancuso performed the studies with the Notch mutants and performed the canal cell ablations. Meera Sundaram also scored Notch mutants.

Figure 2.6. *sos-1* temperature shift experiments reveal continued requirements during duct morphogenesis and differentiation.

(A) *sos-1*(*cs41ts*) lethality at 25°C is rescued by *let-60*(*n1046gf*) or *lin-1*(*e1275lf*). $n>50$ for each genotype. (B,C)*sos-1*(*ts*) animals bearing AJM-1::GFP or *lin-48p*::GFP markers were upshifted or downshifted at the stages indicated. $n\geq20$ for each time point. *sos-1* is required before the 1.5-fold stage to promote *lin-48p*::GFP duct marker expression (B) or duct auto-fusion (C). (D)The *sos-1*(*ts*) temperature-sensitive period (TSP) for lethality extends from the bean stage of embryogenesis to L2. The majority of animals upshifted before L2 arrested with excretory abnormalities (see C,E,F). Animals upshifted during L2 displayed a scrawny phenotype similar to that reported for *egl-15*/FGFR mutants (DeVore et al., 1995; Roubin et al., 1999). (E-F) Fluid (carats) accumulated in or near the duct in threefold upshifted *sos-1*(*ts*) animals (E',F'), while AJM-1::GFP (E) and *lin-48p*::GFP (F) patterns were unaffected in these same animals. Scale bar: 2µm.

Figure 2.7. G1 withdrawal and G2 entry can occur independently.

AJM-1::GFP in L4 larvae. (A,D,G,J) lateral views. (B,E,H,K) ventral views. (C,F,I,L) Schematic diagrams. (A-C)In wild type, G2p forms the pore. (D-F)In *let-60*(*n1046gf*) mutants, G2p usually wraps around the base of the duct. (G-I) In *lin-12*(*n941lf*) mutants, the duct attaches directly to the ventral epidermis after G1 withdrawal. (J-L) In *lin-12*(*n137gf*) mutants, the extra G2p cell wraps around the ventral base of the pore. Lines indicate ventral junctions with the epidermis. (M) Quantification of junction phenotypes. Scale bar: 2µm. Meera Sundaram performed all of these experiments.

Table 2.1. Physical or genetic removal of the canal reduces but does not prevent duct fate specification. Presence of the canal cell or duct cell was assessed based on *vha-1p*::GFP or *lin-48p*::GFP reporter expression, respectively. + or – indicate that presence of canal cell as assessed based on nuclear morphology or AJM-1::GFP. †*m*+*z*– indicates that larvae were obtained from heterozygous *hT2[qIs48]* balancer mothers. For canal cell parent ablation, strain contained *ref-1p*::GFP to aid in target identification. lf, loss-of-function; rf, reduced function; gf, gain-of-function. Vincent Mancuso and Meera Sundaram performed all of these experiments.

Table 2.2. Staging of *sos-1 ts* shifted worms. Worms were shifted at the various time points (hours after egg lay). Developmental stage of worms was confirmed by scoring the worms on a dissecting microscope.

Figure 2.1

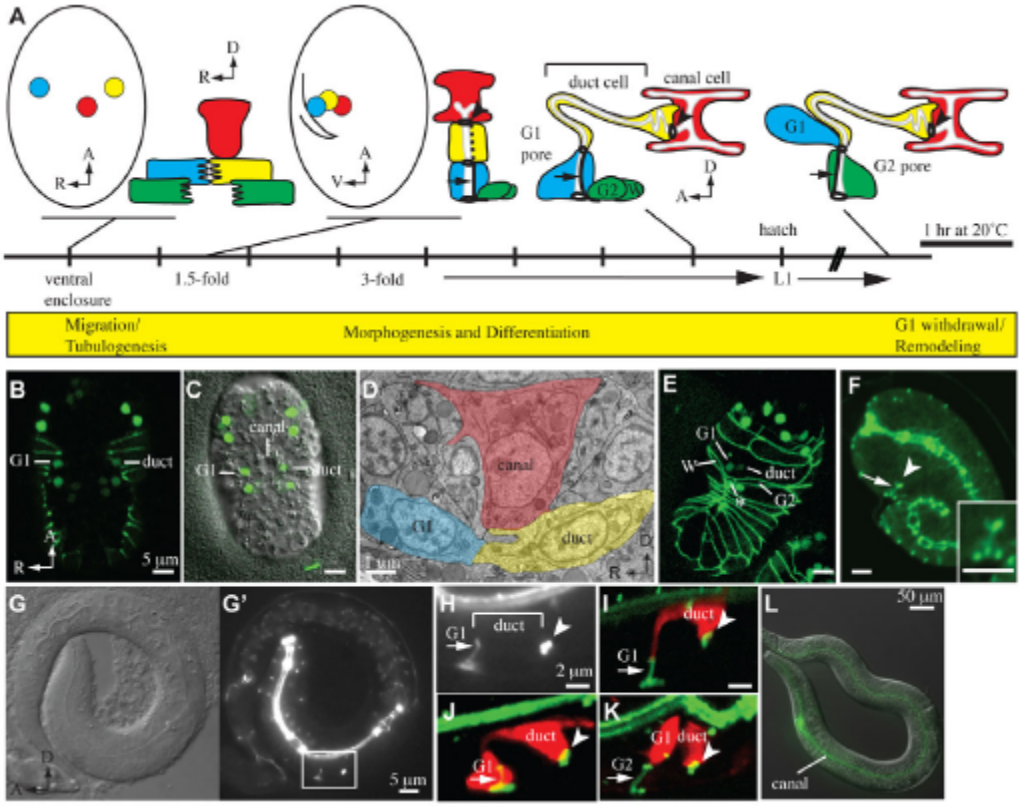
A
duct cell
canal cell
G1 pore
G2 pore
hatch
1 hr at 20°C
ventral enclosure
1.5-fold
3-fold
L1
Migration/ Tubulogenesis
Morphogenesis and Differentiation
G1 withdrawal/ Remodeling
B
C
D
E
F
G
G'
H
I
J
K
L
canal
duct
5 µm
2 µm
50 µm

Figure 2.2

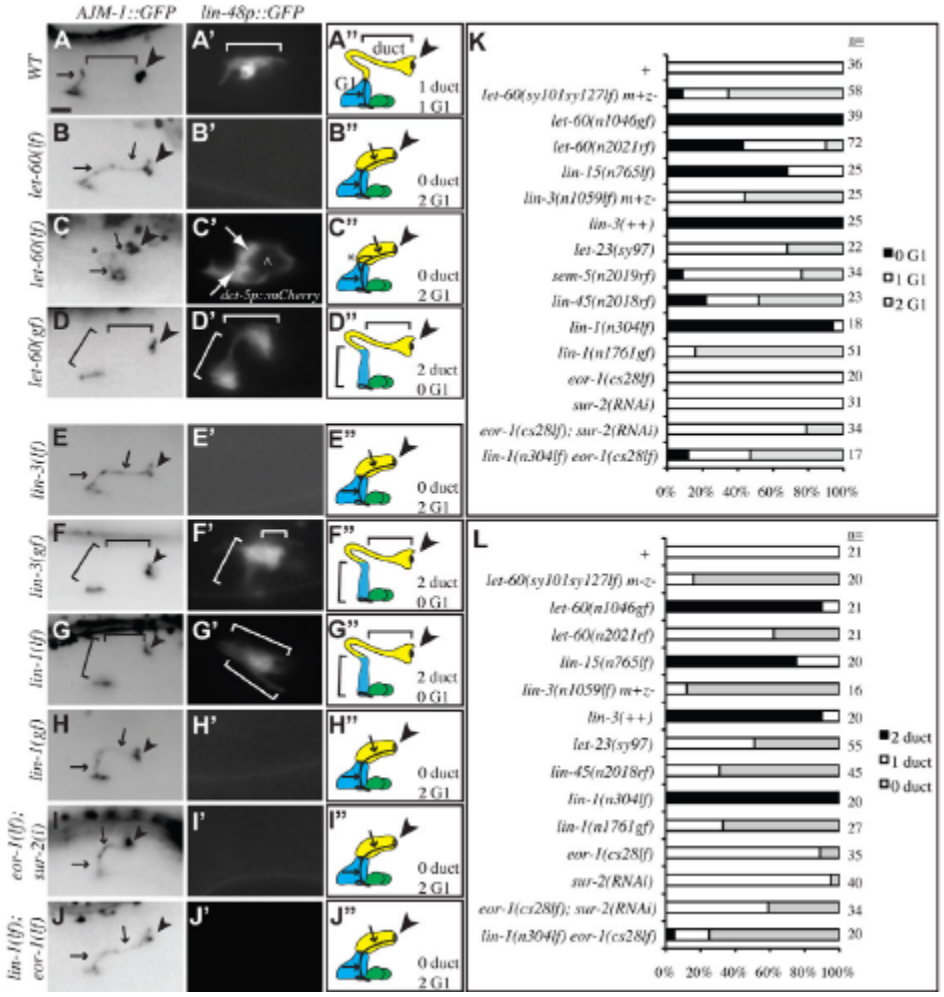
AJM-1::GFP
lin-48p::GFP
WT
let-60(lf)
let-60(lf)
let-60(gf)
lin-3(lf)
lin-3(gf)
lin-1(lf)
lin-1(gf)
eor-1(lf); sur-2(i)
lin-1(lf); eor-1(lf)
duct
G1
1 duct 1 G1
0 duct 2 G1
0 duct 2 G1
2 duct 0 G1
0 duct 2 G1
2 duct 0 G1
2 duct 0 G1
0 duct 2 G1
0 duct 2 G1
0 duct 2 G1
let-60::mCherry
K
+ 36
let-60(sy101sy127lf) m+z- 58
let-60(n1046gf) 39
let-60(n2021rf) 72
lin-15(n765lf) 25
lin-3(n1059lf) m+z- 25
lin-3(++) 25
let-23(sy97) 22
sem-5(n2019rf) 34
lin-45(n2018rf) 23
lin-1(n304lf) 18
lin-1(n1761gf) 51
eor-1(cs28lf) 20
sur-2(RNAi) 31
eor-1(cs28lf); sur-2(RNAi) 34
lin-1(n304lf) eor-1(cs28lf) 17
0% 20% 40% 60% 80% 100%
0 G1
1 G1
2 G1
L
+ 21
let-60(sy101sy127lf) m-z- 20
let-60(n1046gf) 21
let-60(n2021rf) 21
lin-15(n765lf) 20
lin-3(n1059lf) m+z- 16
lin-3(++) 20
let-23(sy97) 55
lin-45(n2018rf) 45
lin-1(n304lf) 20
lin-1(n1761gf) 27
eor-1(cs28lf) 35
sur-2(RNAi) 40
eor-1(cs28lf); sur-2(RNAi) 34
lin-1(n304lf) eor-1(cs28lf) 20
0% 20% 40% 60% 80% 100%
2 duct
1 duct
0 duct

Figure 2.3

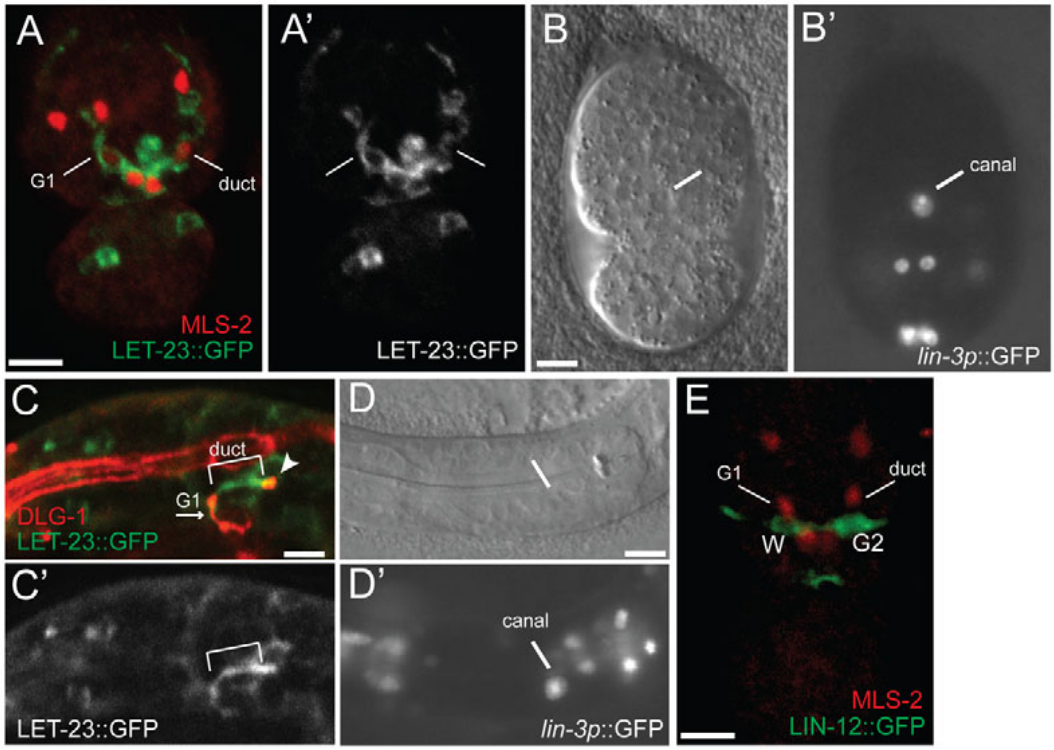
A
G1
duct
MLS-2
LET-23::GFP
A'
LET-23::GFP
B
B'
canal
lin-3p::GFP
C
duct
G1
DLG-1
LET-23::GFP
D
E
G1
duct
W
G2
C'
LET-23::GFP
D'
canal
lin-3p::GFP
MLS-2
LIN-12::GFP

Figure 2.4

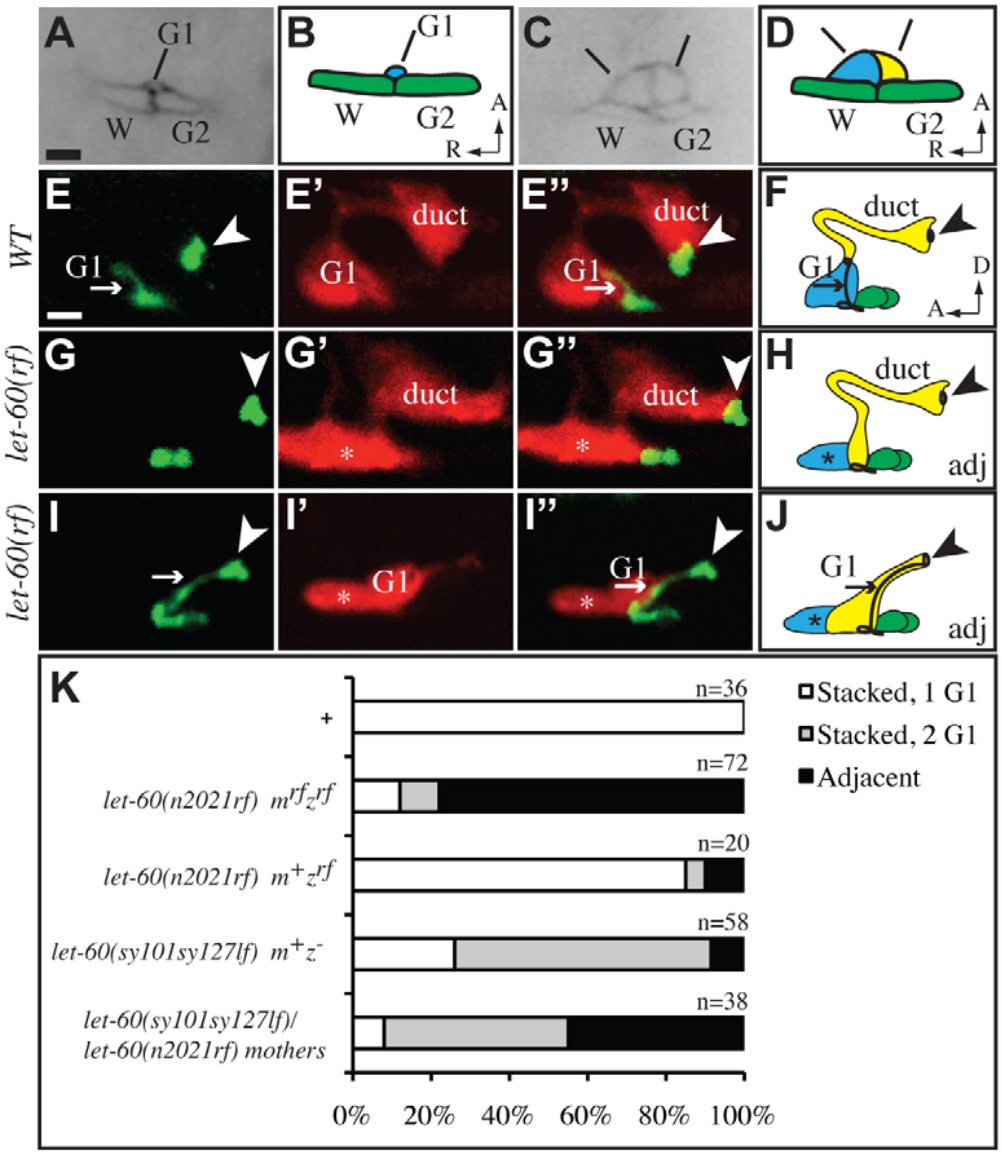
A
G1
W
G2
B
G1
W
G2
A
R
C
W
G2
D
W
G2
A
R
WT
E
G1
E'
duct
G1
E''
duct
G1
F
duct
G1
D
A
let-60(rf)
G
G'
duct
*
G''
duct
*
H
duct
*
adj
let-60(rf)
I
I'
G1
*
I''
G1
*
J
G1
*
adj
K
n=36
+
n=72
let-60(n2021rf) m^rf z^rf
n=20
let-60(n2021rf) m^+ z^rf
n=58
let-60(sy101sy127lf) m^+ z^-
n=38
let-60(sy101sy127lf)/
let-60(n2021rf) mothers
0%
20%
40%
60%
80%
100%
Stacked, 1 G1
Stacked, 2 G1
Adjacent

Figure 2.5

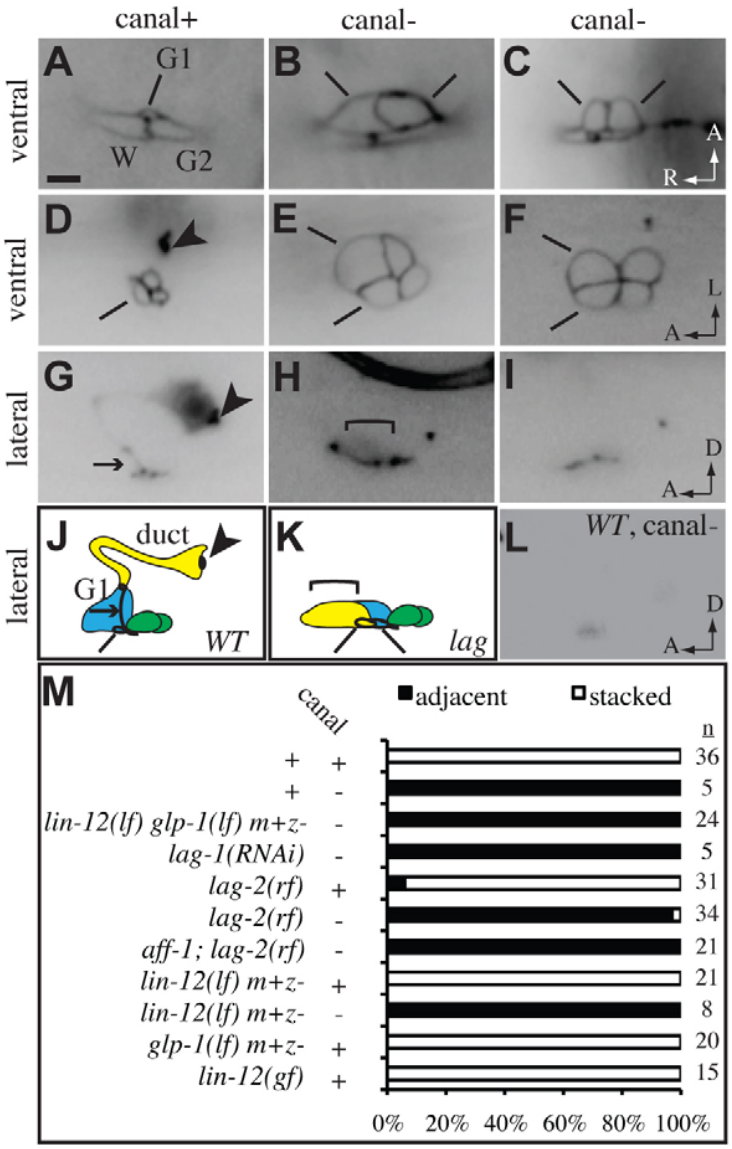
canal+
canal-
canal-
ventral
ventral
lateral
lateral
A
G1
W
G2
B
C
A
R
D
E
F
L
A
G
H
I
D
A
J
duct
G1
WT
K
lag
L
WT, canal-
D
A
M
canal
adjacent
stacked
n
+ +
+ -
lin-12(lf) glp-1(lf) m+z- -
lag-1(RNAi) -
lag-2(rf) +
lag-2(rf) -
aff-1; lag-2(rf) -
lin-12(lf) m+z- +
lin-12(lf) m+z- -
glp-1(lf) m+z- +
lin-12(gf) +
36
5
24
5
31
34
21
21
8
20
15
0% 20% 40% 60% 80% 100%

Figure 2.6

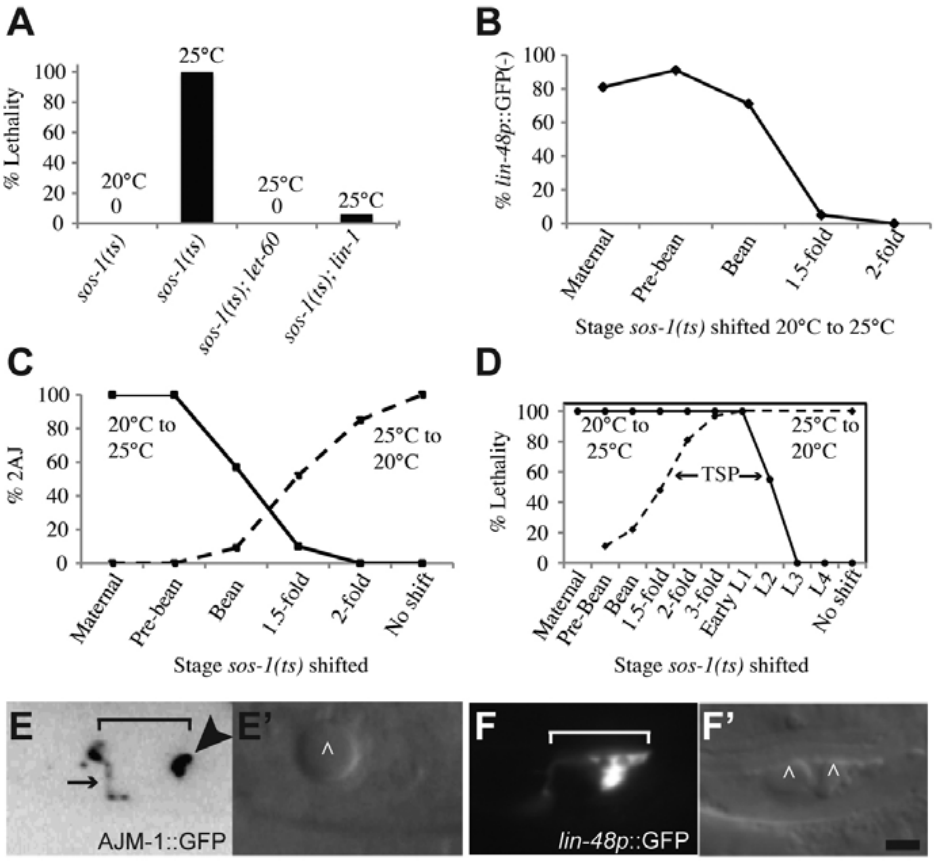
A
% Lethality
100
80
60
40
20
0
20°C
0
25°C
25°C
0
25°C
sos-1(ts)
sos-1(ts)
sos-1(ts); let-60
sos-1(ts); lin-1
B
% lin-48p::GFP(-)
100
80
60
40
20
0
Maternal
Pre-bean
Bean
1.5-fold
2-fold
Stage sos-1(ts) shifted 20°C to 25°C
C
% 2AJ
100
80
60
40
20
0
20°C to 25°C
25°C to 20°C
Maternal
Pre-bean
Bean
1.5-fold
2-fold
No shift
Stage sos-1(ts) shifted
D
% Lethality
100
80
60
40
20
0
20°C to 25°C
25°C to 20°C
TSP
Maternal
Pre-Bean
Bean
1.5-fold
2-fold
3-fold
Early L1
L2
L3
L4
No shift
Stage sos-1(ts) shifted
E
AJM-1::GFP
E'
F
lin-48p::GFP
F'

Figure 2.7

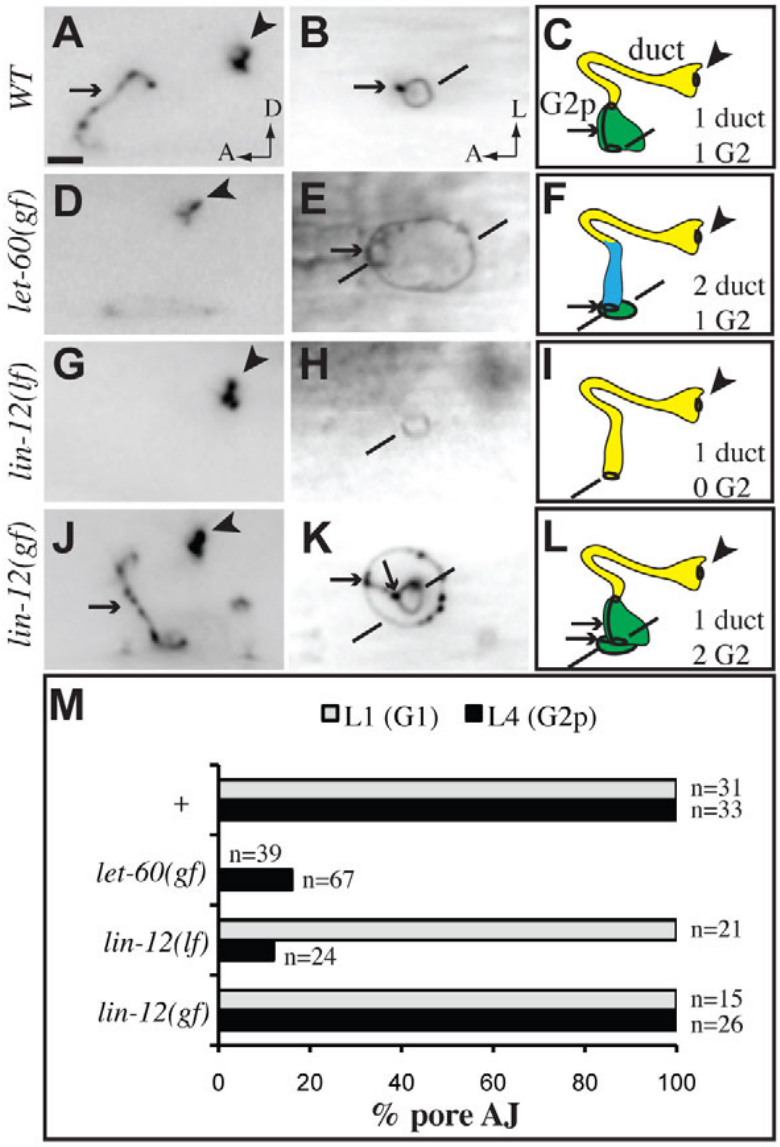
WT
let-60(gf)
lin-12(lf)
lin-12(gf)
A
B
C
D
E
F
G
H
I
J
K
L
M
D
A
L
A
duct
G2p
1 duct
1 G2
2 duct
1 G2
1 duct
0 G2
1 duct
2 G2
L1 (G1)
L4 (G2p)
+
let-60(gf)
lin-12(lf)
lin-12(gf)
n=31
n=33
n=39
n=67
n=21
n=24
n=15
n=26
0
20
40
60
80
100
% pore AJ

Table 2.1

Genotype[†]	Percentage of animals			
	Canal cell	*n*	Duct cell	*n*
+	100	32	97	31
+, canal cell ablated	0	9	100	9
+, canal cell parent ablated	0	8	87	8
lin-12(n941lf) glp-1(q46lf) m+z–	0	30	47	30
lag-1(q385lf) m+z–	0	32	95	40
lag-2(q411lf) m+z–	3	34	44	25
lag-2(q420rf)	+	31	94	31
lag-2(q420rf)	–	34	38	34
lin-12(n137gf)	+	15	100	69
arls12 [lin-12(intra)]	+	40	97	40

Table 2.2

Hours after egg lay (AEL)	Developmental Stage
1	Pre-Bean
4	Bean
6	2-fold
15	Early L1
24	L2
31	L3
60	L4

Chapter Three:

THE NKX5/HMX HOMEODOMAIN PROTEIN MLS-2 IS REQUIRED FOR PROPER TUBE CELL SHAPE IN THE *C.ELEGANS* EXCRETORY SYSTEM

*This chapter was submitted for publication as **Ishmail Abdus-Saboor**, Craig Stone, John I. Murray, and Meera V. Sundaram. (2012) The Nkx5/HMX homeodomain protein MLS-2 is required for proper tube cell shape in the *C.elegans* excretory system.

Summary

Cells perform wide varieties of functions that are facilitated, in part, by adopting unique shapes. Many of the genes and pathways that promote cell fate specification have been elucidated. However, relatively few factors have been identified that promote shape acquisition after fate specification. Here we show that the Nkx5/HMX homeodomain protein MLS-2 is required for cellular elongation and shape maintenance of two tubular epithelial cells in the *C.elegans* excretory system, the duct and pore cells. The Nkx5/HMX family is highly conserved from sea urchins to humans, with known roles in neuronal and glial development. MLS-2 is expressed in the duct and pore, and defects in *mls-2* mutants first arise when the duct and pore normally adopt unique shapes. MLS-2 cooperates with the EGF-Ras-ERK pathway to turn on the LIN-48/Ovo transcription factor in the duct cell during morphogenesis. These results reveal a novel interaction between the Nkx5/HMX family and the EGF-Ras pathway and implicate a transcription factor, MLS-2, as a regulator of cell shape.

Introduction

Many cell types that are commonly found throughout the animal kingdom have quite remarkable shapes. For example, neurons form highly elaborate axonal and dendritic processes to construct networks that support the many functions of the nervous system. The shapes of neurons can vary tremendously depending on the function of the neuron and the distance between the innervating target and the cell body (Kanning et al., 2010;

Marin et al., 2006; Meinertzhagen et al., 2009). Glial cells, which ensheath neurons, can adopt elongated or stellate shapes depending on the functions and shapes of the associated neurons (Mason et al., 1988; Oikonomou and Shaham, 2011). Epithelial cells, which line our organs and external body surfaces, typically are classified as squamous, cuboidal, or columnar in shape (Andrew and Ewald, 2010), but certain epithelial cells, such as tracheal terminal cells in Drosophila and the excretory canal cell in *C.elegans*, adopt more complex, branched morphologies (Buechner, 2002; Schottenfeld et al., 2010). Although each cell type in the body has a characteristic shape, the relationship between cell fate determination and cell shape acquisition is poorly understood.

The cytoskeleton is the major determinant of cell shape, and all three major components of the cytoskeleton (actin, microtubules, and intermediate filaments) play critical roles. Actin monomers polymerize into long stable filaments and webs that provide mechanical structure to cells (Pollard and Cooper, 2009). Microtubule monomers also polymerize into long rigid filaments that provide structure and serve as tracks for long-range transport of other cellular materials, especially at the growing tips of polarized elongated cells such as neurons (Stiess and Bradke, 2010). Intermediate filaments (IFs) organize into more flexible, rope-like structures that help maintain cell shape and resist mechanical stress (Chang and Goldman, 2004; Goldman et al., 1996; Herrmann et al., 2007). The actin, microtubule and IF-based cytoskeletons are interconnected by various bridging proteins, such as formins and plakins (Chesarone et al., 2010; Leung et al., 2002), and work together to establish and maintain cell shape.

Transcription factors play key roles in specifying cell fates and in promoting subsequent steps of terminal differentiation, and thus must ultimately influence the cytoskeleton to confer cell-type appropriate shapes. Indeed, a few transcription factors appear dedicated specifically to the control of cell shape. For example, transcription factors of the Snail family drive cell shape changes during epithelial-to-mesenchymal transition by repressing E-cadherin and other epithelial-specific genes (Peinado et al., 2007). The Drosophila zinc finger transcription factor shavenbaby (svb)/ovo promotes formation of specialized epidermal appendages (denticles) by upregulating multiple genes important for re-organization of the actin cytoskeleton and the extracellular matrix (Chanut-Delalande et al., 2006; Payre et al., 1999). Ovo function appears to be conserved, since the mouse ovo gene, Movo1, also promotes formation of specialized epidermal appendages (hair follicles) (Dai et al., 1998). However, defects in cell fate determination vs. terminal differentiation can be difficult to distinguish in many systems, and few other transcription factors have been identified that function specifically in shape determination downstream of fate specification.

The *C.elegans* excretory (renal-like) system contains three distinct cell types that adopt unique shapes (Abdus-Saboor et al., 2011; Buechner, 2002; Nelson et al., 1983). All three cells of the excretory system (canal, duct, and pore) are unicellular epithelial tubes that connect in tandem via apico-lateral junctions (Fig. 3.1). Unicellular tubes are single cells that form tubes by wrapping or hollowing mechanisms (Kamei et al., 2006; Lubarsky and Krasnow, 2003; Rasmussen et al., 2008). The canal cell is the largest cell in the worm and adopts an H-like shape, with four hollow canals that extend the entire

length of the worm's body (Buechner, 2002). The duct and pore are much shorter in length and connect the canal cell to the outside environment (Fig. 3.1). The duct has a distinctive asymmetric shape, and the region of the duct that connects to the pore is narrow in diameter similar to an axonal extension. The pore has a more regular, conical shape (Fig. 3.1). Thus the cells of the excretory system provide a model to investigate how epithelial cells adopt specialized shapes.

The excretory duct and pore develop from initially equivalent precursors that adopt distinct fates in response to EGF-Ras-ERK signaling (Abdus-Saboor et al., 2011; Sulston et al., 1983; Yochem et al., 1997). The duct and pore fates are distinguished by several properties. For example, during migration of the precursors to the midline, the duct takes a canal proximal position, while the pore moves ventrally (Fig. 3.1). Both cells form unicellular tubes via a wrapping process, but the duct subsequently fuses its autocellular junction while the pore retains its autocellular junction (Stone et al., 2009). During morphogenesis, the duct elongates more extensively than the pore and adopts its unique, asymmetric shape. The duct also expresses the transcription factor LIN-48, an ortholog of Drosphila svb/ovo that influences duct position and/or length (Wang and Chamberlin, 2002).

Here we show that the Nkx5/HMX transcription factor MLS-2 promotes cell shape acquisition in the *C.elegans* excretory duct and pore. MLS-2 cooperates with the EGF-Ras pathway to promote *lin-48/*ovo expression, but MLS-2 must have additional relevant targets since the cell shape defects of *mls-2* mutants are more severe than those of *lin-48* mutants. The roles we identified for MLS-2 in epithelial tube cell development expand

the role of NKX.5/HMX proteins, which have traditionally been shown to act within the nervous system (Wang and Lufkin, 2005). MLS-2 promotes differentiation of two other elongated cells in *C.elegans*, the AWC neuron and the CEP sheath glial cell (Kim et al., 2010; Yoshimura et al., 2008). Therefore, MLS-2 may have a core function in promoting morphogenesis and terminal differentiation in cells that adopt elongated shapes.

Results

An EMS mutagenesis screen for mutants with duct cell abnormalities

Animals mutant for various components of the canonical EGF-Ras-ERK pathway all display a rod-like lethal phenotype associated with absence or abnormal development of the excretory duct cell (Abdus-Saboor et al., 2011; Yochem et al., 1997). To identify additional genes important for duct development, we conducted an EMS mutagenesis screen for rod-like lethal mutants. After screening 3900 haploid genomes, we identified 9 mutants, several of which had incompletely penetrant phenotypes. We used the apical junction marker AJM-1::GFP, which labels the pore autocellular junction, and a duct-specific *lin-48* marker to classify these mutants into two phenotypic groups: 1) Mutants with a duct-to-pore fate transformation; and 2) Mutants with apparently normal duct fate specification. Mapping and complementation tests (Materials and Methods) revealed that the first group included alleles of *lin-3/EGF*, *let-60/Ras* and *ksr-1/Kinase Suppressor of Ras*, as expected based on the known role of EGF-Ras signaling. The second group of mutants included alleles of *vha-5*, *lpr-1* (Stone et al., 2009) and *egg-6* (Mancuso et al.,

2012), which have been described elsewhere.

The incompletely penetrant lethal allele *cs71* fell into a third category (Fig. 3.2). *cs71* mutants sometimes lacked *lin-48* reporter expression, as seen in Ras pathway mutants, but loss of this duct fate marker was not accompanied by duplication of the excretory pore fate (Fig. 3.2D,F,G). Furthermore, the excretory pore sometimes appeared abnormal or missing based on absence or shortening of its characteristic autocellular junction (Fig. 3.2E,F,H). Thus, *cs71* defined a gene important for both excretory duct and pore development.

_cs71_ is an allele of _mls-2_

Linkage mapping placed *cs71* near the *mls-2* gene on the X chromosome. *mls-2(cc615)* null mutants showed a similar rod-like lethal phenotype, and *cs71* and *cc615* failed to complement (Fig. 3.2I). *cs71* mutants contained a nonsense mutation in the *mls-2* coding region (Fig. 3.2J). In addition, a translational GFP::MLS-2 reporter completely rescued *cs71* lethality (Fig. 3.2I). We conclude that *cs71* is an allele of *mls-2*.

mls-2 encodes a homeodomain transcription factor that belongs to the Nkx5/HMX superfamily (Jiang et al., 2005). Most members of the Nkx5/HMX family have the HMX motif [A/S]A[E/D]LEAA[N/S] located immediately downstream of the homeodomain (Wang and Lufkin, 2005; Yoshiura et al., 1998), but MLS-2 and its closest relative, the chick SOHo1 protein, both lack the HMX motif (Deitcher et al., 1994). Accordingly, it has been suggested that MLS-2 be considered a member of the Nkx5 family instead of

HMX (Yoshimura et al., 2008). In sea urchins, zebrafish, fruit flies, and mice, members of the Nkx5/HMX family are expressed in the developing central nervous system and sensory organs (Gongal et al., 2011; Martinez and Davidson, 1997; Wang et al., 2000). The function of Nkx5/HMX family members has not diverged substantially between species as Drosophila *HMX* can fully rescue the otic vesicle defects of *hmx-2/3* null mice (Wang et al., 2004). Consistent with roles in the nervous system, *C.elegans* MLS-2 is expressed predominantly in neurons and glial cells (see below), and MLS-2 is required for differentiation and morphogenesis of the AWC chemosensory neurons and the CEP sheath glial cells (Kim et al., 2010; Yoshimura et al., 2008).

MLS-2 is expressed in the duct and pore lineages

Since *mls-2* promotes duct and pore cell development, we asked if the expression pattern of MLS-2 was consistent with a direct role for MLS-2 in these cells. To visualize MLS-2 expression we used *csIs55,* an integrated version of the GFP::MLS-2 translational reporter that completely rescued *mls-2* lethality (Fig. 3.2I). To gain a complete picture of the MLS-2 expression pattern during embryogenesis, we analyzed confocal time-lapse movies of three developing embryos expressing GFP::MLS-2 and a nuclear histone::mcherry marker (Material and Methods). GFP::MLS-2 expression became detectable around the 50-cell stage of embryogenesis and was restricted to specific, reproducible sublineages of the AB blastomere, most of which gave rise to neuronal

and/or glial descendants (Fig. 3.3). GFP::MLS-2 was also expressed in the duct and pore lineages, but was never observed in the canal cell (Fig. 3.3).

In 3/3 movies, we saw that expression of GFP::MLS-2 initiated in the grandparents of the duct and pore cells (Fig. 3.3A). GFP::MLS-2 expression persisted in the duct and pore cells through the ventral enclosure (Fig. 3.3B) and 1.5-fold stages of embryonic development, during which time fates are specified via EGF-Ras-ERK signaling and the duct and pore cells stack and form tubes (Abdus-Saboor et al., 2011). By the first larval stage of development, when the duct and pore cells have achieved their mature morphologies, GFP::MLS-2 was no longer detected in the duct and pore cells (data not shown). An MLS-2 polyclonal antibody showed the same expression pattern in the duct and pore cells as GFP::MLS-2 (Abdus-Saboor et al., 2011) and (data not shown). We conclude that the temporal and spatial expression pattern of MLS-2 is consistent with MLS-2 acting cell autonomously to promote duct and pore development.

mls-2 mutants have incompletely penetrant and cold-sensitive lethal excretory system defects

Although both *mls-2(cs71)* and *mls-2(cc615)* appear to be null alleles since they truncate or eliminate the protein, their lethal and duct marker phenotypes were incompletely penetrant and cold-sensitive (Fig. 3.2G,I). The pore junction phenotype was also incompletely penetrant but was not cold-sensitive (Fig. 3.2H). In addition to the incompletely penetrant early L1 excretory arrest, some *mls-2* mutants arrested as larvae

without noticeable excretory defects (Fig. 3.2I). MLS-2 is required for ventral CEP sheath glia morphogenesis, and approximately 20% of worms with ablated ventral sheath glial cells arrest as early larvae (Yoshimura et al., 2008). Therefore, the other non-excretory larval arrest seen in *mls-2* mutants is likely the result of glial defects. MLS-2 is also required for differentiation of the AWC neurons, but no lethality is associated with loss of the AWC neurons (Kim et al., 2010). Although the duct and pore are closely related in lineage to the ventral CEP sheath glial cells and the AWC neurons (Fig. 3.3A), *mls-2* mutants fail to express differentiation markers for each cell type with varying levels of penetrance, suggesting independent roles for MLS-2 in each cell. The incomplete penetrance of *mls-2* null mutants suggests that there are redundant factors that work in parallel to MLS-2 to promote excretory system development. The fact that presumptive null alleles are cold sensitive suggests that the process that requires MLS-2 is cold-sensitive, and not the specific alleles.

mls-2 **cooperates with the EGF-Ras pathway to promote duct differentiation and** ***lin-48/Ovo*** **expression**

To address possible redundancy between MLS-2 and other related homeodomain factors, we took a candidate based approach. We screened 9 of the gene products most related by sequence to MLS-2 by RNA-mediated interference (RNAi). We observed no enhancement of *mls-2* excretory phenotypes with this strategy (data not shown), although we cannot exclude the possibility of inefficient RNAi knockdown; RNAi generally works

very poorly in the excretory system (Rocheleau et al., 2008). We also made double mutants between *mls-2* and three other related homeodomain genes for which mutants exist, but this too yielded no enhancement of the *mls-2* excretory phenotype (data not shown). However, a more unbiased genome-wide RNAi screening approach identified two chromatin modifying factors that greatly enhanced *mls-2* rod-like lethality (IA and KH unpublished). One of these, *pbrm-1*, has been previously shown to suppress the multi-vulva phenotype of *let-60 Ras(n1046 gf)* and also interact with other Ras pathway effectors in the vulva (Lehner et al., 2006).

We asked if combining *mls-2* with mutants in the EGF-Ras-ERK pathway could enhance the excretory-related lethality of *mls-2* (Fig. 3.4). Specifically, we examined hypomorphic mutants for *mpk-1/ERK*, which is the terminal kinase in the EGF-Ras pathway (Wu and Han, 1994) and null mutants for *lin-1/ETS*, a downstream transcription factor (Beitel et al., 1995a). In addition, we examined null mutants for two nuclear factors, *eor-1* and *sur-2,* that act redundantly downstream of MPK-1/ERK (Howard and Sundaram, 2002). *mpk-1/ERK, lin-1/ETS, eor-1,* and *sur-2* single mutants all had a weakly penetrant lethal phenotype (Fig. 3.4B). However, when these mutants were combined with *mls-2* mutants, there was a great enhancement of both excretory and total lethality (Fig. 3.4B). These data suggested that *mls-2* cooperates with the EGF-Ras-ERK pathway to promote excretory duct development.

Importantly, we found no evidence for defects in duct vs. pore cell fate specification in *mls-2* mutants. Although many mutants lacked markers indicative of the duct or pore cell fate, in no case did we observe duplication of either fate; thus, apparent

loss of one cell type was not associated with conversion to the other. *mls-2* enhanced defects in duct terminal differentiation, as reflected by enhanced loss of the *lin-48* duct marker in a *sur-2* background (Fig. 3.4C). *mls-2* did not suppress the pore-to-duct fate transformations of *let-60 ras* gain-of-function (gf) mutants (Fig. 3.4D), but did reduce *lin-48* marker expression in *let-60(gf)* and *lin-1* backgrounds (Fig. 3.4C). These data placed *mls-2* genetically downstream or in parallel to the EGF-Ras-ERK pathway with respect to turning on *lin-48* in the duct cell (Fig. 3.4A). Thus, *mls-2* cooperates with EGF-Ras-ERK to promote terminal differentiation of the excretory duct cell.

mls-2 affects duct and pore tube cell shape

To better understand the *mls-2* mutant phenotype, we used additional markers to visualize the shapes of excretory system cells in *mls-2* mutants. To visualize the canal cell, we used the *vha-1p*::GFP marker, which labels the entire cytoplasm of this cell (Mattingly and Buechner, 2011). In *mls-2* mutants, the canal cell extended its canals normally the entire length of the worm, and fluid rarely accumulated within the canal lumen (3/104) (data not shown), suggesting that *mls-2* excretory lethality is not the result of canal cell defects.

We visualized the cytoplasm of the duct and pore cells with *dct-5p*:mcherry in combination with AJM-1::GFP (Fig. 3.5). The duct and pore cells in *mls-2* mutants frequently had abnormal globular shapes rather than their normal elongated morphologies (Fig. 3.5C-H). These cell shape defects were variable, with individual animals exhibiting

defects in only the pore (Fig. 3.5C), only the duct (Fig. 3.5G), or in both cells (Fig. 3.5E). *mls-2* mutants scored with *lin-48p*::mcherry and AJM-1::GFP also had variable defects, with either the duct (Fig. 3.2D), pore (Fig. 3.2E), or both cells affected (Fig. 3.2F). Pore cell shape defects were strongly correlated with absence of the pore autocellular junction. In mutants where only the pore cell was affected, the duct often reached to the ventral epidermis (Fig. 3.5C); this phenotype was compatible with animal survival. In rare *mls-2* mutants where only the duct cell was affected, the pore cell appeared to connect directly to the canal cell, and the *dct-5p*::mcherry marker was not expressed in the duct or pore cells (Fig 3.5G). Therefore, it was difficult to define the position of the duct cell with this particular phenotype, but we hypothesize that the duct cell either failed to elongate or was displaced. In summary, *mls-2* affects the shape of both the excretory pore and duct cells.

mls-2 cell shape defects begin during duct and pore elongation

To determine when the *mls-2* cell shape and junctional defects began, we measured the length of the pore autocellular junction (AJ) and the distance between the pore AJ and duct-canal junction (an estimate of duct length) at four time-points between the1.5-fold stage of embryogenesis and the first larval stage of development (Fig. 3.6). In wild type worms at the 1.5-fold stage, the duct and pore cells have stacked in tandem and wrapped into tubular structures with simple, block-like shapes (Figs. 3.1 and 3.6C) (Abdus-Saboor et al., 2011; Stone et al., 2009). Each cell initially has an autocellular junction, but the duct rapidly auto-fuses to dissolve its junction. *mls-2* mutants appeared

similar to wild-type at this stage (Fig. 3.6D), suggesting that the duct and pore had stacked and formed tubes normally. Consistent with the duct and pore stacking normally, at the early 3-fold stage *mls-2* mutants had a single ventral pore opening similar to wild type, as opposed to adjacent non-stacked cells (Abdus-Saboor et al., 2011) (Fig. 3.6E,F). However, while the cells in wild type continued to elongate up until the first larval stage, the cells in some *mls-2* mutants failed to elongate or actually collapsed and became shorter (Fig. 3.6G-J). Thus, the *mls-2* phenotype first became apparent two hours after the 1.5-fold stage, when the duct and pore cells were beginning to elongate and take distinct shapes.

mls-2 **mutants have a more severe duct shape phenotype than** ***lin-48*** **mutants**

mls-2 mutants have reduced expression of *lin-48* reporters in the excretory duct, suggesting that *mls-2* might affect duct cell shape at least in part via upregulation of *lin-48*. *lin-48* is the *C. elegans* ortholog of Drosophila *svb/ovo*, which is known to regulate expression of a variety of cytoskeletal genes to control cell shape in the epidermis (Chanut-Delalande et al., 2006). Furthermore, *lin-48* mutants were previously described to have defects in duct positioning or shape (Wang and Chamberlin, 2002). We used markers AJM-1::GFP and *dct-5p*::mcherry to visualize the duct in *lin-48* mutants. While the duct cell body appeared somewhat narrower in *lin-48* mutants than in wild-type, the duct retained its distinctive process and asymmetric cell shape, and pore morphology was normal (Fig. 3.5I). The *lin-48* mutant phenotype is relatively subtle compared to the *mls-*

2 phenotype, indicating that *mls-2* must regulate additional genes in the duct besides *lin-48*. *mls-2* also affects pore shape via mechanisms that are independent of *lin-48*. *lin-48; mls-2* double mutants were not more severe than *mls-2* mutants alone (data not shown), suggesting that *mls-2* and *lin-48* do not have redundant functions in promoting duct cell shape.

Discussion

We have shown that the Nkx5/HMX homeodomain transcription factor MLS-2 promotes terminal differentiation and morphogenesis of the epithelial duct and pore cells in *C. elegans*. In *mls-2* mutants, both cells adopt simple tube shapes as in wild-type, but subsequently fail to elongate to their more complex, mature morphologies. In the duct, MLS-2 cooperates with the EGF-Ras-ERK pathway in turning on the terminal differentiation gene *lin-48/ovo*. We propose that MLS-2 regulates additional genes important for cytoskeletal organization and cell elongation, and that MLS-2 plays widespread roles in promoting morphogenesis of cells with complex shapes.

mls-2 **acts in parallel to the EGF-Ras-ERK pathway to upregulate** ***lin-48/ovo***

The EGF-Ras-ERK pathway is used repeatedly throughout metazoan development to promote numerous cell fates. In *C. elegans,* the EGF-Ras-ERK pathway specifies the excretory duct versus pore fate, and there is a continued requirement for

signaling to maintain duct tube architecture after initial fate specification (Abdus-Saboor et al., 2011). How signaling ultimately promotes specific aspects of duct fate such as cell shape, and how continued signaling affects later tube architecture, is unclear. Most effects of EGF-Ras-ERK signaling depend on the combined action of the core downstream transcription factors LIN-1/Ets and EOR-1/BTB-Zinc finger and the Mediator subunit SUR-2, which must then control expression of various other target genes that together influence duct terminal differentiation. MLS-2 cooperates with SUR-2 to turn on one known duct-specific target, the LIN-48/Ovo transcription factor, and acts downstream or in parallel to LIN-1/Ets.

We favor a model whereby MLS-2 works in parallel to the EGF-Ras-ERK pathway and is not itself a target of signaling. Several observations have led us to this conclusion, including: 1) MLS-2 expression begins well before the time that Ras signaling is thought to occur in the duct, and is observed equally in the duct and pore; 2) *mls-2* mutants do not have a duct-to-pore fate switch like Ras signaling mutants, and 3) *mls-2* mutants have shape defects in both the duct and pore, whereas Ras signaling mutants only affect the duct. We cannot exclude the possibility that Ras signaling enhances MLS-2 expression after it has already been initiated. Neither can we exclude the possibility that the activity of MLS-2 is post-transcriptionally regulated by Ras signaling. Nonetheless, our data are most consistent with the model that MLS-2 and the Ras pathway converge to turn on common targets such as *lin-48*.

lin-48 plays only a subtle role in shape acquisition and position in the duct cell (Wang and Chamberlin, 2002) and (this work), and therefore is probably just one of a

host of target genes downstream of Ras signaling and MLS-2 that promote duct morphogenesis. The Drosophila ortholog of *lin-48*, Shavenbaby (svb), also is upregulated by EGF-Ras-ERK signaling (Payre et al., 1999) and promotes specialized cell shape in the fly epidermis by turning on at least a dozen genes that affect either the cytoskeleton or the extracellular matrix (Chanut-Delalande et al., 2006). Transcriptional upregulation of svb depends on the combined action of at least seven distinct enhancer elements (Frankel et al., 2010; Frankel et al., 2011), and transcription factors that bind directly to these enhancers have not yet been identified. We also do not know if MLS-2 or Ras-regulated transcription factors act directly or indirectly to upregulate *lin-48.*

MLS-2 may regulate expression of cytoskeletal genes to control duct and pore cell shape

We hypothesize that, in addition to *lin-48*, MLS-2 targets may include genes more directly involved in cytoskeletal organization. The cold-sensitivity of *mls-2* null mutants is consistent with defects in a microtubule-dependent process, since microtubules have been shown to depolymerize at low temperatures in all systems studied, including *C. elegans* (Chalfie and Thomson, 1982; Melki et al., 1989). Both the actin and microtubule-based cytoskeletons have known roles in cellular elongation contexts (Lloyd and Chan, 2004; Otani et al., 2011; Pollard and Cooper, 2009), so disorganization of either could potentially explain the *mls-2* duct and pore shape defects.

Like other organisms, *C. elegans* has multiple isoforms of actin and tubulin, and many types and isoforms of cytoskeletal bridging proteins, and these various isoforms are expressed in cell-type specific patterns (Bobinnec et al., 2000; Fukushige et al., 1995; Hurd et al., 2010)(Cartier et al., 2006; Fuchs and Karakesisoglou, 2001; McKean et al., 2001; McLean et al., 2008). A given cell's repertoire of cytoskeletal subunits, combined with its repertoire of bridging proteins, may determine how the different parts of the cytoskeleton work together, contributing to cell-type appropriate morphologies. We currently know very little about which cytoskeletal isoforms are expressed in the excretory duct and pore cells, but predict that the MLS-2 transcription factor promotes expression of a subset of these factors that are important for generating the unique morphologies of these cells.

MLS-2 promotes terminal differentiation of cells with complex shapes

In addition to the duct and pore, *mls-2* affects differentiation of the AWC neurons and the CEP sheath glia cells, which all derive from common precursor cells (Kim et al., 2010; Yoshimura et al., 2008) (see Fig. 3A). However, the loss of terminal fate markers occurs at varying penetrance in these different cell types, suggesting that *mls-2* plays a specific role in each of these related cell types, and not a general role in the common precursors of the three cell types. In addition to lineage history, one feature shared by all three cell types is a complex shape.

The AWC left and right neurons are a pair of amphid sensory neurons required to chemotax to volatile odors (Bargmann et al., 1993). The AWC neurons have long, unbranched dendrites terminating in elaborate sheet-like cilia that are buried within the amphid glial sheath (Ward et al., 1975). These dendrites elongate via a novel retrograde extension mechanism in which their tips are anchored at the nose while the cell body migrates posteriorly (Heiman and Shaham, 2009). *ceh-36* is a terminal selector gene for the AWC neuron (Lanjuin et al., 2003), and *mls-2* promotes *ceh-36* expression in the AWC neurons (Kim et al., 2010). We note, however, that *ceh-36* expression actually precedes *mls-2* expression in the embryonic AWC lineages (J.I.M submitted) suggesting that *mls-2* might be part of a feedback loop that maintains *ceh-36* expression in larvae. The AWC neurons are not converted to an alternate neuronal fate in *mls-2* mutants, but they often fail to express *ceh-36* and other AWC-specific marker genes; cells that do express these markers (and therefore can be visualized) display abnormal dendrite morphology (Kim et al., 2010).

The CEP sheath glial cells envelope the *C. elegans* nerve ring, which is considered the worm's brain, and send elongated processes to surround some synaptic sites (Ward et al., 1975). In *mls-2* mutants, ventral CEP sheath cells fail to express sheath-specific marker genes and fail to ensheath relevant neurons (Yoshimura et al., 2008). *mls-2* is also strongly expressed in CEP socket glia and OLQ sheath glia (Fig. 3B, Supplementary Fig. 3), although its requirements there have not been tested.

The excretory duct and pore tubes have complex cell shapes that are somewhat comparable to those of neurons and glia. The duct and pore, like sheath and socket glia,

form unicellular tubes with a hollow interior. The duct also has a long narrow process similar to a neuronal extension. These cells make initial junction attachments to partners at both ends, and then subsequently elongate to maintain those attachments as the embryo elongates and the partners move further and further apart. This phenomenon is similar to the stretch-dependent elongation of many neurons that form synapses early in development and then must maintain those synaptic connections as the animal grows (Smith, 2009). It may also be functionally related to the retrograde extension mechanism of AWC elongation (Heiman and Shaham, 2009).

Many conserved transcription factors control similar developmental processes across distantly related phyla. For example, master transcriptional regulators FoxA, Pax6 and Nkx2.5 specify foregut, eye or heart organ identity in both invertebrate and vertebrate systems (Friedman and Kaestner, 2006; Gehring and Ikeo, 1999; Mango, 2009; Qian et al., 2011), while the Snail family of transcription factors drives epithelial-to-mesenchymal transitions (Peinado et al., 2007). In all animals where they have been studied, Nkx5/Hmx transcription factors are expressed primarily in neurons and neuronal support cells such as glia (Wang and Lufkin, 2005). We hypothesize that this expression pattern could reflect a conserved role for MLS-2 and other Nkx5 factors in regulating common sets of cytoskeletal genes important for the process of cellular elongation.

Materials and Methods

Strains and alleles

Bristol N2 was the wild-type strain. Strains were maintained and manipulated by standard methods unless otherwise noted. Mutant alleles used are *III: mpk-1(ku1), lin-48(sa469). IV: eor-1(cs28), let-60(n1046), lin-1(n304). X: lon-2(e678), mls-2(cc615), mls-2(cs71).* Balancers used are: *hT2[qIs48] (I; III), mIn1[mIs14 dpy-10(e128)] (II)*, or *nT1[qIs51]* (IV, V)*]*. Transgenes used are: *jcIs1* (AJM-1::GFP) (Koppen et al., 2001a), *saIs14* (*lin-48p*::GFP) (Johnson et al., 2001), *wIs78* (AJM-1::GFP) (Koh and Rothman, 2001) *, csEx146* (*lin-48p*::mcherry) (Abdus-Saboor et al., 2011), *qpIs11 (vha-1p*::GFP) (Mattingly and Buechner, 2011), *qnEx59 (dct-5p*::mcherry) (Abdus-Saboor et al., 2011). *csIs55* (GFP::MLS-2) was generated from a pYJ59-containing array (Jiang et al., 2005) by gamma-irradiation-induced integration.

EMS Mutagenesis Screen

Wild-type animals were mutagenized with 50 mM EMS as described previously (Brenner, 1974), and allowed to self-fertilize. F1 progeny were picked to individual plates. From each F1 plate, 8 F2 progeny were picked to individual *ksr-2(RNAi)* plates, and F3 progeny were screened for rod-like lethal larvae. Mutants were isolated by picking live siblings of rod-like lethal larvae and allowing them to self fertilize. 9 mutants with a rod-like lethal phenotype of greater than 15% penetrance were kept for further analysis. *ksr-2(RNAi)* was performed to generate a sensitized background for identifying *ksr-1*-like mutations. Three *ksr-1* alleles (*cs66, cs74, cs76*) were obtained that showed phenotypes that strongly depended on *ksr-2(RNAi),* as expected based on the known

redundancy between the *ksr-1* and *ksr-2* paralogs (Ohmachi et al., 2002). All other mutants showed phenotypes that were independent of *ksr-2(RNAi)*.

Mapping and complementation tests

Genetic mapping and complementation tests were performed using standard methods. All mutations were roughly mapped by crossing mutant hermaphrodites with males carrying a balancer chromosome marked with GFP. Green hermaphrodite progeny of either the genotype *m/+; Bal/+* (where *m* = mutation and *Bal*=balancer) or *m/Bal* were picked to individual plates and allowed to self-fertilize. Rod-like lethal progeny segregating from these animals were examined for GFP expression to assess presence of the balancer chromosome. Animals that segregated only non-GFP rods were presumed to be of the genotype *m/Bal*. Mutations were then fine-mapped to specific chromosomal regions and candidate loci by further two-factor and/or three-factor linkage mapping.

cs66 mapped close to *dpy-6* on the X chromosome. *cs66, cs74,* and *cs76* all showed strong genetic interactions with *ksr-2(RNAi)* and failed to complement *ksr-1(n2526)*. *cs67* mapped close to *unc-29* on chromosome I and failed to complement *egg-6(ok1506)* (Mancuso et al., 2012). *cs71* mapped close to *lon-2* on the X chromosome and failed to complement *mls-2(cc615)*. *cs72* mapped close to *unc-24* on chromosome IV and failed to complement *vha-5(ok1588)*. *cs73* mapped close to *bli-3* on chromosome I and failed to complement *let-124(h276)*. This locus has been re-named *lpr-1* (lipocalin-related-1) (Stone et al., 2009). *cs75* mapped close to *dpy-20* on chromosome IV and failed to

complement *let-60(sy101sy127)*. Genomic sequencing revealed a single G-to-A nucleotide change within the *let-60*/Ras coding region, leading to an Isoleucine to Phenylalanine amino acid change at codon 120. *cs127* mapped approximately 3 cM away from *dpy-20* on chromosome IV and failed to complement *lin-3(n1059)*.

Marker Analysis and Imaging

Images were captured by differential interference contrast (DIC) and epi-fluorescence microscopy using a Zeiss Axioskop and Hamamatsu C5985 camera, or by confocal microscopy using a Leica SP5. Images were processed for brightness and contrast using Photoshop or ImageJ.

Duct and pore measurements were performed using ImageJ software with worms expressing AJM-1::GFP, which marks the pore autocellular junction (AJ) and the duct-canal junction. To measure the height of the pore AJ, a straight line was drawn in ImageJ from the base of the pore AJ to the top the pore AJ. To measure the duct length, a straight line was drawn in ImageJ from the top of the pore AJ to the duct-canal junction.

To visualize expression of MLS-2 in the duct and pore lineages, we generated 3D confocal movies of strains UP2051 (pie-1::mCherry::HIS-58::pie-1utr; his-72pro::HIS-24::mCherry::let-858utr; GFP::MLS-2) and RW10890 (pie-1::mCherry::HIS-58::pie-1utr; his-72pro::HIS-24::mCherry::let-858utr; PAL-1::GFP) as previously described (Murray et al., 2006) on a Leica TCS SP5 resonance-scanning confocal microscope with 0.5 micron z slice spacing and 1.5 minute time point spacing. Temperature was 22.5˚C.

We used a hybrid blob-slice model and StarryNite (Bao et al., 2006; Santella et al., 2010) for automated lineage tracing and curated the full lineage through the stage when ~600 nuclei are present (bean stage, approximately 275 minutes) with AceTree (Boyle et al., 2006).

Acknowledgements

I am deeply grateful to Craig Stone, John Murray, and Meera Sundaram (see figure legends for corresponding contributions). Craig also performed an RNAi candidate based screen to find redundant factors with *mls-2* (data were not shown). Meera Sundaram helped greatly with editing and revising the submitted manuscript. I would also like to thank Jun Liu, whose lab published the first role for MLS-2 in the *C.elegans* M lineage. Jun Liu also generously shared a translational MLS-2::GFP reporter that the lab has made great utility of.

Figure Legends

Figure 3.1: Timeline of excretory system development. Schematics of excretory canal cell (red), duct (yellow), and pore (blue) at different developmental stages. DIC images correspond to developmental stage listed on timeline; colored circles on the DIC images represent positions of the canal, duct, and pore. Dark black lines indicate apical junctions. Dotted line, duct auto-fusion. Arrow, pore autocellular junction. Arrowhead, duct-canal

cell intercellular junction. Bracket, duct cell body. Schematics are modified from (Abdus-Saboor et al., 2011). EGF-Ras-ERK-dependent duct vs. pore cell fate specification occurs just prior to the 1.5-fold stage (Abdus-Saboor et al., 2011). The duct elongates extensively between the 1.5-fold and early 3-fold stages (Stone et al., 2009).

Figure 3.2. *mls-2* mutants have incompletely penetrant and cold sensitive lethal excretory system defects. (A) WT L1 stage larva. (B) *mls-2(cs71)* L1 stage larva showing fluid accumulation near duct and pore (arrowhead). (C-F) L1 worms with AJM-1::GFP junction marker and *lin-48p*::mcherry duct marker. (C) WT larva with one duct and one pore. (D) *mls-2* mutant with normal AJM-1::GFP but no *lin-48* expression. (E) *mls-2* mutant with normal *lin-48* duct expression and collapsing pore. (F) *mls-2* mutant with no *lin-48* duct expression and no pore autocellular junction. (G,H) Quantification of marker loss phenotypes in *mls-2* mutants. (I) Rod-like (excretory) lethality shown as a fraction of total lethality. Other lethality scored as any worm that failed to reach L4 within 4 days. Note: GFP::MLS-2 rescue data scored by DIC microscopy looking for presence or absence of fluid cysts in L1s. Non-transgenic siblings were scored as controls. Complete genotype in this experiment was: *mls-2(cs71); pha-1(e2123); Ex[GFP::MLS-2; pha-1(+)]*. (J) Protein structure of MLS-2 showing the homeodomain and mutant alleles. *cs71* changes a CAA codon (Q250) to TAA (stop). Craig Stone identified *mls-2* in mutagenesis screen, performed complementation tests with *cc615*, and identified lesion in *cs71*.

Figure 3.3. *mls-2* is expressed in the duct and pore cell lineages. (A) Lineage tree showing florescence intensity of GFP::MLS-2 expression from 3D automated lineage analysis. Only 1 of 3 embryos that were lineaged is shown here. Only the ABplpa lineage is shown, but GFP::MLS-2 is symmetrically expressed in the ABprpa lineage, which gives rise to the excretory pore. See Supplemental Fig.3 for complete lineage analysis of all 3 embryos. (B) Ventral enclosure embryo expressing GFP::MLS-2, and (C) corresponding DIC image. Identities of some nuclei are indicated. CEPsh nuclei are dim and not visible at this stage. AWC nuclei are not in plane of focus. The pair of nuclei directly above the CEPsoVL/R nuclei are the sisters of the CEPsoVL/R that are fated to die (Sulston et al., 1983). The DB1/DB3 ventral cord motor neurons are sisters of the duct and pore, respectively. AIAL/R are amphid inter-neurons and DB6/DB7 are ventral cord motor neurons; expression in these cells initiates at this stage and is very faint. John I.Murray performed automated lineage analysis of GFP::MLS-2.

Figure 3.4. *mls-2* cooperates with the EGF-Ras-ERK pathway to promote duct differentiation and *lin-48/ovo* expression. (A) EGF-Ras-ERK signaling pathway downstream of *let-60*/Ras. *eor-1, lin-1/*ETS, and *sur-2/*Med23 are downstream nuclear effectors. *mls-2* acts downstream or parallel to the EGF-Ras-ERK pathway. (B) Rod-like (excretory) lethality shown as a fraction of total lethality. Other lethality scored as any worm that failed to reach L4 within 4 days. (C) Percentage of L1 worms that lacked *lin-48p::*GFP expression in duct. Note: *let-60(n1046)* and *lin-1(n304)* worms frequently had two *lin-48p*::GFP positive nuclei instead of one. (D) Percentage of L1 worms that lacked

a pore autocellular junction and worms that had a pore AJ junction connected directly to the canal cell (Pore AJ to canal), as scored with AJM-1::GFP. Note: *let-60(n1046)* and *let-60(n1046); mls-2(cs71)* were scored at late 3-fold instead of L1. Craig Stone built double mutant strains between *mls-2* and *eor-1* and *mpk-1* and characterized the excretory and non-excretory lethality. Craig Stone also built the *n1046;mls-2; lin-48p::*GFP strain.

Figure 3.5. *mls-2* affects duct and pore tube shape. AJM-1::GFP (left column) and *dct-5p*::mCherry (second column) in early L1s grown at 15°C, lateral view. Third column shows overlay. Fourth column shows schematic interpretation of phenotypes. (A,B) WT; n=20. (C-H) *mls-2(cs71); n=25*. (C,D) Pore cell collapsed and duct extending ventrally; n=11/25. Note: In both wild type and *mls-2* mutants, the duct sometimes displays a dorsal extension as seen here. (E,F) Both the duct and pore cells collapsed ventrally; n=3/25 (G,H) Pore cell AJ connected to canal cell, with duct cell presumably small or mispositioned; n=5/25. The remaining 6/25 *mls-2* mutants looked similar to *WT*. Asterisks indicate ventral cells with collapsed cell shapes. (I, J) *lin-48(sa469);* n=15. Duct cell shape appears similar to wild-type.

Figure 3.6. *mls-2* cell shape defects begin around the elongation stage of embryogenesis. (A, B) Schematics of wild type AJM-1::GFP junction pattern at 1.5 fold (A) and late 3-fold (B) stages. Parameters measured in I, J are indicated. (C-H) Excretory duct and pore junction patterns visualized with AJM-1::GFP. Images were inverted in

ImageJ for clarity. (C) WT and (D) *mls-2* embryos at 1.5-fold, lateral view. (E) WT and (F) *mls-2* mid 3-fold embryos, ventral view. Single pore opening lies just adjacent to the G2 and W epidermal cells. Note proximity of the canal cell junction (arrowhead) to the pore opening in F. (G, H) Measurements of AJ height and distance between AJ and canal cell junction at different time-points. Note: at 1.5-fold stage, height of AJ is duct and pore, and at all other stages, height of AJ is only the pore. Each point is a measurement from a single worm. Early 3-fold corresponds to 2 hours after the 1.5-fold stage. Late 3-fold corresponds to 6 hours after the 1.5-fold stage.

Figure 3.1

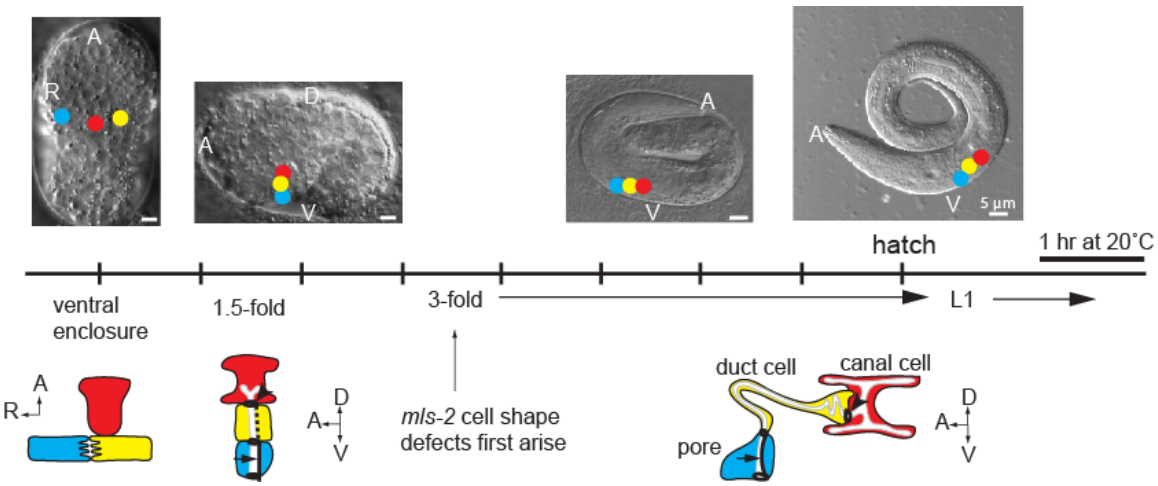
A
R
D
A
V
A
V
A
V
5 µm
hatch
1 hr at 20°C
ventral enclosure
1.5-fold
3-fold
L1
A
R
D
A
V
mls-2 cell shape defects first arise
duct cell
canal cell
pore
D
A
V

Figure 3.2

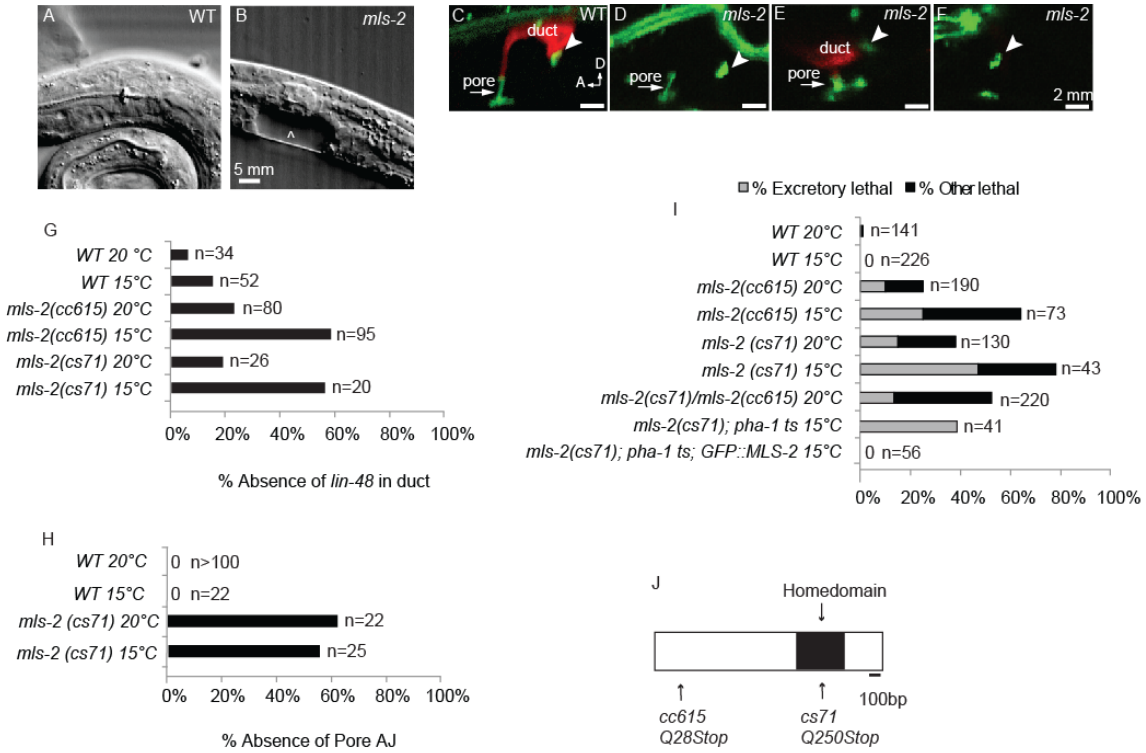
A
WT
B
mls-2
5 mm
C
WT
duct
pore
D
A
D
mls-2
pore
E
mls-2
duct
pore
F
mls-2
2 mm
G
WT 20 °C
WT 15°C
mls-2(cc615) 20°C
mls-2(cc615) 15°C
mls-2(cs71) 20°C
mls-2(cs71) 15°C
n=34
n=52
n=80
n=95
n=26
n=20
0%
20%
40%
60%
80%
100%
% Absence of lin-48 in duct
% Excretory lethal
% Other lethal
I
WT 20°C
WT 15°C
mls-2(cc615) 20°C
mls-2(cc615) 15°C
mls-2 (cs71) 20°C
mls-2 (cs71) 15°C
mls-2(cs71)/mls-2(cc615) 20°C
mls-2(cs71); pha-1 ts 15°C
mls-2(cs71); pha-1 ts; GFP::MLS-2 15°C
n=141
0 n=226
n=190
n=73
n=130
n=43
n=220
n=41
0 n=56
0%
20%
40%
60%
80%
100%
H
WT 20°C
WT 15°C
mls-2 (cs71) 20°C
mls-2 (cs71) 15°C
0 n>100
0 n=22
n=22
n=25
0%
20%
40%
60%
80%
100%
% Absence of Pore AJ
J
Homedomain
100bp
cc615
Q28Stop
cs71
Q250Stop

Figure 3.3

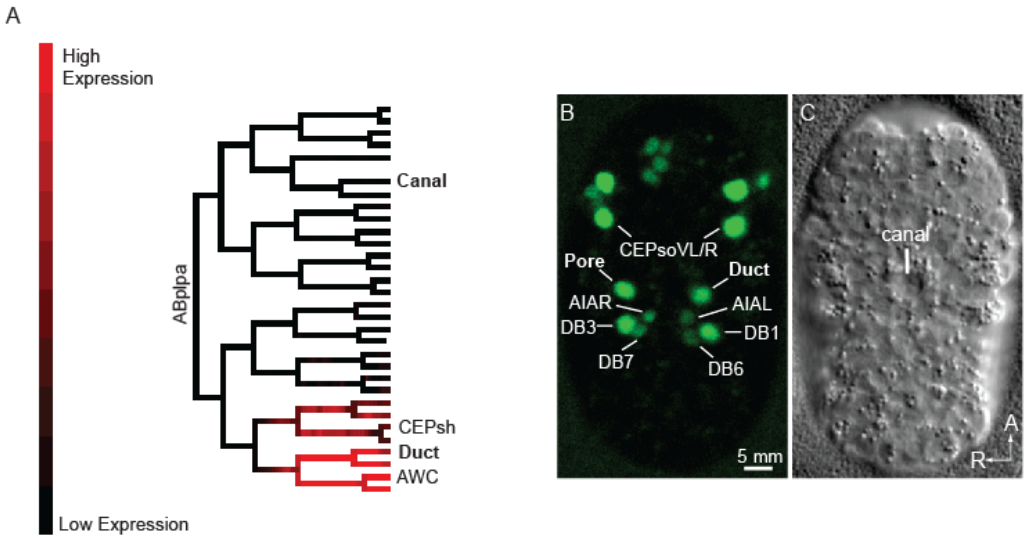
A
High
Expression
Low Expression
ABplpa
Canal
CEPsh
Duct
AWC
B
CEPsoVL/R
Pore
Duct
AIAR
AIAL
DB3
DB1
DB7
DB6
5 mm
C
canal
A
R

Figure 3.4

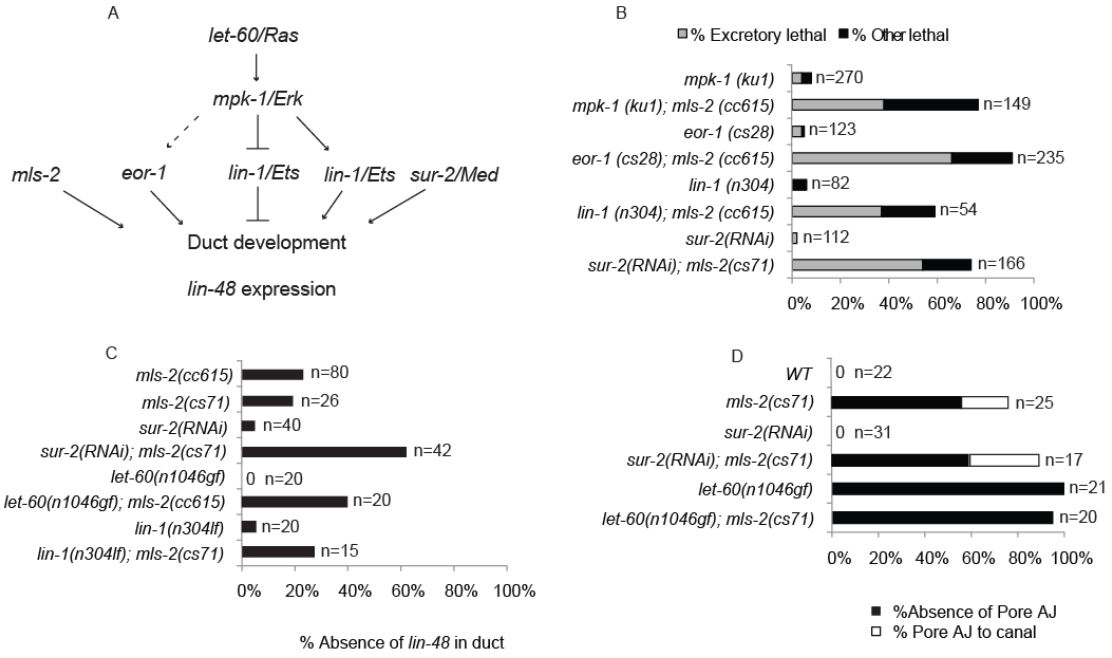
A
let-60/Ras
mpk-1/Erk
mls-2
eor-1
lin-1/Ets
lin-1/Ets
sur-2/Med
Duct development
lin-48 expression
B
% Excretory lethal
% Other lethal
mpk-1 (ku1)
n=270
mpk-1 (ku1); mls-2 (cc615)
n=149
eor-1 (cs28)
n=123
eor-1 (cs28); mls-2 (cc615)
n=235
lin-1 (n304)
n=82
lin-1 (n304); mls-2 (cc615)
n=54
sur-2(RNAi)
n=112
sur-2(RNAi); mls-2(cs71)
n=166
0% 20% 40% 60% 80% 100%
C
mls-2(cc615)
n=80
mls-2(cs71)
n=26
sur-2(RNAi)
n=40
sur-2(RNAi); mls-2(cs71)
n=42
let-60(n1046gf)
0 n=20
let-60(n1046gf); mls-2(cc615)
n=20
lin-1(n304lf)
n=20
lin-1(n304lf); mls-2(cs71)
n=15
0% 20% 40% 60% 80% 100%
% Absence of lin-48 in duct
D
WT
0 n=22
mls-2(cs71)
n=25
sur-2(RNAi)
0 n=31
sur-2(RNAi); mls-2(cs71)
n=17
let-60(n1046gf)
n=21
let-60(n1046gf); mls-2(cs71)
n=20
0% 20% 40% 60% 80% 100%
%Absence of Pore AJ
% Pore AJ to canal

Figure 3.5

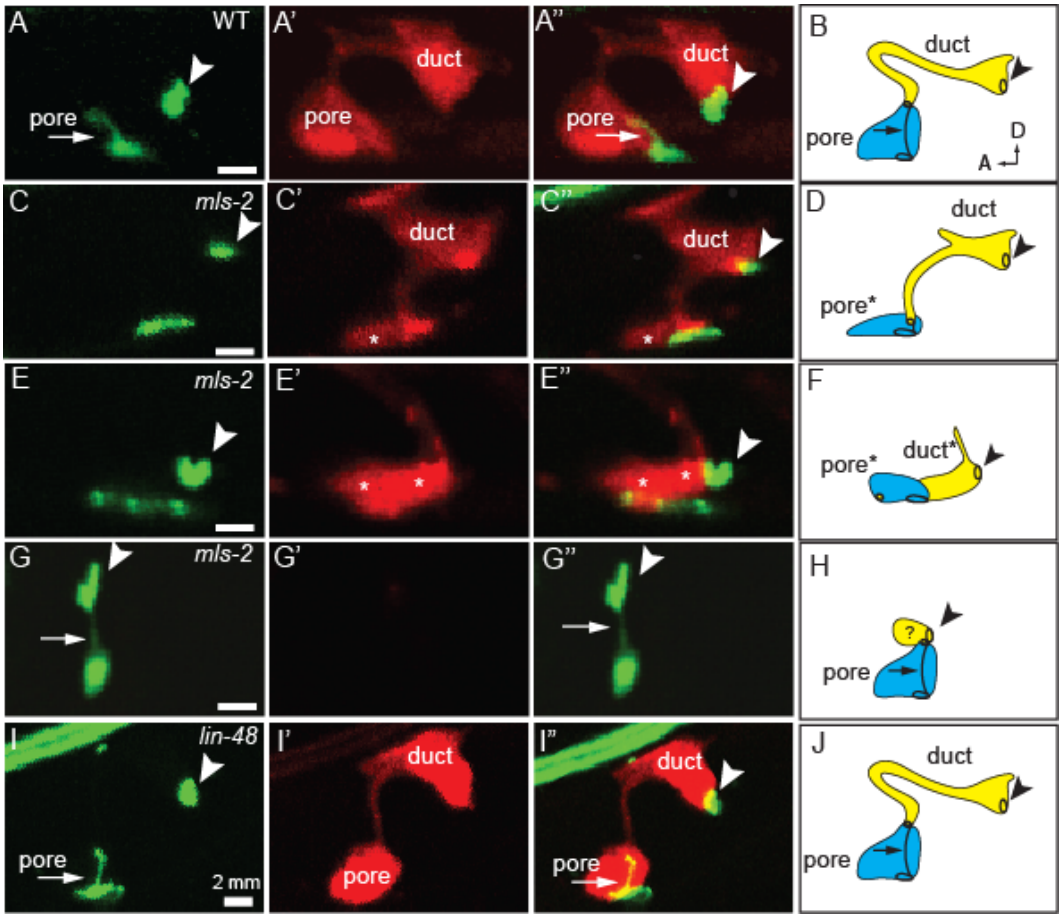
A
WT
pore
A'
duct
pore
A"
duct
pore
B
duct
pore
D
A
C
mls-2
C'
duct
C"
duct
D
duct
pore*
E
mls-2
E'
E"
F
pore*
duct*
G
mls-2
G'
G"
H
?
pore
I
lin-48
pore
2 mm
I'
duct
pore
I"
duct
pore
J
duct
pore

Figure 3.6

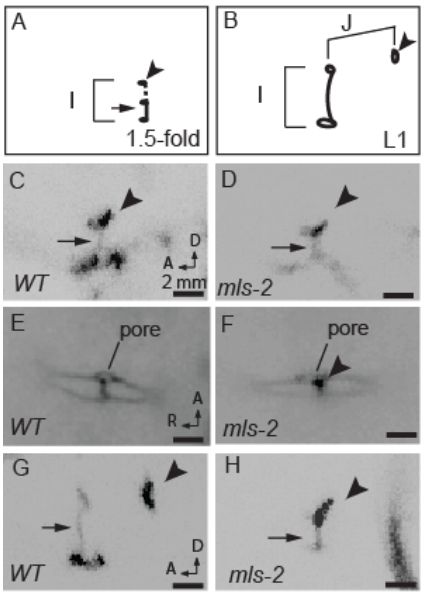
A
I
1.5-fold
B
J
I
L1
C
D
WT
2 mm
mls-2
E
pore
WT
F
pore
mls-2
G
WT
H
mls-2

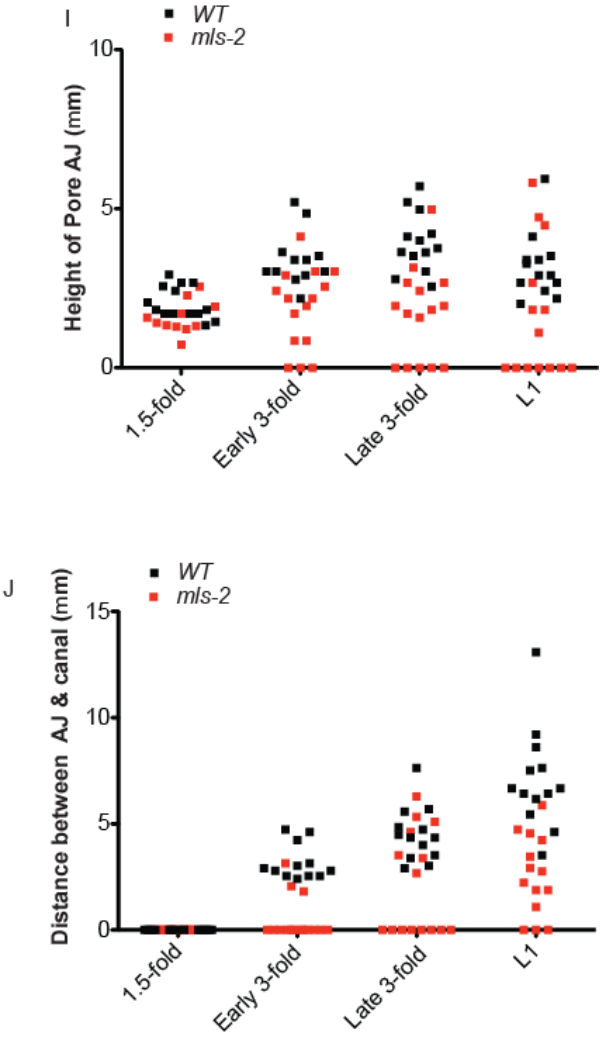
I
WT
mls-2
Height of Pore AJ (mm)
10
5
0
1.5-fold
Early 3-fold
Late 3-fold
L1
J
WT
mls-2
Distance between AJ & canal (mm)
15
10
5
0
1.5-fold
Early 3-fold
Late 3-fold
L1

Chapter Four:

ASSESSING THE ROLE OF THE CYTOSKELETON IN PROMOTING MORPHOGENESIS IN THE *C.ELEGANS* EXCRETORY SYSTEM

Summary

The cytoskeleton, which consists of actin, microtubule, and intermediate filaments, is the main determinant in establishing cell shape. All three cells of the *C.elegans* excretory system adopt complex elongated morphologies, analogous in structure to neurons and glia. Many cytoskeletal genes are expressed in cell type specific patterns to influence cell appropriate shapes. I took an unbiased RNAi approach in a sensitized background to identify individual cytoskeletal isoforms involved in promoting morphogenesis in the excretory system. Our screening did not uncover a role for any specific cytoskeletal isoform. However, we did uncover a novel genetic interaction in the early embryo between the Nkx5/HMX homeodomain protein *mls-2* and several microtubule and actin isoforms.

Introduction

The *C.elegans* excretory system provides a genetically tractable system to uncover roles for individual cytoskeletal isoforms during epithelial tube morphogenesis. Neurons are elongated cells that require the cytoskeleton for shape and polarization (Lee and Van Vactor, 2003), and the cells of the *C.elegans* excretory system are similar in structure to neurons. As is the case in the nervous system, it is also unclear which specific cytoskeletal genes promote and maintain shape in the *C.elegans* excretory system.

MLS-2 is an Nkx5/HMX homeodomain transcription factor that is required for proper shape in the duct and pore cells (Chapter Three). Cell shape defects first arise in *mls-2* mutants at the time when the duct and pore normally begin elongating into complex morphologies (Chapter Three). The cell shape defects in *mls-2* mutants suggest a failure of the duct and pore to maintain their cytoskeleton. The *mls-2* lethal excretory phenotype is cold sensitive (Chapter Three), and microtubules have been shown to depolymerize at low temperatures in all systems studied, including *C. elegans* (Chalfie and Thomson, 1982; Melki et al., 1989). I hypothesized that MLS-2 may regulate cytoskeletal genes that directly impact the microtubule cytoskeleton.

I sought to identify which microtubule, actin, or intermediate filament isoform is required for excretory system morphogenesis, and/or interact with MLS-2. Since functional redundancy is always an issue with large gene families (9 α-tubulins, 6 β-tubulins, 1 γ-tubulin; 5 actins, 9 IFs), I reduced each microtubule, actin, and intermediate filament (IF) isoform using RNA interference (RNAi) in both a wild type and *mls-2* background. I used *mls-2* as a genetically sensitized background, with the idea that this may alleviate the problem of genetic redundancy. However, it appears that genetic redundancy might still have been an impediment , as I did not identify a role of any cytoskeletal isoform in excretory system morphogenesis. Nonetheless, I did reveal a surprising genetic interaction between *mls-2* and several microtubule and actin isoforms in a role outside of excretory system development.

Results

RNAi enhancer screen to identify specific subunits involved in excretory system morphogenesis

To identify a role for cytoskeletal isoforms in excretory system development, wild type and *mls-2* worms were treated from the fourth larval stage and onwards with RNAi against 8 α-tubulin, 5 β-tubulin, 1 γ-tubulin, 4 actin, and 9 IF isoforms in the *C.elegans* genome. The F1 progeny from the L4 treated worms were screened for rod-like (excretory) lethal larvae. At least 4 separate plates were scored for each RNAi clone, and the results were averaged. Results from the RNAi screening are described below.

mls-2 has synthetic embryonic interactions with tubulin and actin

RNAi against each α, β, and γ-tubulin isoform in wild type worms did not yield any excretory lethal phenotypes (Fig 4.1 A). In addition, RNAi against the tubulin genes in *mls-2* mutants did not enhance the excretory lethal phenotype of *mls-2* mutants (Fig 4.2). Similarly, RNAi against actin and IF isoforms did not cause excretory phenotypes in wild type, or enhancement of excretory phenotypes in *mls-2* mutants (Figs 4.2, 4.3). However, genetic interactions were detected between *mls-2* and actin and microtubule isoforms in early embryos.

When *tba-1* was reduced by RNAi, more than half the worms arrested with embryonic lethality (Fig 4.1). The open reading frame of TBA-1 is 89% identical to TBA-2, and RNAi of *tba-1* has been shown to also reduce *tba-2* (Phillips et al., 2004). RNAi specifically targeted against *tba-1* results in only 10% embryonic lethality, while

combined RNAi targeted specifically against *tba-1* and *tba-2* results in 100% embryonic lethality (Lu and Mains, 2005). Therefore, the 75% embryonic lethality we observed knocking down *tba-1* RNAi is likely a combined knockdown of *tba-1* and *tba-2*. We could not grow the *tba-2* RNAi clone for unknown technical reasons. *mls-2* mutants significantly enhanced the embryonic lethality of *tba-1* RNAi (Fig 4.1). RNAi against *tbg-1* and *tbb-4* did not result in embryonic lethality (Fig 4.1). However, when *mls-2* mutants were treated with *tbb-4* or *tbg-1* RNAi, significant embryonic lethality was observed (Fig 4.1). *tbb-1* RNAi knocks down both *tbb-1* and *tbb-2* (Ellis et al., 2004), making embryonic lethality too high to test for enhancement by *mls-2* (Fig 4.1).

To confirm that the embryonic interactions between *mls-2* and these tubulin genes was not an artifact of using one particular *mls-2* allele, I used a second null allele of *mls-2* repeating the RNAi protocol in quadruplicate. I observed similar results with both *mls-2* alleles, suggesting that these were true genetic interactions with tubulin genes (Fig 4.1 B). Based on my observation by stereomicroscopy, I estimate that embryos arrested before the 300 cell stage, which is in the first half of embryogenesis. In summary, *mls-2* genetically interacted with *tba-1*, *tbg-1*, and *tbb-4* during a critical process during early embryonic development.

Reduction of *act-1* and *act-5* by RNAi resulted in embryonic lethality that was significantly increased in *mls-2* mutants (Fig 4.2). Embryonic lethality of *act-2* and *act-3* was nearly 100%, making it difficult to test for genetic interactions (Fig 4.2). An *act-2* deletion allele or RNAi specifically targeting *act-3* alone results in no observable phenotypes (Willis et al., 2006). However, combining the *act-2* deletion allele with *act-3*

specific RNAi results in 100% embryonic lethality (Willis et al., 2006). Therefore, our depletion of either *act-2* or *act-3* using RNAi likely reduced both genes simultaneously. Despite the 100% embryonic lethal phenotype of *act-2* or *act-3* RNAi, we still observed genetic interactions with *mls-2* (Fig 4.2). *mls-2* mutants treated with *act-2* RNAi were completely sterile (Fig 4.2), suggesting a potential role for *mls-2* in the germline.

Reducing all 9 IF genes by RNAi did not result in embryonic lethality or excretory lethality in either wild type or *mls-2* worms (Fig 4.3). Reduction of *ifa-2* (previously known as *mua-6*) results in first larvae stage (L1) arrest due to defects in muscle attachment (Plenefisch et al., 2000). We consistently saw L1 arrest when depleting *ifa-2* by RNAi, demonstrating that our RNAi knockdown of IFs was sufficient to reproduce known phenotypes (data not shown). Nonetheless, we did not uncover a role in excretory system morphogenesis for any IF, or detect a genetic interaction between IFs and *mls-2*.

mls-2 and tubulin null mutants do not genetically interact

We next analyzed tubulin null mutants alone and in combination with *mls*-2 mutants. Null mutations should eliminate maternal and zygotic expression of the tubulin gene of interest and affect all cell types equally, including the excretory system. Therefore using null mutants should circumvent some of the caveats of the RNAi screening (see Discussion). We focused on microtubules because we demonstrated that the microtubule cytoskeleton is disorganized in the duct and pore in *mls-2* mutants

(Chapter Three). *mls-2* mutants also have cold sensitive defects (Chapter Three), and microtubules have been shown to depolymerize at low temperatures (Chalfie and Thomson, 1982; Melki et al., 1989).

When I scored the two null mutants *tba-1(ok1135)* and *tbb-1(gk207)* at both 20°C and 15°C, we did not detect any embryonic or excretory lethality (Fig 4.4). I did detect very little embryonic lethality of *tbb-1(gk207)* at 15°C (Fig 4.4). *tbg-1(t1465)* is a hypomorphic allele that disrupts interactions between γ-tubulin and αβ-tubulin heterodimers (Hannak et al., 2002). *tbg-1(t1465)* is also a maternal effect lethal mutant so I had to obtain homozygous worms from heterozygous mothers. I observed almost no embryonic lethality or excretory lethality with *tbg-1(t1465)* (Fig 4.4). Consistent with the single mutant phenotypes, none of the tubulin mutations combined with *mls-2* enhanced excretory or embryonic lethality (Fig 4.4). Although I did not observe any excretory phenotypes with the tubulin mutants, I did expect to recapitulate the embryonic phenotypes caused by RNAi (Fig 4.1). The non-specific RNAi knocked down multiple tubulin genes, while the mutants only targeted one gene. Therefore, embryonic and possibly excretory phenotypes may only be uncovered with a knockdown of multiple tubulin isoforms.

tubulin temperature sensitive mutants do not have excretory phenotypes

In a final attempt to determine which tubulin isoforms are involved in excretory system morphogenesis I utilized two tubulin temperature sensitive *(ts)* mutants, *tba-1 (or346)* and *tbb-2(or362)*, that are wild type when grown at 15°C and completely embryonic lethal when grown at 25°C (Phillips et al., 2004). The fully penetrant

embryonic lethality at high temperatures suggested that multiple tubulin isoforms were affected by these dominant *ts* mutations. I first grew both *ts* mutants at an intermediate temperature of 20°C, in an effort to identify excretory phenotypes. However, both *ts* mutants grown at 20°C displayed a mix of wild type worms and embryonic lethality, but no other observable phenotypes (data not shown).

I next used the tubulin *ts* mutants to reduce tubulin activity at two different time-points in development. It is clear that most tubulin isoforms have critical roles in early embryogenesis. I hypothesized that if I reduced tubulin genes after early critical roles in embryonic development, but before excretory system morphogenesis, I would recover some worms that died with rod-like (excretory) lethality. When I shifted *tba-1 (or346)* worms from the permissive to non-permissive temperature at either 1 hour or 3 hours after egg lay (AEL), all laid eggs grew up and hatched normally (Fig 4.5), indicating that the critical window when this tubulin is required for embryonic development is after 3 hours post egg lay. *tba-1 (or346)* shifts also suggested that *tba-1* and the other tubulin isoforms affected by the dominant *tba-1* mutation, are not required for excretory system morphogenesis.

When I shifted *tbb-2(or362)* mutants from the permissive to non-permissive temperature at 1 hour AEL, most embryos died (Fig 4.5). However, when *tbb-2(or362)* mutants were shifted from the permissive to non-permissive at 3 hours AEL, most of the embryos lived (Fig 4.5). Therefore the critical time when *tbb-2* and the tubulin genes affected by the dominant *tbb-2* mutation are required is just a few hours after egg lay.

However, at either time I shifted *tbb-2 ts* mutants, I never observed any excretory lethality (Fig 4.5).

Tubulin is still expressed in *mls-2* mutants with cell shape defects

Since I could not identify any tubulin isoform that genetically interacted with *mls-2*, I wanted to determine if microtubules were disorganized or not expressed in the duct and pore in *mls-2* mutants. To visualize microtubules, I utilized the DM1A mouse polyclonal alpha-tubulin antibody, which has been shown to cross react with *C.elegans* alpha-tubulin (Gonczy et al., 1999). In both wild-type and *mls-2* mutants at the 1.5-fold stage, anti-tubulin labeled both the duct and pore cells (Fig. 4.6A,B) with a pattern similar to AJM-1::GFP and DLG-1::GFP (Abdus-Saboor et al., 2011). In wild-type newly hatched L1 larvae, tubulin was apically enriched in both the duct and pore (Fig 4.6C). In *mls-2* mutants tubulin was still present in the duct and pore (Fig 4.6D,E). Some *mls-2* L1 larvae had a normal AJM-1::GFP pattern and tubulin localization, corresponding to the percentage of *mls-2* worms that grow up to look wild type (Fig 4.6D). Not surprisingly, in 7/7 *mls-2* mutants with cell shape defects, tubulin appeared slightly disorganized, although still managing to display some sub-cellular localization (Fig 4.6E). I hypothesize that as the duct and pore lose shape in *mls-2* mutants, the microtubule cytoskeleton may become disorganized or tangled in the collapsed duct and pore cells. The best way to visualize the microtubule cytoskeleton in *mls-2* mutants would be to analyze a tubulin reporter *in vivo*. *In vivo* analysis could determine if microtubule disorganization is a primary or secondary defect in *mls-2* mutants.

Discussion

Targeting single cytoskeletal isoforms by RNAi did not uncover a requirement for any individual gene in excretory system morphogenesis. RNAi knockdown of cytoskeletal genes did produce embryonic lethality comparable to previously published reports. I unexpectedly found that embryonic lethality caused by knocking down several actin or tubulin genes was enhanced in an *mls-2* background. Cell shape abnormalities in *mls-2* mutants are accompanied by abnormalities in microtubule cytoskeleton organization. However, it is unclear how MLS-2 could be affecting the microtubule cytoskeleton. Below I discuss technical reasons that might have prevented me from discovering roles for individual cytoskeletal genes in excretory morphogenesis, and also ways to alleviate these difficulties. I conclude the discussion by exploring the embryonic requirement for MLS-2.

Insufficient knockdown of cytoskeletal isoforms by RNAi

C.elegans can be treated with RNAi by three different methods: injecting, soaking, feeding, or transgenesis. Feeding is the simplest but least effective and most variable of the four methods (Ahringer, 2006). Obtaining negative results from RNAi can be difficult to interpret, as the false negative result over all genes by feeding RNAi is 30% (Kamath et al., 2003). To confirm negative RNAi results secondary tests need to be performed such as RT-PCR and antibody staining (Ahringer, 2006). In our RNAi screening of cytoskeletal genes, RNA knockdown was sufficient to produce embryonic lethality and larval lethality (*ifa-2* RNAi), but may not have been reduced enough to

produce excretory lethality. In addition to RNAi by feeding being variable at times, some tissues in *C.elegans*, such as neurons, are recalcitrant to RNAi (Kamath et al., 2001; Tavernarakis et al., 2000).

Our lab has known for years that RNAi works very poorly in the *C.elegans* excretory system. Few genes however, do produce robust excretory phenotypes when targeted with RNAi in sensitized genetic backgrounds (see Chapter Five). A current postdoctoral fellow in the lab, Jean Parry, is attempting to improve the efficacy of RNAi in the excretory system by driving the *sid-1* gene in the duct and pore. SID-1 is a transmembrane protein required for systemic RNAi in *C.elegans* (Winston et al., 2002). SID-1 expressed in neurons by a pan-neuronal driver allows RNAi to work more efficiently in neurons (Calixto et al., 2010), a cell type that had previously been recalcitrant to RNAi. If we can make the duct and pore hyper-sensitive to RNAi in a SID-1 expressing strain, we can perform the cytoskeletal screening over again, with more confidence that we are reducing RNA in our cells of interest.

Overcoming redundancy of microtubule isoforms

A second caveat to this screen is that many cytoskeletal isoforms are required during excretory system morphogenesis. Functional redundancy between microtubule isoforms in *C.elegans* has been observed in numerous processes (Driscoll et al., 1989; Lu et al., 2004; Phillips et al., 2004; Wright and Hunter, 2003). Recently, several groups have been able to overcome redundancy, not by knocking down individual isoforms, but rather by targeting all pools of stable microtubules.

The Bargmann and Chuang labs designed a protocol to depolymerize microtubules in *C.elegans* embryos using the microtubule depolymerizing chemical nocodazole (Chang et al., 2011). Treating embryos between 0-6 hours after egg lay with nocodazole resulted in a pair of olfactory neurons called AWC, having shortened axons and defective synaptic signaling at the nerve ring (Chang et al., 2011). In addition, other cell types were affected by nocodazole treatment, resulting in worms with uncoordinated phenotypes (Chang et al., 2011). This unbiased approach for targeting stable microtubules uncovered a novel role for microtubules in localizing a calcium signaling complex during neuronal differentiation (Chang et al., 2011).

At a recent International *C.elegans* Meeting the Labouesse lab described a protocol that used the microtubule severing protein Spastin to depolymerize all microtubules (Sophie Quintin, personal communication). The Labouesse lab expressed *spastin* under cell specific drivers, or in all cells under a heat-shock promoter. Microtubules were disrupted in cells that expressed *spastin*, demonstrating that their protocol did disrupt microtubules. Interestingly, expressing *spastin* in all cells after mid-embryogenesis did not result in any lethal phenotypes, suggesting that microtubule function is not required for morphogenesis in late embryogenesis (Sophie Quintin, personal communication). The cells of the excretory system undergo considerable morphogenesis during late embryogenesis (see Chapter One). Therefore, the Labouesse lab's results may directly impact the interpretations from our experiments reducing individual tubulin isoforms. While microtubules may promote shape in the excretory

system, depleting microtubules may only lead to subtle excretory defects and not lethal defects.

An analogous approach of treating embryos with microtubule depolymerizing agents can be taken to define a window when microtubules are required for excretory system morphogenesis. In addition to looking for robust lethal phenotypes when disrupting microtubules, we should also look for defects in cell shape in the excretory system. If depolymerizing stable microtubules leads to cell shape defects in the duct and pore, this would lend support to the hypothesis that MLS-2 turns on specific microtubule isotypes to promote cell shape.

Embryonic role for MLS-2 uncovered

The embryonic genetic interaction between *mls-2* and several tubulin and actin isoforms was surprising for several reasons. Firstly, the expression pattern of MLS-2 is not consistent with an early role for MLS-2 in embryonic development. A rescuing MLS-2::GFP translational reporter cannot be detected until the 50-cell stage (Jiang et al., 2005)(Chapter Three), and *mls-2* RNA is not detected in the maternal germline or early embryos by Fluorescence In-Situ Hybridization(http://nematode.lab.nig.ac.jp/). Secondly, *mls-2* single mutants rarely have any embryonic lethality, and most of the reported phenotypes are in larvae (Jiang et al., 2005; Kim et al., 2010; Yoshimura et al., 2008).

tbg-1, tbb-4, tba-1, act-2, and *act-3* all act during the one-cell stage, and depletion of these isoforms results in early embryonic arrest (Hannak et al., 2002; Phillips et al.,

2004; Willis et al., 2006). TBG-1 is required during interphase to assemble centrosomal asters, but not to nucleate stable populations of cytoplasmic microtubules (Hannak et al., 2002). TBA-1 subunits incorporate into microtubules, and *tba-1* is redundant with the highly similar isoform *tba-2* (Phillips et al., 2004). *tba-1* and *tba-2* double mutants have abnormal mitotic spindles that result in the mis-segregation of key developmental determinants (Phillips et al., 2004). *act-2* and *act-3* are redundant in early embryos for microfilament dependent processes such as cytokinesis (Willis et al., 2006). TBB-4 acts post-embryonically to promote differentiation of sensory cilia and ray neurons in the male tail (Hao et al., 2011; Hurd et al., 2010; Portman and Emmons, 2004). To our knowledge, the data presented above is the first evidence of embryonic lethality caused by *tbb-4* depletion. Therefore TBB-4, like MLS-2, has both embryonic and post-embryonic roles. The genetic interactions between *mls-2* and the tubulin and actin isoforms (*tba-1, tbb-4, tbg-1, act-2, act-3*), suggest that *mls-2* acts in a parallel pathway with these genes. Thus MLS-2 may turn on genes in the embryo that also regulate processes ranging from assembling centrosomal asters to promoting cytokinesis.

The genetic interactions between *mls-2* and the tubulin and actin isoforms could result from MLS-2 acting at one of two time-points in development. MLS-2 could be required in the maternal germline or zygotically around the one-cell stage, or alternatively, MLS-2 could be required after the 50-cell stage. The expression pattern of MLS-2 is more consistent with the latter model. In the alternative scenario, the embryonic lethality observed in the *mls-2* and cytoskeletal double knockdowns, would consists of both early and mid-stage embryonic lethality. A precise study of the stages

when all embryos arrest would help decipher between these two models of when MLS-2 acts. These data have not only uncovered a role for MLS-2 during mid-stage embryogenesis, but also for several cytoskeletal isoforms, which had previously been shown to work only in early embryogenesis or in larvae. To what extent any of the genetic interactions between *mls-2,* and tubulin or actin isoforms in the embryo also extend to the excretory system, awaits further investigation.

Materials and Methods

Strains and alleles

Bristol N2 was the wild-type strain. Strains were maintained and manipulated by standard methods unless otherwise noted. Descriptions of each gene can be found at www.wormbase.org. Mutant alleles used are LG1*: tba-1(or346)* (Phillips et al., 2004), *tba-1(ok1135)* (Baran et al., 2010). LGIII*: tbb-1(gk207)* (Lu et al., 2004)*, tbb-2(or362)* (Ellis et al., 2004)*, tbg-1(t1465)* (Hannak et al., 2002). LGX*: lon-2(e678), mls-2(cc615)* (Jiang et al., 2005)*, mls-2(cs71)*.

RNA interference (RNAi)

RNAi was performed by placing wild type and *mls-2(cs71)* L4 stage worms on feeding plates with HT-115 E. coli expressing RNA against *unc-22* (negative control) or *tba-1, tba-2, tba-4, tba-5, tba-5, tba-6, tba-7, tba-8, tba-9, tbb-1, tbb-2, tbb-3, tbb-4, tbb-6, tbg-1, act-1, act-2, act-3, act-5, ifa-1, ifa-2, ifa-3, ifa-4, ifb-1, ifc-1, ifc-2, ifd-1, ifd-2*. Feeding

plates were made by growing *E.coli* cultures for overnight, adding IPTG to 1mM concentration, and then plating. 48 hours after being placed onto feeding plates of control RNAi or RNAi against a single cytoskeletal isoforms, multiple worms from each original RNAi plate were picked to new RNAi plates and allowed to lay eggs for approximately 6 hours.

Phenotypic Scoring

To score for rod-like (excretory) lethality, hermaphrodites treated with control or experimental RNAi for 48 hours were allowed to lay eggs for approximately 6 hours. Percent rod-like lethal was determined by the proportion of progeny that were visible as rods 48 hours post-egg lay. Percent embryonic lethal was determined by the proportion of progeny that did not hatch by 24 hours post-egg lay.

Immunostaining

Embryos were permeabilized by freeze-cracking and fixed in methanol as described (Duerr et al., 1999) and incubated with primary antibodies overnight at 4°C and with secondary antibodies for 2hrs at room temperature. The following antibodies were used: preadsorbed rat anti-MLS-2 (CUMCR6; 1:400) (Jiang et al., 2005), goat polyclonal anti-GFP (Rockland; 1:50), rabbit polyclonal anti-DLG-1 (1:50 to 1:100) (Segbert et al., 2004), mouse monoclonal anti-tubulin, clone DM1A (Sigma; 1:50). All secondary antibodies were from Jackson ImmunoResearch Laboratories and were used at a dilution of 1:50 to 1:200.

Acknowledgements

I thank the Caenorhabditis Genetics Center (University of Minnesota, USA) for providing all the tubulin strains analyzed in this chapter. All of the RNAi clones were from the Julia Ahringer RNAi feeding library.

Figure Legends

Figure 4.1. *mls-2* and tubulin have synthetic embryonic interactions. (A) Bar graph showing percentage of worms with either embryonic lethality or rod-like (excretory lethality). Results from 3-4 plates were averaged together. *unc-22* used as negative RNAi control. n>100 for each genotype. All statistics were performed using the Fisher's exact test. $p<0.05$ considered statistically significant. **$p<0.001$ for embryonic lethality comparing *mls-2; (unc-22 RNAi)* and *mls-2* in combination with *tba-1(RNAi),tbb-4(RNAi),* and *tbg-1(RNAi).* p is not statistically significant for any other combinations, including excretory and embryonic lethality. Note: embryonic lethality caused by RNAi of most tubulin isoforms leads to high embryonic lethality, making it appear that *mls-2* rod-like lethality is reduced in these backgrounds. However, *mls-2* worms that die as embryos do not live long enough to die from excretory lethality. (B) Bar graphs showing percentage of worms with either embryonic lethality or rod-like (excretory lethality). Results from 3-4 plates were averaged together. *unc-22* used as negative RNAi control. The two bar graphs were taken from the same data, but separated by embryonic and rod-like lethality. A second null allele of mls-2*(cc615)* was also used. n>100 for each

genotype. **p<0.001 for embryonic lethality for both *mls-2* alleles with *unc-22(RNAi)* compared to *mls-2* in combination with *tba-1(RNAi),tbb-4(RNAi),* and *tbg-1(RNAi)*.

Figure 4.2. *mls-2* and actin have synthetic embryonic interactions. (A) Bar graph showing percentage of worms with either embryonic lethality or rod-like (excretory lethality). Results from 3-4 plates were averaged together. *unc-22* used as negative RNAi control. n>100 for each genotype. All statistics were performed using the Fisher's exact test. p<0.05 considered statistically significant. **p<0.001 for embryonic lethality comparing *mls-2; (unc-22 RNAi)* and *mls-2* in combination with *act-5(RNAi);* ***p=0.0006 embryonic lethality comparing *mls-2;(unc-22 RNAi)* and *mls-2; (act-1 RNAi)*. p is not statistically significant for any other combinations, including excretory and embryonic lethality. Note: embryonic lethality caused by RNAi of actin isoforms leads to high embryonic lethality, making it appear that *mls-2* rod-like lethality is reduced in these backgrounds. However, *mls-2* worms that die as embryos do not live long enough to die from excretory lethality.

Figure 4.3. *mls-2* does not genetically interact with intermediate filaments. (A) Bar graph showing percentage of worms with either embryonic lethality or rod-like (excretory lethality). Results from 3-4 plates were averaged together. *unc-22* used as negative RNAi control. n>50 for each genotype. All statistics were performed using the Fisher's exact test. p<0.05 considered statistically significant. p is not statistically significant for any *mls-2; unc-22(RNAi)* versus *mls-2; IF RNAi* combinations, including excretory and embryonic lethality.

Figure 4.4. *mls-2* and tubulin null mutants do not genetically interact. Bar graph showing percentage of worms with either embryonic lethality or rod-like (excretory lethality) at two different temperatures. Note: *tbg-1(t1465)* homozygous worms were obtained from *tbg-1(t1465)* heterozygous mothers. n>30 for each genotype and temperature. All statistics were performed using the Fisher's exact test. $p<0.05$ considered statistically significant. p is not statistically significant for any single versus double mutant combinations comparing similar temperatures, including excretory and embryonic lethality.

Figure 4.5. tubulin temperature sensitive mutants do not have excretory phenotypes. Worms were grown at 15C then shifted to 25C at either 1 hour after egg lay (AEL) or 3 hours after egg lay (AEL). Bar graph shows percentage of shifted embryos that lived or died as embryos after being shifted to 25C. n>30 for each genotype and shift.

Figure 4.6. Tubulin is still expressed in *mls-2* mutants with cell shape defects. (A,B) 1.5-fold embryos carrying a *lin-48p*::GFP reporter, stained with anti-tubulin (red) and anti-GFP (green) antibodies. Tubulin marks both the duct and pore cells in Wild-type (A) and *mls-2* (B), but *mls-2* fails to express *lin-48p*::GFP. (C-E) L1 worms expressing AJM-1::GFP, stained with anti-tubulin (red) and anti-GFP (green) antibodies. (C) WT. Tubulin localized apically in both the duct and pore cells. (D) *mls-2* mutant with normal junction and tubulin pattern. (E) *mls-2* mutant with no pore AJ. Tubulin pattern is disorganized. (C'''- E''') Schematic interpretations of C-E.

Figure 4.1 A

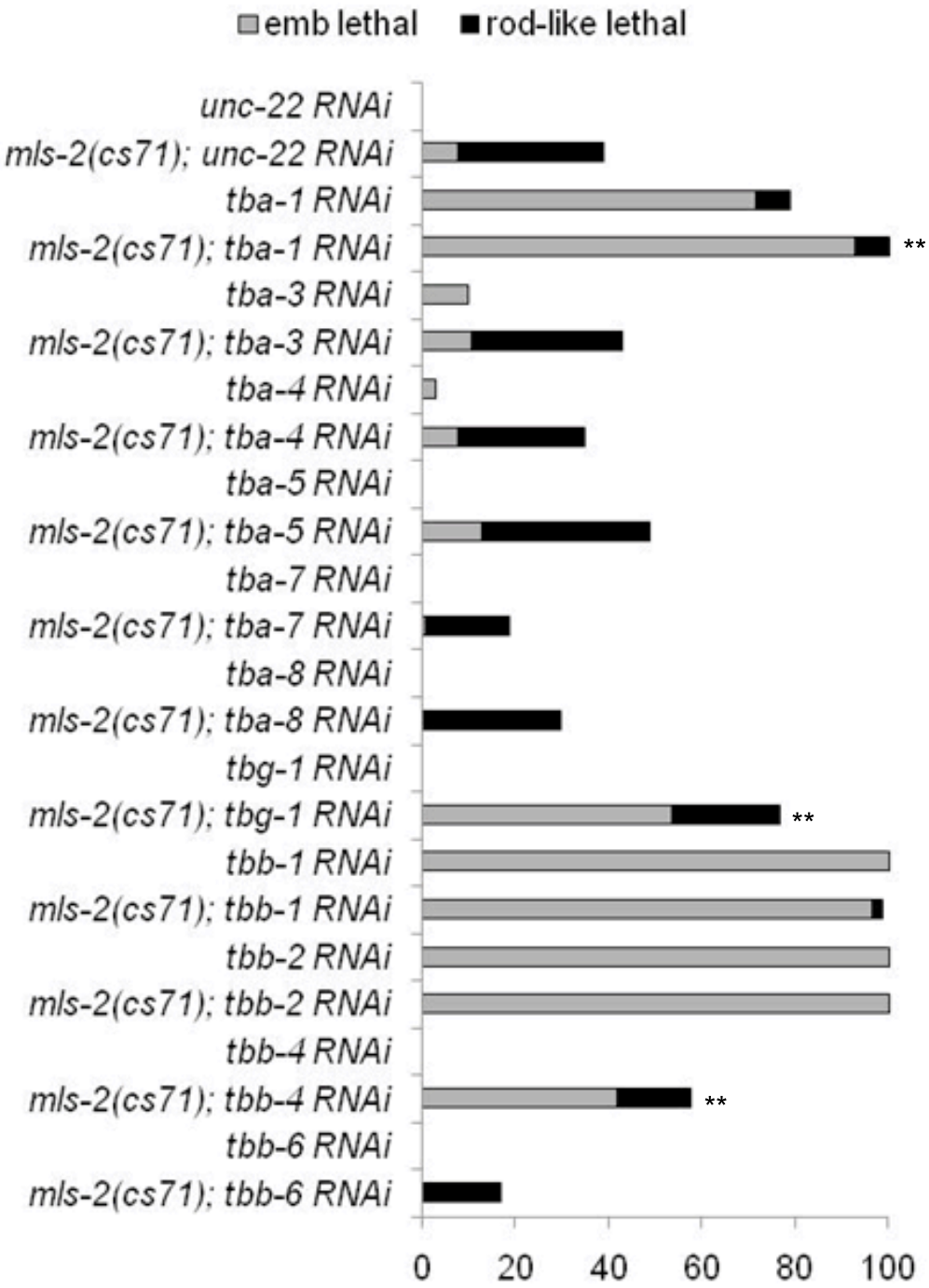
emb lethal
rod-like lethal
unc-22 RNAi
mls-2(cs71); unc-22 RNAi
tba-1 RNAi
mls-2(cs71); tba-1 RNAi
tba-3 RNAi
mls-2(cs71); tba-3 RNAi
tba-4 RNAi
mls-2(cs71); tba-4 RNAi
tba-5 RNAi
mls-2(cs71); tba-5 RNAi
tba-7 RNAi
mls-2(cs71); tba-7 RNAi
tba-8 RNAi
mls-2(cs71); tba-8 RNAi
tbg-1 RNAi
mls-2(cs71); tbg-1 RNAi
tbb-1 RNAi
mls-2(cs71); tbb-1 RNAi
tbb-2 RNAi
mls-2(cs71); tbb-2 RNAi
tbb-4 RNAi
mls-2(cs71); tbb-4 RNAi
tbb-6 RNAi
mls-2(cs71); tbb-6 RNAi
**
**
**
0
20
40
60
80
100

Figure 4.1 B

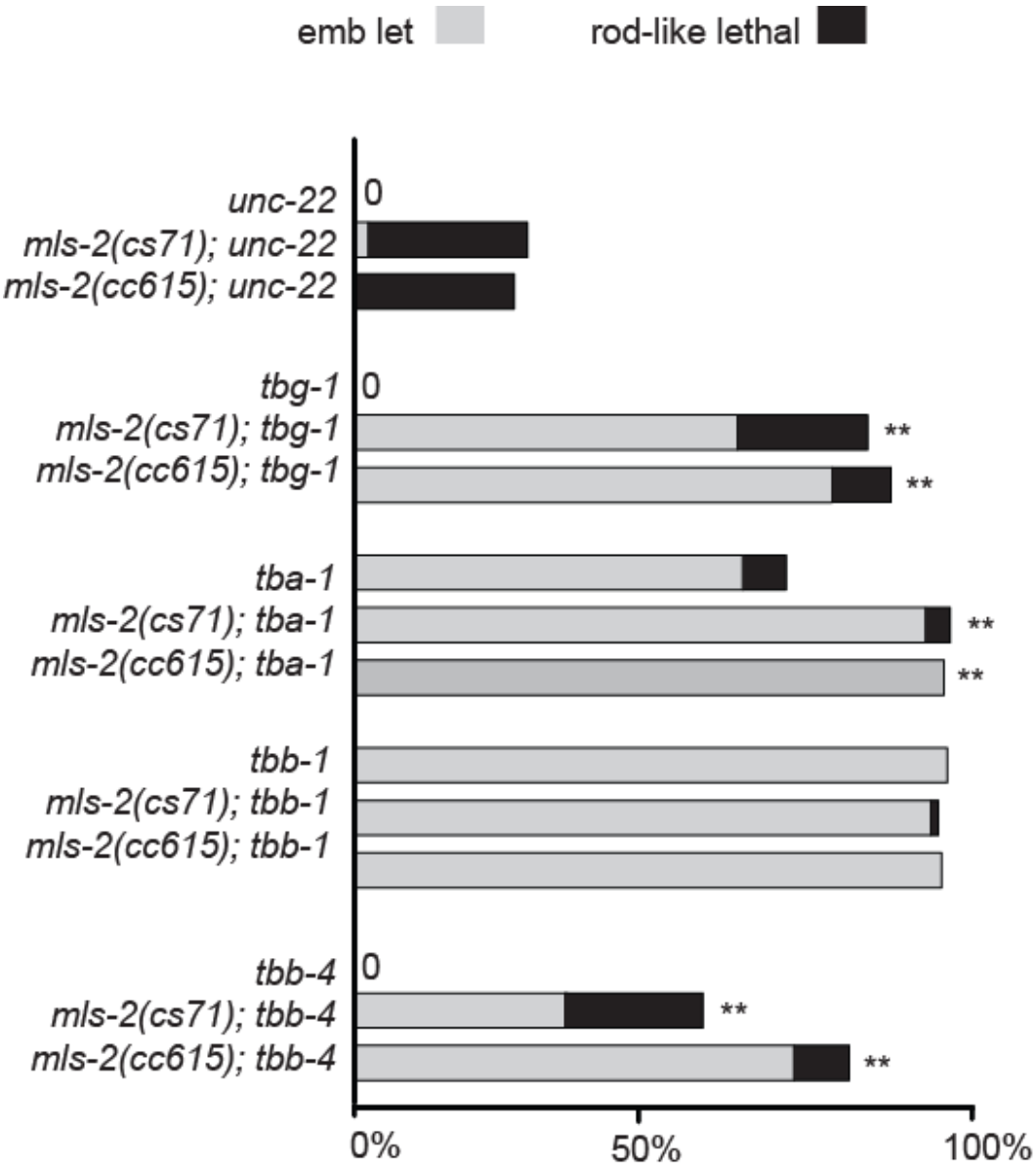
emb let
rod-like lethal
unc-22
mls-2(cs71); unc-22
mls-2(cc615); unc-22
0
tbg-1
mls-2(cs71); tbg-1
mls-2(cc615); tbg-1
0
**
**
tba-1
mls-2(cs71); tba-1
mls-2(cc615); tba-1
**
**
tbb-1
mls-2(cs71); tbb-1
mls-2(cc615); tbb-1
tbb-4
mls-2(cs71); tbb-4
mls-2(cc615); tbb-4
0
**
**
0%
50%
100%

Figure 4.2

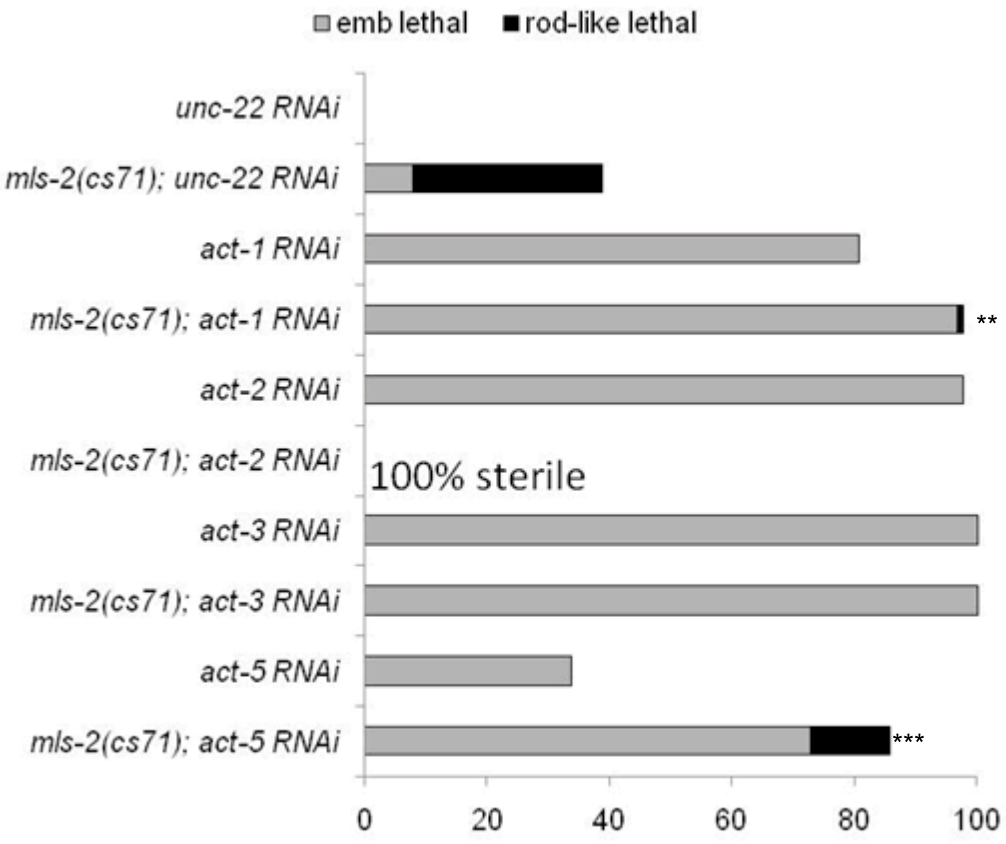
emb lethal
rod-like lethal
unc-22 RNAi
mls-2(cs71); unc-22 RNAi
act-1 RNAi
mls-2(cs71); act-1 RNAi
act-2 RNAi
mls-2(cs71); act-2 RNAi
act-3 RNAi
mls-2(cs71); act-3 RNAi
act-5 RNAi
mls-2(cs71); act-5 RNAi
100% sterile
**
***
0
20
40
60
80
100

Figure 4.3

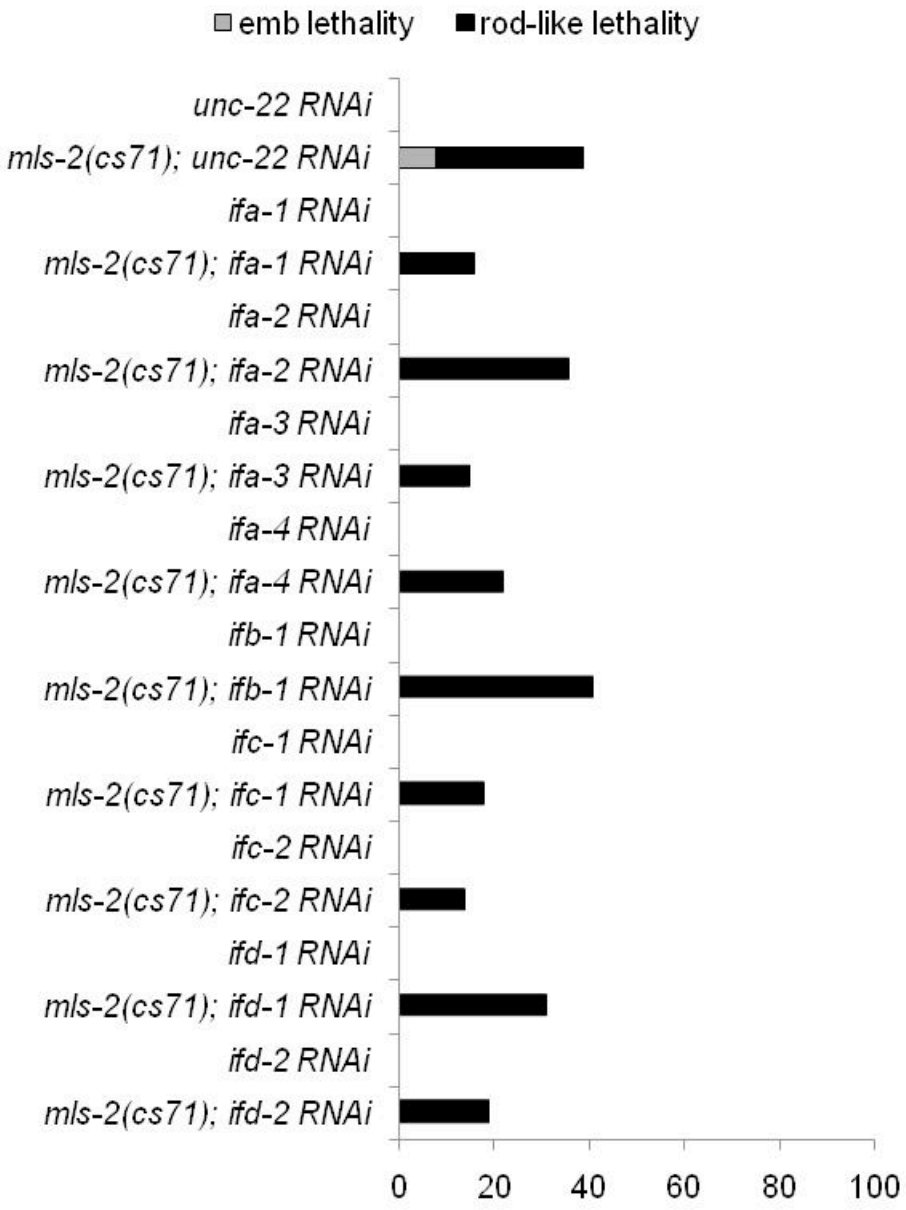
emb lethality
rod-like lethality
unc-22 RNAi
mls-2(cs71); unc-22 RNAi
ifa-1 RNAi
mls-2(cs71); ifa-1 RNAi
ifa-2 RNAi
mls-2(cs71); ifa-2 RNAi
ifa-3 RNAi
mls-2(cs71); ifa-3 RNAi
ifa-4 RNAi
mls-2(cs71); ifa-4 RNAi
ifb-1 RNAi
mls-2(cs71); ifb-1 RNAi
ifc-1 RNAi
mls-2(cs71); ifc-1 RNAi
ifc-2 RNAi
mls-2(cs71); ifc-2 RNAi
ifd-1 RNAi
mls-2(cs71); ifd-1 RNAi
ifd-2 RNAi
mls-2(cs71); ifd-2 RNAi
0
20
40
60
80
100

Figure 4.4

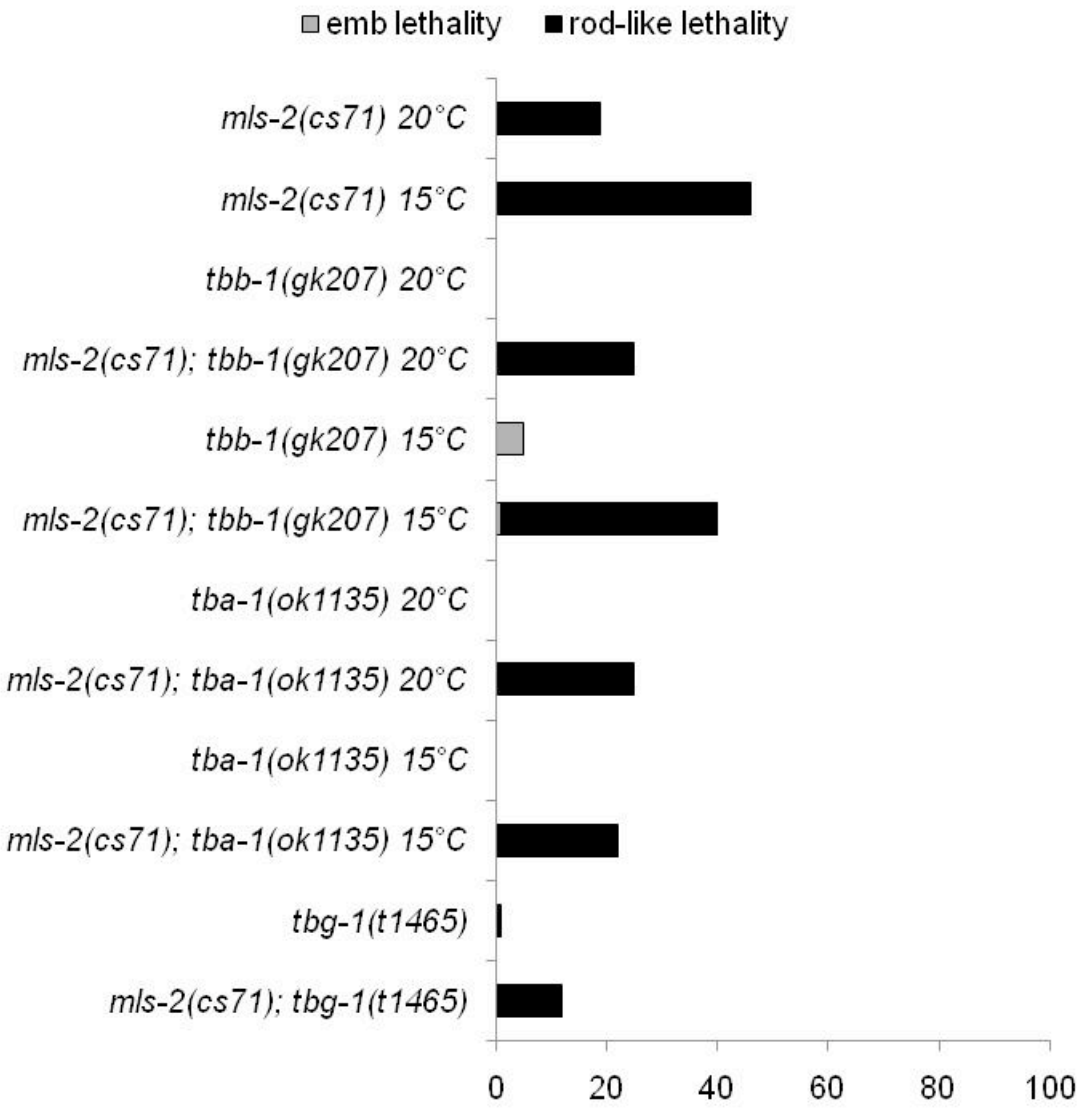
emb lethality
rod-like lethality
mls-2(cs71) 20°C
mls-2(cs71) 15°C
tbb-1(gk207) 20°C
mls-2(cs71); tbb-1(gk207) 20°C
tbb-1(gk207) 15°C
mls-2(cs71); tbb-1(gk207) 15°C
tba-1(ok1135) 20°C
mls-2(cs71); tba-1(ok1135) 20°C
tba-1(ok1135) 15°C
mls-2(cs71); tba-1(ok1135) 15°C
tbg-1(t1465)
mls-2(cs71); tbg-1(t1465)
0
20
40
60
80
100

Figure 4.5

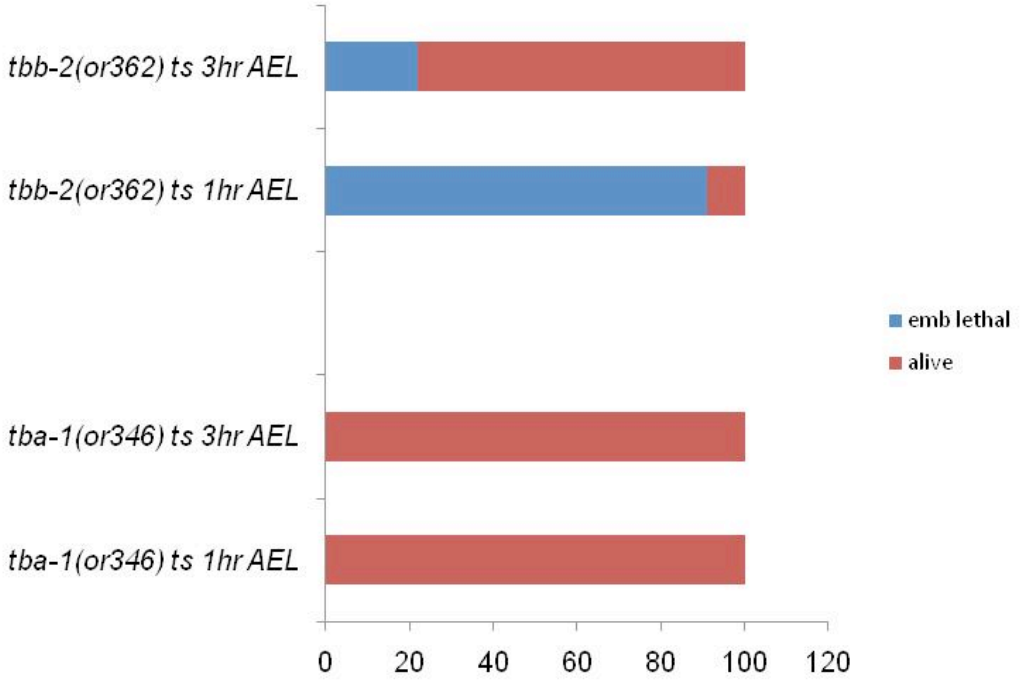
tbb-2(or362) ts 3hr AEL
tbb-2(or362) ts 1hr AEL
tba-1(or346) ts 3hr AEL
tba-1(or346) ts 1hr AEL
0
20
40
60
80
100
120
emb lethal
alive

Figure 4.6

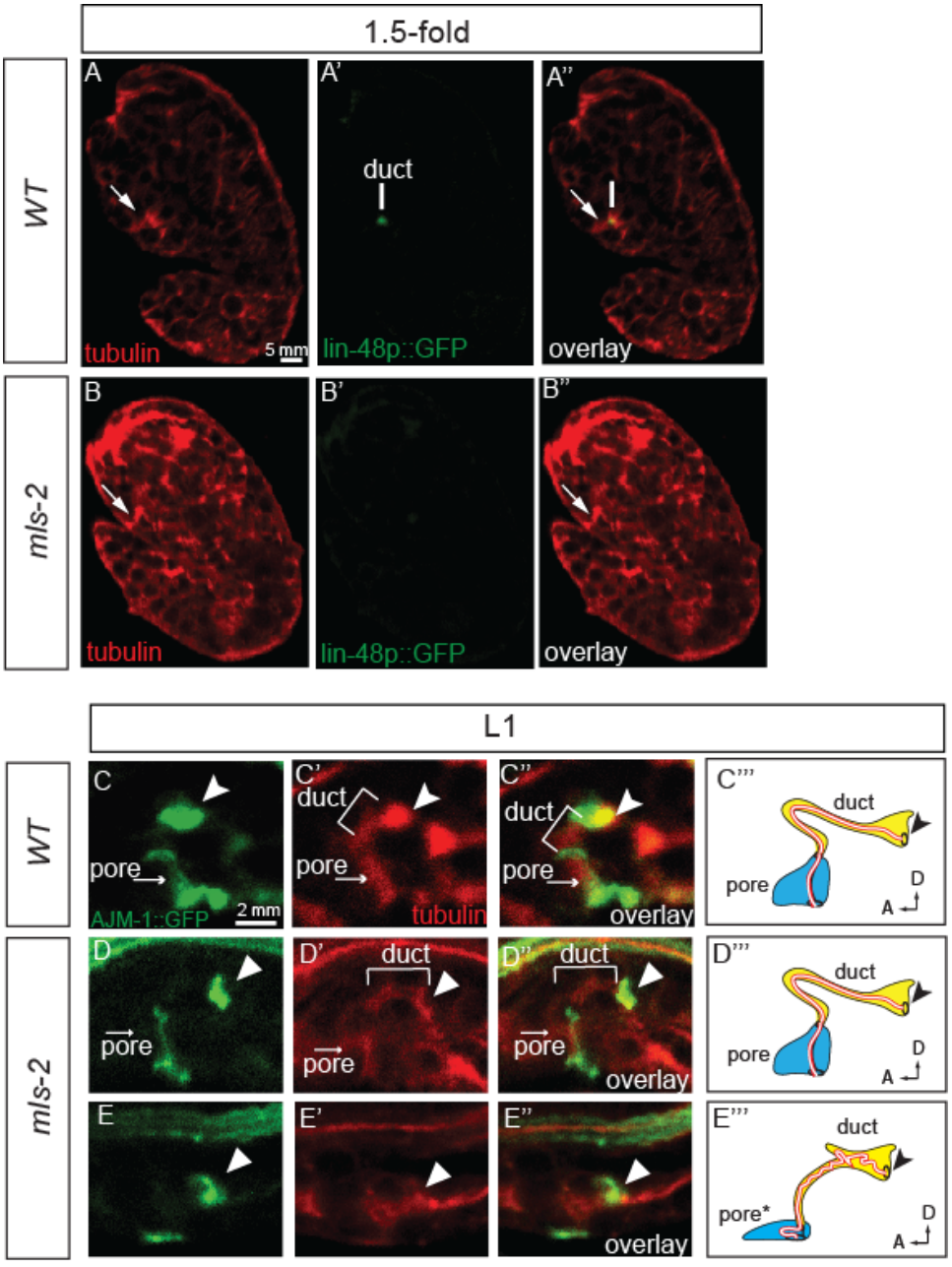
1.5-fold
WT
mls-2
A
A'
A''
duct
tubulin
5 mm
lin-48p::GFP
overlay
B
B'
B''
tubulin
lin-48p::GFP
overlay
L1
WT
mls-2
C
C'
C''
C'''
duct
pore
AJM-1::GFP
2 mm
tubulin
overlay
D
D'
D''
D'''
E
E'
E''
E'''
pore*
A
D

Chapter Five:

RNAi ENCHANCER SCREEN TO IDENTIFY *MLS-2* REDUNDANT FACTORS

Summary

Genetic redundancy is a developmental strategy observed throughout the animal kingdom. Genetic redundancy bolsters a system against complete malfunction if one of its gene products is mutated or absent. The duct and canal cells of the *C.elegans* excretory system are essential for viability of the organism. Therefore, it is not surprising that some genes that promote duct or canal cell development have redundant factors. The Nkx5/HMX homeodomain protein MLS-2 promotes cell shape in the duct and pore. However, two genetic null alleles of *mls-2* have incompletely penetrant lethal excretory system defects, suggesting that *mls-2* has redundant factors that also promote excretory system development. To find the *mls-2* redundant factors I performed an RNAi enhancer screen in an *mls-2* mutant background of 650 transcription factors in the *C.elegans* genome. My screen identified *pbrm-1*, a chromatin modifying factor that greatly enhanced the *mls-2* excretory lethality. In addition, *pbrm-1* genetically interacted with downstream effectors in the EGF-Ras-ERK pathway. *PB1*, the mammalian homologue of PBRM-1, opens chromatin to allow transcription factors to bind DNA and initiate transcription. Therefore, *mls-2* redundant factors may utilize *pbrm-1* to turn on target genes important for excretory system morphogenesis.

Introduction

MLS-2 is a homeodomain transcription factor that promotes cell shape acquisition in the duct and pore cells of the *C.elegans* excretory system (Chapter Three). Two null

alleles of *mls-2* have fully penetrant defects in other cells that require MLS-2 such as the M-lineage (Jiang et al., 2005), but incompletely penetrant lethal excretory defects (Chapter Three). I hypothesized that *mls-2* redundant factors were acting to protect the worm from excretory lethality when MLS-2 was absent.

The EGF-Ras-Erk pathway specifies the duct versus pore cell fate (Abdus-Saboor et al., 2011). Not surprisingly, combining *mls-2* mutants with Ras pathway mutants enhances *mls-2* excretory lethality (Chapter Three). However, the *mls-2* and *Ras* mutant phenotypes are largely distinct, suggesting that their synergy is the result of two independent pathways acting in parallel. My goal was to find genes that act within the same pathway as MLS-2, have a similar phenotype as *mls-2*, and share common sets of target genes as MLS-2.

In previous work performed in the lab by Craig Stone, the 12 genes most similar to MLS-2 by sequence were reduced in an *mls-2* mutant background (Chapter Three, Abdus-Saboor et al., submitted). However, no candidate redundant factors were identified by Craig's approach to target genes similar to *mls-2* (Chapter Three, Abdus-Saboor et al., submitted). Therefore, I turned towards an unbiased approach to identify *mls-2* redundant factors by performing an RNAi enhancer screen, testing most transcription factors in the *C.elegans* genome. Surprisingly, knocking down approximately 650 transcription factors in an *mls-2* mutant background, identified only one new candidate of interest.

Results

mls-2 RNAi enhancer screen

To identify *mls-2* redundant genes I performed RNAi against transcription factors in an *mls-2* mutant background. The transcription factors we screened were taken from a published list (wTF2.0) of transcription factors in *C.elegans* (Reece-Hoyes et al., 2005). wTF2.0 was compiled by scanning all protein coding genes with the GO terms 'transcription factor activity', 'DNA binding', and 'transcriptional regulation' (Reece-Hoyes et al., 2005). To gain specificity and reduce the number of false positives, almost 400 genes were removed from the list that had functions in general transcription, chromatin, DNA replication and repair, or genes that had no DNA binding domain (Reece-Hoyes et al., 2005). Finally, almost 400 genes were added back to the list that were found to have a predicted DNA binding domain by a different algorithm and also genes that acted with specific pathways despite being listed as general transcriptional machinery (Reece-Hoyes et al., 2005). The final list of genes in wTF2.0 contains 934 putative transcription factors (Reece-Hoyes et al., 2005).

I utilized a sub-library of RNAi clones that was arrayed from the Ahringer RNAi feeding library and based on wTF2.0. The arrayed sub-library, courtesy of the Lamitina lab, contained about 800 of the 934 transcription factors listed in wTF2.0, of which 650 I was able to screen. *mls-2* second and third stage larvae were treated with control RNAi and RNAi against each transcription factor. Approximately 5 worms from each genotype were seeded onto each RNAi feeding plate. Four days after initial RNAi exposure, worms were assessed for enhancement of the ~30% excretory lethality caused by *mls-2* alone. A screen of this kind was biased towards identifying strong interactions, as going

from 30% to 40% excretory lethality would be difficult to appreciate by eye. Of all 650 transcription factors tested one gene was identified, *pbrm-1*, which greatly enhanced *mls-2* excretory lethality (Fig 5.1). PCR and analytical restriction digests confirmed that the *pbrm-1* RNAi clone was correct (data not shown). A deletion allele of *pbrm-1* is homozygous viable (Shibata et al., 2012) and *pbrm-1* RNAi in wild type worms does not cause lethality (Fig 5.1).

PBRM-1 is the *C.elegans* homologue of mammalian PB1, a subunit of the PBAF (Polybromo, Brg1-Associated Factors) chromatin-remodeling complex (Thompson, 2009). The PBAF complex is commonly known as RSC in yeast and PBAP in Drosophila. The PBAF complex moves nucleosomes away from nucleosome positioning sequences, to provide transcription factors with access to previously occupied sites (Kwon and Wagner, 2007). Interestingly, some subunits within chromatin remodeling complexes can have distinct functions (Kwon and Wagner, 2007). Recently in *C.elegans* it was shown that *pbrm-1* regulates the asymmetric expression of *psa-1/Meis* during gonad primordium formation in a manner independent of other PBAF subunits (Shibata et al., 2012). *pbrm-1* also genetically interacts with the EGF-Ras-Erk pathway during *C.elegans* vulval development (Lehner et al., 2006). *pbrm-1* suppresses the multivulva phenotype of hyper-activated Ras and also enhances the vulvaless phenotype of several Ras pathway effectors (Lehner et al., 2006). The genetic interactions between *pbrm-1* and the EGF-Ras-Erk pathway intrigued us because of the known roles for Ras signaling in duct cell development (Chapter Two).

pbrm-1 genetically interacts with EGF-Ras effectors in the excretory system

To test for genetic interactions in the excretory system between *pbrm-1* and the EGF-Ras-Erk pathway I used Ras pathway mutants that had weakly penetrant phenotypes. These included hypomorphic alleles of *lin-45/Raf* and *mpk-1/Erk*, and a null allele of *eor-1*. *lin-45/Raf* is a kinase upstream in the Ras pathway, while *mpk-1/Erk* is the terminal kinase in the Ras pathway that translocates to the nucleus (see Fig 1.4). *eor-1* is a downstream effector in the Ras pathway that is redundant with the *lin-1/ets* factor (Howard) (see Fig 1.4). When *lin-45* hypomorphs were given *pbrm-1* RNAi, the weak excretory lethal phenotype of *lin-45* hypomorphs was not enhanced (Fig 5.2). However, when *mpk-1* hypomorphs and *eor-1* null mutants were treated with *pbrm-1* RNAi their weak excretory phenotypes were greatly enhanced (Fig 5.2). Thus *pbrm-1* RNAi enhanced the excretory lethality of mutants downstream in the Ras pathway, but not a kinase upstream in the Ras pathway.

PBRM-1 is expressed in most cells

To determine if the expression pattern of PBRM-1 was consistent with a cell autonomous role for PBRM-1 in the excretory system, I assessed PBRM-1 expression with a transcriptional reporter that contained ~2kb of the *pbrm-1* promoter fused to GFP. In early embryos around the 200-cell stage, *pbrm-1*::GFP localized to the nucleus of almost every cell (Fig 5.3). Ubiquitous expression of a subunit of a chromatin remodeling complex is not surprising. However, during larval stages *pbrm-1*::GFP was no longer

expressed in every cell, but displayed cell type specificity (Fig 5.3). In larvae I observed *pbrm-1*::GFP in several neurons in the head (Fig 5.3), and also in the vulva during the fourth larval stage (data not shown). I also observed *pbrm-1*::GFP in a cell whose identity has not been confirmed by co-localization studies, but appears to be the duct cell (Fig 5.3). However, I presume that the *pbrm-1*::GFP reporter lacks some important regulatory regions, as a full length rescuing translational PBRM-1::GFP reporter is expressed in every cell during larval stages (Shibata et al., 2012). Nonetheless, the *pbrm-1*::GFP reporter has enough regulatory information to drive GFP expression in neurons, the vulva, and potentially the duct cell (Fig 5.3). Taken together, PBRM-1 is probably transcribed and localized in most cells of the worm throughout development, including the cells of the excretory system.

An unknown mechanism for PBRM-1 in excretory system morphogenesis

To investigate how *pbrm-1* RNAi was enhancing excretory lethality in *mls-2* and *eor-1* mutants, I examined several excretory system markers. As a control for penetrance of *pbrm-1* RNAi , I performed pulse lays with siblings of the scored worms and confirmed the enhanced excretory lethality shown in Figs 5.1, 5.2 (data not shown). *lin-48p*::GFP is a marker for both duct fate specification and differentiation. Unfortunately, the *pbrm-1(RNAi);eor-1* strain with *lin-48p*::GFP in the background was too sick to score. AJM-1::GFP is an epithelial junction marker that labels the autocellular junction(AJ) of the pore cell (Stone et al., 2009). Mutants with duct-to-pore fate

transformations have 2 pore AJs (Abdus-Saboor et al., 2011). The 2AJ phenotype was never observed in *pbrm-1* or *eor-1* single mutants (Fig 5.4A). However, approximately 15% of *pbrm-1(RNAi);eor-1* double mutants displayed the 2AJ phenotype (Fig 5.4A), suggesting that PBRM-1 may have a small role in duct fate specification. In comparison to the low penetrance 2AJ phenotype in *pbrm-1(RNAi);eor-1* double mutants, a high penetrance excretory lethality was observed in this strain. This result (Fig 5.2), suggests that PBRM-1 has additional roles in the excretory system besides duct fate specification.

mls-2 single mutants and *pbrm-1(RNAi); mls-2* double mutants never displayed the 2AJ phenotype (Fig 5.4A, Chapter Three), a result that is consistent with both MLS-2 and PBRM-1 acting mainly outside of duct fate specification. Approximately ~20% of *mls-2* mutants did not express *lin-48* in the duct, indicating that MLS-2 promotes morphogenesis of the duct cell (Fig 5.4B, Chapter Three). However, treating *mls-2* mutants with *pbrm-1* RNAi did not enhance loss of *lin-48* in the duct (Fig 5.4B). *mls-2* mutants also have cell shape defects in the duct and pore that lead to loss of the pore AJ and collapse of the duct cell (Chapter Three). However, the cell shape defects of *mls-2* mutants were not enhanced or altered by treatment with *pbrm-1* RNAi (data not shown). In summary, the mechanism by which *pbrm-1* RNAi enhances excretory lethality of *mls-2* and *Ras* pathway effectors remains largely unknown.

Discussion

An RNAi enhancer screen was performed to identify MLS-2 redundant factors. Although many genes were tested, only *pbrm-1* reproducibly enhanced *mls-2* excretory lethality. *pbrm-1* has been shown to genetically interact with the EGF-Ras-Erk pathway in the vulva, and I have demonstrated similar genetic interactions in the excretory system. RNAi or deletion of *pbrm-1* alone does not lead to excretory system defects. Only reduction of *pbrm-1* combined with loss of *mls-2* or Ras effectors resulted in excretory system lethality. With the panel of markers I used to visualize the duct and pore, I could not determine how *pbrm-1* contributes to excretory lethality. Below I discuss a potential model for PBRM-1 cooperation with MLS-2 and Ras, and an alternative way to find MLS-2 redundant factors. I end the discussion by highlighting a recent report about a common class of genes that may be acting as MLS-2 redundant factors.

PBRM-1, MLS-2, and EGF-Ras-Erk may all function in parallel

pbrm-1 excretory phenotypes are only revealed when either *mls-2* or Ras pathway effectors are reduced, knockdown of *pbrm-1* on its own has no effect. *pbrm-1* genetically interacts with two Ras downstream genes during excretory system development, *mpk-1* and *eor-1*. *pbrm-1(RNAi);eor-1* double mutants have a high percentage of excretory lethality and a lower percentage of fate specification defects. The *eor-1* and *pbrm-1* genetic interactions suggests that *pbrm-1* may act downstream of Ras signaling during fate specification, but possibly parallel to Ras outside of fate specification. *pbrm-1(RNAi)* greatly enhanced *mls-2* excretory lethality, but not loss of *lin-48* in the duct or

cell shape defects. Although I cannot exclude the possibility that *mls-2* directly depends upon *pbrm-1*, my analyses suggest that *mls-2* and *pbrm-1* function largely in independent parallel pathways.

If *pbrm-1* is acting in a pathway partially independent of *mls-2* and Ras, what could PBRM-1 be doing to promote excretory system development? PBRM-1 appears to be expressed in most cells in the worm (Shibata et al., 2012), leading to several possible modes of action for enhancing excretory lethality. One simple possibility that we have not tested, is that PBRM-1 is affecting the canal cell, as opposed to the duct or pore like MLS-2 and Ras. We could easily test this by visualizing the canal cell in a *pbrm-1(RNAi)* single or double mutant background. A second possibility, which appears less likely, is that *pbrm-1* is acting cell non-autonomously outside of the excretory system. Secreted proteins that promote excretory system development can be driven in non-excretory cells and have rescuing capability (Stone et al., 2009). PBRM-1 is mainly nuclear and not secreted, thus the cells where phenotypes are observed probably require PBRM-1 cell autonomously. However, I cannot exclude the possibility that PBRM-1 affects the expression of a secreted factor. A third possibility is that PBRM-1 acts in the duct cell either downstream and/or parallel to both MLS-2 and Ras.

How could PBRM-1 act in the duct cell downstream or parallel to Ras to promote excretory system development? Several groups have shown that PBRM-1 and the PBAF complex are required for Ras dependent processes. For example, during oncogene mediated senescence, Ras activates p53, which promotes the transcription of the CDK inhibitor p21 (Burrows et al., 2010). The PBAF subunit BRD7 physically interacts with

p53 and directly promotes p21 transcription (Burrows et al., 2010). Thus, when the PBAF subunit *BRD7* is reduced, activated Ras can no longer promote senescence through the p53-p21 pathway (Burrows et al., 2010). Likewise in *C.elegans,* hyper-activating Ras leads to a multi-vulva phenotype, which is suppressed when *pbrm-1* is reduced (Lehner et al., 2006). Hyper-activating Ras in *C.elegans* also results in two duct cells being specified (Abdus-Saboor et al., 2011). It will be interesting to determine if reduction of *pbrm-1* can also suppress the 2-duct phenotype caused by hyper-activated Ras. A speculative model combining my data with other reports, is that *pbrm-1* may help transcription factors that are activated in part by Ras, to access DNA and turn on genes important for excretory system development.

We have shown that *mls-2* genetically interacts with the Ras pathway during duct morphogenesis (Chapter Three). While the identification of the interaction between *pbrm-1* and *mls-2* adds more evidence for *mls-2* and Ras interaction, it has not given us an additional *mls-2* interacting pathway beyond what was already known.

A forward genetic screen to find MLS-2 redundant genes

There are several reasons to obtain negative results with RNAi treatment in the excretory system (see Chapter Four discussion). Even though one RNAi clone (pbrm-1) did produce robust results, 1/650 is a fairly low recovery rate. I discussed a way to improve RNAi in the excretory system for subsequent RNAi screens (Chapter Four discussion). Another way to alleviate the pitfalls of RNAi screening is to perform a

different kind of screen. A forward mutagenesis screen is the most unbiased way to let the worm tell us what genes are functioning redundantly with *mls-2*.

Forward genetic screens lead researchers to study genes that would have been overlooked based on *a priori* knowledge. The RNAi enhancer screen I performed was unbiased in that it contained all classes of transcription factors, but highly biased because no other genes besides transcription factors were tested. I propose doing a forward mutagenesis screen, but in an *mls-2* mutant background with markers for the duct and pore cells. Having excretory system markers in the mutagenized strain would allow me to quickly screen which mutants were worth further pursuit. For example, mutants that cause enhanced excretory lethality, and duct-to-pore fate transformations, would probably be alleles of Ras pathway genes and not worth mapping and cloning. However, mutants that enhance *mls-2* cell shape defects are more likely to be *mls-2* redundant factors and worth mapping, cloning, and performing subsequent assays with. Others in the lab are currently performing similar forward screens with worms bearing duct and pore markers, and it would be feasible to mutagenize an *mls-2* strain alongside the current screens.

MLS-2 redundant genes may not be limited to transcription factors

Two presumptive null alleles of *mls-2* have incompletely penetrant lethal excretory phenotypes (Chapter Three). In an effort to find the *mls-2* redundant genes I tested cytoskeletal genes that may have the same function as *mls-2* (Chapter Four), and

transcription factors that may turn on the same genes as MLS-2. When null alleles do not have fully penetrant phenotypes, the most common assumption is that similar genes are compensating for the loss of the absent gene. However, the genetic logic that many similar genes are performing the same function, does not account for all cases of genetic redundancy. Recently, Burga et al. in *Nature* showed that at least two compensation pathways exist to protect organisms against losses of critical gene products.

Burga et al. used a null mutant of the *C.elegans* T-box transcription factor *tbx-9* to identify genetic compensatory pathways. The *tbx-9* null mutant causes an incompletely penetrant abnormal muscle and epidermal phenotype in larvae (Andachi et al., 2004, Pocock et al., 2004). TBX-9 is highly related to another T-box transcription factor TBX-8. Combined loss of *tbx-8* and *tbx-9* leads to fully penetrant muscle and epidermal phenotypes in larvae (Andachi et al., 2004, Pocock et al., 2004). Over-expression of TBX-8 partially rescues the *tbx-9* null mutant, and *tba-8* transcription is upregulated in a *tbx-9* null background (Burga et al., 2011). However, some *tbx-9* null mutants that do not upregulate *tbx-8* grow up wild type (Burga et al., 2011) indicating that a second compensatory pathway was involved.

To find the second compensatory pathway in *tbx-9* null mutants Burga et al. turned to molecular chaperones, proteins that when inhibited, can enhance the effects of diverse mutations (Queitsch et al., 2002, Van Dyk et al., 1989). To visualize chaperones the authors made reporters for daf-21 (hsp90) and hsp-4 (orthologous to mammalian BiP). *tbx-9* null mutants expressed the chaperones at higher levels, and embryonic expression of the chaperone was generally predictive of the future outcome (Burga et al.,

2011). *tbx-9* null mutants that expressed both *tba-8* and the chaperones at high levels in embryos almost always grew up wild type (Burga et al., 2011). While *tbx-9* null mutants that expressed both *tba-8* and the chaperones at low levels almost always grew up to display the phenotype (Burga et al., 2011). In summary, protection from loss of a null mutant, came from upregulation of a similar gene and from commonly used chaperones.

We have attempted without huge success, to identify *mls-2* redundant genes by knocking down genes similar to *mls-2* in sequence, and genes we assumed were similar to *mls-2* in function. It may be possible, as was observed with *tbx-9*, that a pathway involving chaperones is protecting *mls-2* null mutants from dying at a higher percentage. I could test the chaperone hypothesis by directly knocking down select chaperones by RNAi or using mutants where available. I could also cross reporters for chaperones into *mls-2* mutants to see if they are upregulated. If chaperones are protecting *mls-2* null mutants, some chaperones may be identified in the *mls-2* forward genetic screen that I proposed to perform in the previous section. Our prior reverse genetic approaches to find the *mls-2* redundant genes (barring technical limitations) were likely performed accurately, but may not have targeted the correct set of genes.

Materials and Methods

Strains and alleles

Bristol N2 was the wild-type strain. Strains were maintained and manipulated by

standard methods unless otherwise noted. Descriptions of each gene can be found at www.wormbase.org. Mutant alleles used are: LG1V: *eor-1(cs28)* (Rocheleau et al., 2002)*, lin-45 (ku112)* (Sundaram and Han, 1995). LGIII: *mpk-1(ku1)* (Wu and Han, 1994). LGX*: mls-2(cs71)*.

RNA interference (RNAi)

RNAi was performed by placing *mls-2(cs71)* L2/3 stage worms on feeding plates with HT-115 E.coli expressing RNA against *GFP* (negative control) or each transcription listed in wTF2.0 (Reece-Hoyes et al., 2005) that is available in the Ahringer feeding library.

The RNAi screen was based on the following 9-day protocol: *Monday* – I grew up lots of *mls-2* worms at 25°C. *Tuesday* – I prepared 6-well NGM feeding plates. *Wednesday* – I bleached *mls-2* worms to recover eggs and rocked the eggs overnight in M9 on the Nutator. I also grew up RNAi clones in LB-amp-tet and incubated them at 37°C overnight. *Thursday* – I transferred synchronized L1s to fresh OP50 plates to continue growth. I also added IPTG to 1mM concentration to overnight RNAi cultures and then seeded the feeding plates with the cultures and put the plates to 37°C overnight. *Friday* – I washed L2/3 stage *mls-2* worms with M9 to 15mL tubes. From the 15ml tubes I pipetted ~5 worms to seeded RNAi plates to incubate at 20°C over the weekend. The following *Monday* and *Tuesday* I scored the plates that had now laid F1 progeny, for enhancement of *mls-2* excretory lethality.

Phenotypic Scoring

To score for rod-like (excretory) lethality, hermaphrodites treated with control or experimental RNAi for 4-5 days were allowed to lay eggs for approximately 2 days. Percent rod-like lethal was determined by the proportion of progeny that were visible as rods 48 hours post-egg lay.

Marker Analysis and Imaging

Images were captured by differential interference contrast (DIC) and epi-fluorescence microscopy using a Zeiss Axioskop and Hamamatsu C5985 camera, or by confocal microscopy using a Leica SP5.

Acknowledgements

I would like to thank the Caenorhabditis Genetics Center (University of Minnesota, USA) for providing the strains analyzed in this chapter, including the *pbrm-1*::GFP transcriptional reporter. All of the RNAi clones were from the Julia Ahringer RNAi feeding library. The list of transcription used was taken from Reece-Hoyes et al. The arrayed library, which made the screen many fold easier, was generously provided by Todd Lamitina. The 9-day RNAi protocol was adopted from Kai Huang, a former undergraduate student in the lab.

Figure Legends

Figure 5.1. *pbrm-1* enhances *mls-2* excretory lethality. Bar graph showing percentage of worms with rod-like (excretory lethality). Results from multiple worms from individual plates were averaged together. *GFP* used as negative RNAi control. n>100 for each genotype.

Figure 5.2. *pbrm-1* genetically interacts with the Ras pathway in the excretory system. Bar graph showing percentage of worms with rod-like (excretory lethality). Results from multiple worms from individual plates were averaged together. *GFP* used as negative RNAi control. n>100 for each genotype.

Figure 5.3. *pbrm-1*::GFP is dynamically expressed. (A,B) Florescence and corresponding DIC image of ~200-cell stage embryo. *pbrm-1*::GFP is nuclear localized in almost of every cell. (C,D) Florescence and corresponding DIC image of an L4 larva. *pbrm-1::GFP* is no longer nuclear localized in every cell, and is now expressed in head neurons and possibly the excretory duct cell (white line).

Figure 5.4. Main process in excretory development affected by *pbrm-1* is unclear. (A) Bar graph showing percentage of L1 worms that had a 2 pore auto-cellular junction(AJ) phenotype, as scored with AJM-1::GFP. n at least 20 for each genotype. (B) Bar graph showing percentage of L1 worms that lacked *lin-48p::*GFP expression in duct. n at least 20 for each genotype.

Figure 5.1

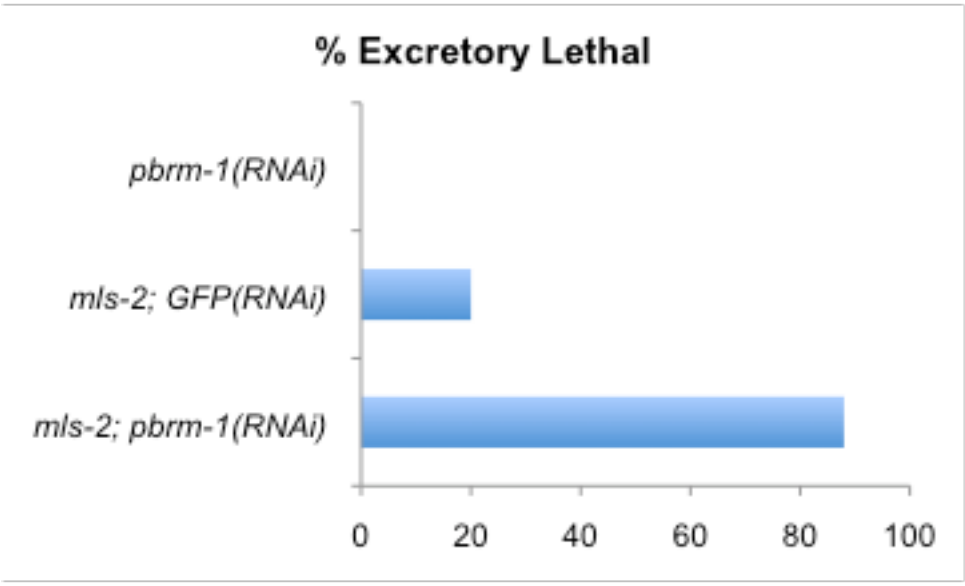
% Excretory Lethal
pbrm-1(RNAi)
mls-2; GFP(RNAi)
mls-2; pbrm-1(RNAi)
0
20
40
60
80
100

Figure 5.2

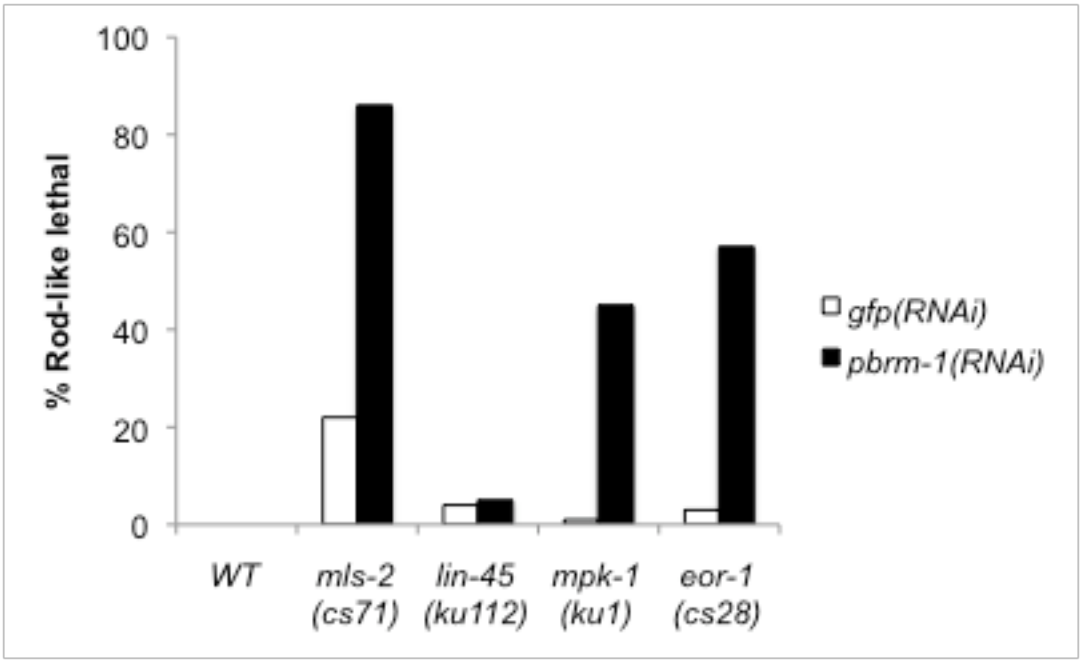
100
80
60
40
20
0
% Rod-like lethal
WT
mls-2 (cs71)
lin-45 (ku112)
mpk-1 (ku1)
eor-1 (cs28)
gfp(RNAi)
pbrm-1(RNAi)

Figure 5.3

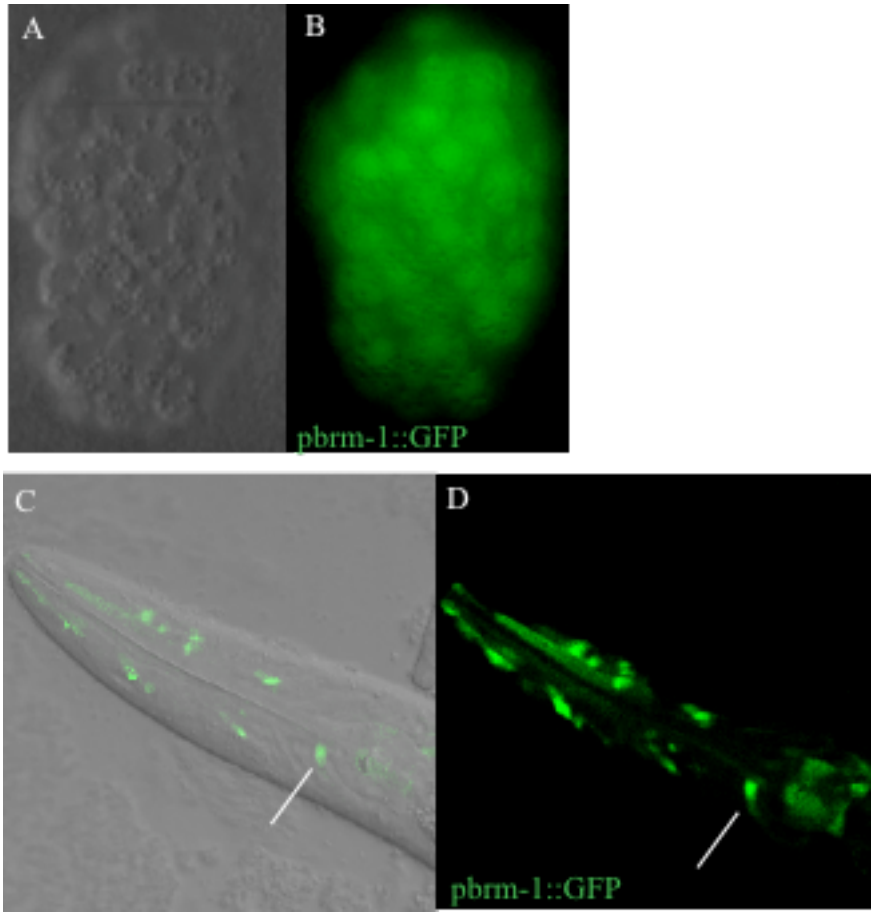

Figure 5.4

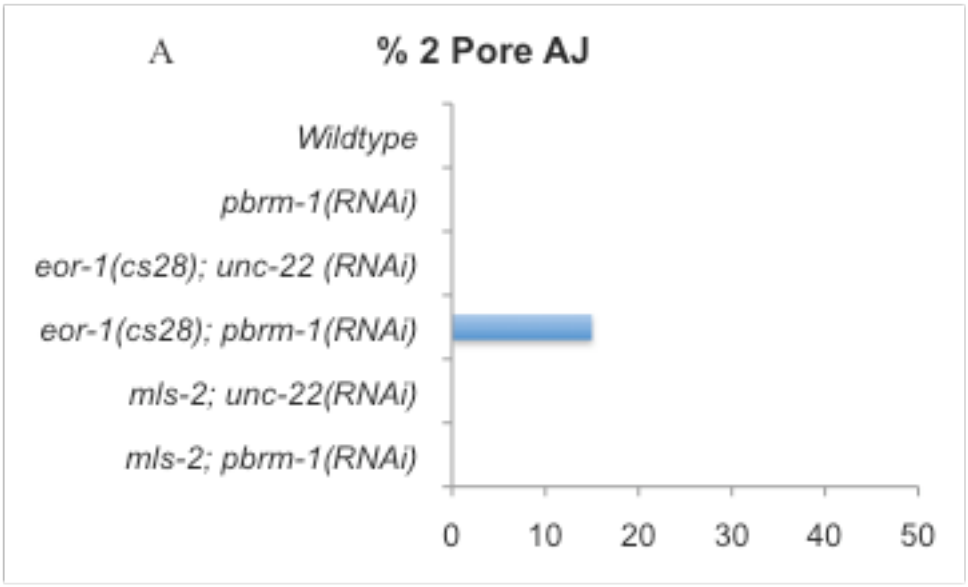
A
% 2 Pore AJ
Wildtype
pbrm-1(RNAi)
eor-1(cs28); unc-22 (RNAi)
eor-1(cs28); pbrm-1(RNAi)
mls-2; unc-22(RNAi)
mls-2; pbrm-1(RNAi)
0
10
20
30
40
50

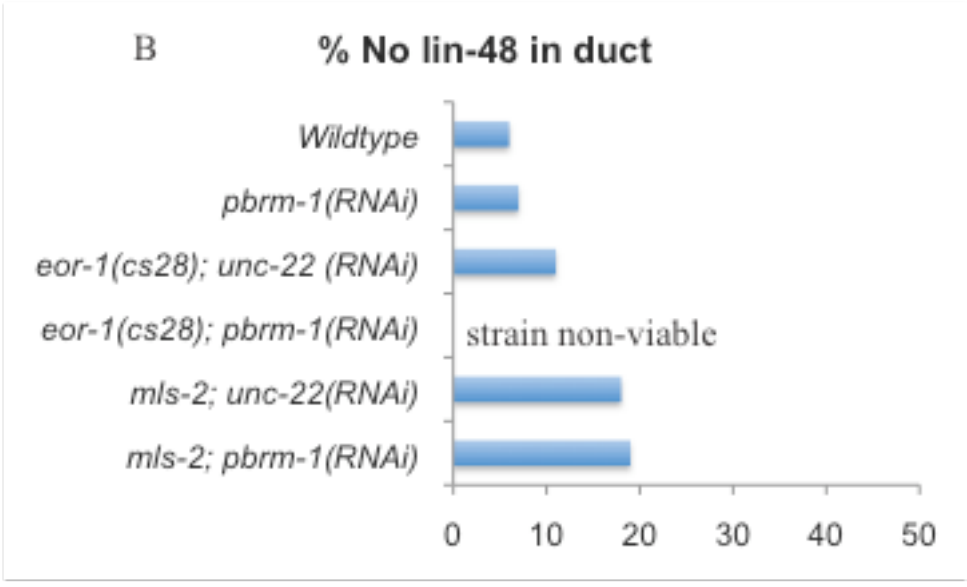
B
% No lin-48 in duct
Wildtype
pbrm-1(RNAi)
eor-1(cs28); unc-22 (RNAi)
eor-1(cs28); pbrm-1(RNAi)
strain non-viable
mls-2; unc-22(RNAi)
mls-2; pbrm-1(RNAi)
0
10
20
30
40
50

Chapter Six:

DISCUSSION:

SPECULATIONS, ONGOING AND FUTURE EXPERIMENTS

Summary

For my thesis research I utilized a network of epithelial tubes in the *C.elegans* excretory system as a model to study fate specification, cell-cell interactions, and morphogenesis. I was able to expand upon earlier work from others implicating Ras in development of the duct cell. I was able to demonstrate that the canonical EGF-Ras-Erk pathway has at least three genetically distinct roles in the excretory system: 1) to specify the duct versus the pore cell fate, 2) to bias the positions the duct and pore adopt in the tubular network, and 3) to maintain organ architecture in the duct. However, the maintenance or late role for Ras signaling in the excretory system remains unclear. I also demonstrated that a homeodomain transcription factor, MLS-2, acts in parallel to EGF-Ras-ERK signaling to promote shape acquisition in the duct and pore. I hypothesize that MLS-2 is acting to stabilize the cytoskeleton in the duct and pore by turning on specific cytoskeletal isoforms.

In this discussion I compare RTK regulation of excretory development to RTK regulation in more complex tubular organs. In addition, I present preliminary data that suggests the late requirement for Ras is during the G1/G2 pore exchange. I conclude the discussion by highlighting collaborations to find MLS-2 target genes in the duct and pore.

Duct versus pore competition is analogous to tip versus stalk competition

Cell competition mediated by RTK signaling is a strategy observed in several tubular organs including the mammalian kidney and vasculature, and the Drosophila trachea (Chi et al., 2009; Eilken and Adams, 2010; Ghabrial and Krasnow, 2006). In response to RTK growth factors, one or few cells emerge as leader or tip cells from a sheet of equivalent precursor cells (Tung et al., 2012). The tip cell is of seminal importance, especially in branched tubular organs like the Drosophila trachea, as new branches form from the migrating tip cell (Ghabrial et al., 2003). The follower or stalk fate is also important, as the stalk cells proliferate and contribute to the nascent sprout (Tung et al., 2012). Interestingly, despite negative feedback to insure the tip fate decision, tip cell identity can be dynamic, with cells shuttling back and forth between being a tip or stalk cell during tubulogenesis (Jakobsson et al., 2010). The duct and pore precursor cells of the *C.elegans* excretory system are lineal homologs and are also initially equivalent until RTK signaling specifies the duct cell fate (Abdus-Saboor et al., 2011; Sulston et al., 1983). Duct versus pore positioning and specification is highly similar to RTK mediated tip versus stalk specification in more complex tubular organs. The competition to become a duct ("tip") versus pore ("stalk") is much simpler than the multi-cellular competition observed in more complex tubes.

The study of duct versus pore competition can be exploited to learn more about tip versus stalk specification in complex tubular organs such as the mammalian kidney. In the kidney, the chemo-attractive growth factor GDNF signals from the surrounding mesenchymal cells to the ureteric bud epithelium through the Ret RTK, to specify the tip

versus stalk cell fate (Costantini, 2010). The cells that are specified as tip cells appear to respond to GDNF and migrate away from a sheet of equivalent epithelial cells towards the tip of the ureteric bud (Costantini, 2010). GDNF is a potent inducer of the tip cell fate in the immature kidney, as no ureteric tip forms in *GNDF -/-* mice, and mutations that block inhibition of GDNF cause the formation of multiple ureteric tips (Costantini, 2010). However, additional reports about GDNF induction of the tip cell fate have made some of the previous conclusions and working models difficult to interpret. For example, mice that were engineered to express GDNF in the ureteric bud epithelium (receiving cell) instead of the surrounding mesencyhme, were still able to specify tip cells and make kidneys (Shakya et al., 2005a). This result suggests that the expression of the growth factor signal at the location of migration and specification is not required for tip cell specification. In addition, it has been shown that FGF10 can act as an inducer of tip cell specification in the absence of GDNF (Michos et al., 2010). The FGF10 rescue of GDNF mice does not result in completely normal kidneys, indicating that GDNF has specific roles that cannot be compensated by adding back FGF10 (Michos et al., 2010). While it is clear that GDNF is required to specify a tip cell, it is unclear if the precursors need to respond to GDNF at the place of their migration, if their migration is controlled by a parallel pathway, or if migration is simply the result of intrinsic programming of the cells.

Studies of the duct and pore can provide insight into the precise role of growth factors in specifying leader versus stalk cell fates. The duct and pore are born on opposite sides of the embryo and migrate towards the canal cell (Sulston et al., 1983), which is the source of the *lin-3/Epidermal Growth Factor (EGF)* (Chapter Two). The duct and pore

migrate and stack normally in *lin-3* zygotic mutants (Chapter Two). However, *lin-3* null mutants were obtained from heterozygous mothers, meaning that there was still maternally supplied *lin-3/EGF*. I hypothesize that maternally supplied *lin-3/EGF* localizes to the canal cell, resulting in normal duct and pore stacking in *lin-3* zygotic mutants. We know that maternal Ras signaling is important, as reducing maternal Ras leads to defects in duct and pore stacking (Chapter Two). Therefore, because maternal *lin-3/EGF* was still present in our experiments, it is unclear if *lin-3/EGF* needs to be expressed at the place of migration for normal stacking and specification of the duct and pore.

With the simplicity of the excretory system, there are ways to test the required location of EGF in duct cell specification. One way I could do this is by using a mutant that expresses *lin-3/EGF* from multiple locations in the embryo. A mutant is available from the Horvitz lab that has two canal cells because of a failed cell death execution (Daniel Denning, personal communication). I have not examined the two canal cell mutants in detail, but they do not die from excretory lethality like many other mutants we have examined. A proof of principle in using this mutant will be to locate both canal cells in the embryo and confirm that they both express EGF. If each canal cell expresses EGF, and each precursor migrates towards one of the canals, this would suggest that location of the growth factor signal is critical in specifying the tip cell fate. However, if the cells still migrate to their normal positions, despite the competing EGF signal from the other canal, this would suggest that location of the RTK growth factor is not critical for tip cell specification. To my knowledge, no tubulogenesis studies have been performed where

precursors with equivalent competency to respond to signaling, were given multiple sources of their stimulating chemo-attractant. Performing this analysis in the worm could suggest a model worth testing in the immature kidney, to gain insight into where GDNF is required during ureteric bud tip cell specification.

What are the targets of EGF-Ras-ERK signaling during duct tubulogenesis?

Building an epithelial tube requires numerous processes ranging from cell migration and polarization to cell elongation (Andrew and Ewald, 2010; Lubarsky and Krasnow, 2003). In Chapter Two I described several genetically separable steps for EGF-Ras-Erk signaling in the development of the duct cell. I described roles for Ras signaling in mediating competition as the duct and pore stacked, roles for Ras in fate specification, and a late requirement for Ras signaling in maintaining duct tube organ architecture (see next section for speculation about late requirement for Ras). However, at least two key questions emerged from our findings, including: 1) What are the targets of the Ras signaling that allow the pathway to carry out each step? 2) Are the same targets of signaling utilized at each step? Although I do not have answers to these questions, I will describe several possibilities and avenues for further research.

The data presented in Chapter Two suggest that most of the Ras dependent steps during duct tubulogenesis are dependent on transcription from a downstream effector (s). For example, *sos-1 ts* defects are rescued when reducing the Ras downstream transcription factor *lin-1/Ets* (Chapter Two). *lin-1/Ets* normally represses the duct cell

fate, and this repression is relieved by MPK-1 Erk phosphorylation of LIN-1 (Jacobs et al., 1998). In addition, a combinatorial loss of *lin-1* and another Ras downstream transcription factor *eor-1*, results in duct specification defects (Chapter Two). In the immature kidney, the Ets transcription factors *etv-4* and *etv-5* act downstream of GDNF and the Ret RTK to specify the tip cell fate (Kuure et al., 2010b). In the Drosophila trachea, the Ets transcription factor *pointed* acts downstream of the *Breathless* FGFR. *pointed* is not required to specify the tip cell position, but for other tip cell characteristics (Ghabrial and Krasnow, 2006; Schottenfeld et al., 2010). Thus, activation of Ets transcription factors by RTK signaling during tip cell specification, appears to be a common them in tube development. Our work suggests that RTK activation of ETS transcription factors is critical for later steps of tubulogenesis, and not only cell fate specification (Fig. 6.1).

If activation of LIN-1 by MPK-1 is critical for all the Ras dependent steps during tubulogenesis, what are the targets of LIN-1 at each step? Are the LIN-1 targets different at each Ras dependent step? There are only two known targets for LIN-1 in *C.elegans,* the hox factor LIN-39 (Maloof and Kenyon, 1998; Wagmaister et al., 2006), and the Notch ligand LAG-2 (Zhang and Greenwald, 2011). During vulval patterning LIN-1 binds to the *lin-39* promoter to upregulate *lin-39* expression in the P6.p VPC (Wagmaister et al., 2006). Also during vulval patterning, LIN-1 presumably binds to the *lag-2* promoter and represses *lag-2*, until LIN-1 repression is relieved by EGF-Ras pathway activation (Zhang and Greenwald, 2011). We do not have data that suggests that LIN-39 or LAG-2 could be LIN-1 targets during duct development. LIN-1 may act in

combination with other transcription factors on common sets of target genes. For example, Ras works in parallel to the Nkx5/HMX homeodomain transcription factor MLS-2 to turn on *lin-48* in the duct (Chapter Three) (Figure 6.1). LIN-1 and MLS-2 may have common target genes including *lin-48* during duct development (see approach in final section to identify LIN-1/MLS-2 target genes). One potential strategy to find LIN-1 target genes is to perform whole genome RNA sequencing from an isolated duct cell in a *lin-1* gain-of-function background. Techniques have been described in the worm to perform laser microsurgery of individual cells followed by RNA sequencing (Kato and Sternberg, personal communication). Transcripts that are differentially expressed in the duct compared to a cell where the EGF-Ras pathway is not activated, would be candidate LIN-1 target genes. To limit the list of potential LIN-1 target genes in the duct, we could analyze mutants and make reporters for selected candidate genes.

MPK Erk phosphorylation of transcription factors appears to be another common theme in tube development. MPK-1 phosphorylation of LIN-1 appears to be critical during duct development, and MAPK phosphorylation of *pointed* is critical during Drosophila trachea development (Schottenfeld et al., 2010). Finding LIN-1 targets will help determine how signaling controls tubulogenesis, and finding other transcription factors that are regulated by MPK-1 during duct development will also be informative. Several *in vitro* studies have been conducted to find novel MPK Erk target genes in mammals (Johnson and Hunter, 2005). One study performed in cell culture combining functional proteomics and mass spectrometry, identified 25 Erk target genes, 5 of which were previously known (Lewis et al., 2000). Another recent study used a phospho-

proteomic approach combined with a steroid receptor fusion system to identify 38 new Erk target genes (Kosako et al., 2009). Because many genes in higher organisms have homologs in *C.elegans*, we can use the lists generated from other organisms, to identify novel MPK-1 targets in the duct.

The lab now has a panel of markers to label the excretory system and I can easily visualize which step in duct development is defective in any given mutant. Therefore, as the lab identifies new genes by screening methods or literature searches, I can place a gene into a functional bin based on what process or processes are defective in duct development. As I begin to put functional bins together, I will be able to make predictions about what genes are regulated by Ras signaling at various steps. My predictions can be tested by looking for changes in activity or expression of the candidate target genes when Ras signaling is altered. The core EGF-Ras signaling cascade has been known for years, now the work for the field has shifted to identifying what genes are downstream of signaling.

Does EGF-Ras-ERK signaling affect the G1-to-G2 pore swap?

SOS-1 and Ras signaling have a continued role in maintaining duct organ architecture (Chapter Two). To my surprise, when I shifted *sos-1 ts* mutants from the permissive to non-permissive temperature shortly after hatch during the first larval stage, a high percentage of worms died from excretory lethality (Fig. 2.6). The *sos-1 ts* mutants that died from late temperature shifts still turned on the duct fate marker *lin-48* and fused

the duct auto-cellular junction (AJ) (Fig. 2.6). However, a late process in excretory system development that requires Ras signaling must have been defective to cause excretory lethality in *sos-1 ts* mutants shifted late. Importantly, *sos-1* ts worms shifted after the second larval stage grew up normally without excretory defects (Chapter Two), suggesting that the late role for Ras is a development role and not a continuous physiological role. The only developmental process that I am aware of that occurs late, after the worm hatches and the excretory system has begun to function, is the G1/G2 pore exchange (see Introduction).

The *sos-1 ts* shifts described in Chapter Two implicate a late requirement for Ras signaling in excretory system development, but the precise time when Ras signaling is required is unknown. *sos-1 ts* mutants shifted at 3-fold or early L1 were scored for excretory lethality around the late L1 to early L2 stage, meaning that approximately 6-9 hours elapsed between the time of shift and the time of score (Chapter Two). I hypothesized that if I could determine when defects first began in *sos-1 ts* mutants shifted late, I could infer which process required Ras signaling.

To determine when excretory defects began in *sos-1 ts* mutants shifted late, I shifted hand-picked newly hatched *sos-1 ts* L1 worms bearing AJM-1::GFP from the permissive to non-permissive temperatures and visualized the excretory system every hour. I also crossed the *aff-1* mutation into the *sos-1 ts* background to visualize the duct cell with AJM-1:GFP. The duct cell normally fuses its AJ, but in an *aff-1* mutant background the duct cell AJ remains (Stone et al., 2009). The *aff-1* mutation does not significantly affect excretory system development, and it was used as a tool to label the

duct cell. (Note: at the time of these experiments I did not have the *dct-5p*::mcherry marker that labels the duct and pore cytoplasm. If so, *dct-5p::mcherry* would have been the best marker to use for these studies). *sos-1 ts* worms that were never shifted were almost always wild type, except for a few abnormal junctions with fluid accumulation (Fig. 6.2). The few abnormalities in non-shifted *sos-1 ts* worms may have been caused by leakiness of the *sos-1 ts* mutation or a slight effect of the *aff-1* mutation. *sos-1 ts* mutants scored between 1-5 hours after shift were almost always wild type (Fig. 6.2). However, approximately 25% of *sos-1 ts* mutants that were scored between 6-7 hours after shift displayed excretory phenotypes including large intercellular loops between the duct and pore and apparent disconnection between the duct and pore (Fig. 6.2). The junctional abnormalities of *sos-1 ts* worms scored 6-7 hours after shift were accompanied by abnormal fluid accumulation in the excretory system (data not shown). In summary, the time excretory defects begin in *sos-1 ts* mutants, and presumably the time when Ras signaling is required, is 6-7 hours after hatch.

Work from a post-doctoral fellow in the lab, Jean Parry, has demonstrated that the G1 pore withdrawal and G2 pore entry begins around 6-7 hours after hatch. The G1/G2 pore swap is a tightly regulated developmental process that results in a seamless exchange of the old pore with the new pore. In wild type, the pore exchange never causes abnormal fluid accumulation. Thus, when the duct cell loses connections with the old pore, the new pore is ready instantaneously to connect to the duct to maintain normal osmoregulation in the worm.

My work suggests that Ras signaling may play a role in keeping the excretory system intact during the pore exchange process. Prior mosaic analysis has shown that the only cell that requires Ras for viability is the duct cell (Yochem et al., 1997). Also signaling between the G1 pore and G2 pore is not required for exit of one pore and entry of the other (Fig. 2.7). Therefore, if Ras signaling acts cell autonomously in the duct and not the G1 or G2 pore, how could Ras signaling affect the pore exchange process? I hypothesize that Ras signaling affects the pore exchange by promoting G1 exit. If G2 arrives at the duct to establish a connection and G1 has not withdrew, an unhealthy competition may ensue between the pore cells to determine which one will connect to the duct. I hypothesize that Ras signaling promotes G1withdraw by promoting break down of the duct junction that connects to the G1 pore.

A study performed in MDCK cells has shown that Ras signaling promotes adherens junction disassembly and breakdown of intercellular adhesions (Potempa and Ridley, 1998). MDCK epithelial cells become motile in cell culture when treated with Ras pathway growth factors (Potempa and Ridley, 1998; Ridley et al., 1995). However, when Ras signaling is blocked downstream with MAPKK inhibitors, MDCK cells lose the ability to spread after stimulation by Ras pathway ligands (Potempa and Ridley, 1998). β-catenin and E-cadherin localize to intercellular junctions between un-stimulated MDCK cells to hold them together (Potempa and Ridley, 1998). Upon Ras growth factor stimulation, β-catenin and E-cadherin expression are lost at junctions, allowing for cell spreading and motility (Potempa and Ridley, 1998). When MAPKK or PI3K, downstream genes in the Ras pathway, were inhibited, β-catenin and E-cadherin

expression persisted at intercellular junctions even in the presence of Ras growth factor stimulation (Potempa and Ridley, 1998). Therefore, Ras signaling is required for MDCK cells to down-regulate junctional proteins that connect cells together (Potempa and Ridley, 1998).

I hypothesize that continued Ras signaling in the duct cell is required to down-regulate proteins at the junctional complex that connects the duct to the pore. Since the G2 pore doesn't need a signal from the G1 pore to enter (Fig. 2.7), G2 will still attempt to connect to the duct with G1 still present. It is possible that a competition between the two pores leads to neither cell connecting to the duct correctly, thus resulting in excretory lethality. Further studies using time-lapse imaging of the G1/G2 pore exchange in both wild type and Ras mutants should clarify the preliminary data and hypothesis I have presented.

A search for MLS-2 target genes

MLS-2 promotes cell shape acquisition in the duct and pore by an unknown mechanism (Chapter Three). Craig Stone (a former graduate student in the lab) and I, attempted to take advantage of the incompletely penetrant *mls-2* phenotype and identify MLS-2 redundant genes (Chapters Four and Five). Knowing what genes could substitute for *mls-2* in its absence, could have predicted what function MLS-2 normally performs. However, the attempts do find *mls-2* redundant genes, either due to technical limitations or targeting the wrong genes, were largely unsuccessful. Since MLS-2 is a transcription

factor, the best way to determine how MLS-2 promotes cell shape in the duct and pore, is to determine what genes MLS-2 is turning on.

A sequence that MLS-2 binds to while turning one of its target genes has been validated *in vitro* and *in vivo*. The Sengupta lab identified a 9 base pair motif GCAAATGGG that MLS-2 binds to while regulating the expression of the Otx gene *ceh-36* (Kim et al., 2010). In gel shift assays MLS-2 can bind to this 9-mer sequence that is found in the ceh-36 promoter, and mutating this motif in worms prevents MLS-2 regulation of CEH-36 (Kim et al., 2010). CEH-36 appears to be a bona fide target of MLS-2 during differentiation of the AWC chemosensory neuron. In embryos CEH-36 expression precedes MLS-2 expression (J.I.Murray, personal communication), suggesting that MLS-2 doesn't regulate CEH-36 expression in the duct and pore during excretory system development. Nonetheless, these studies provide a motif that we could potentially utilize to find other MLS-2 targets relevant to our cells of interest.

Binding motifs for Nkx5/HMX family members have also been identified with transcription factors from mouse and Drosophila. Berger et al. determined the binding preferences of nearly all homeodomain proteins in the mouse to all possible 8-base sequences. To identify the DNA-binding preference of all homeodomain proteins Berger et al. used protein binding microarrays that contained every possible combination of 8-mer sequence. The preferred binding motif identified for the Nkx5/HMX family is CAATTAA (Berger et al., 2008). Another group identified the binding preference of all homeodomain proteins in Drosophila using a bacterial one-hybrid system. The Drosophila HMX preferred binding motif identified is tTAATTGc (Noyes et al., 2008).

Importantly, the homeodomain (DNA binding domain) of MLS-2 is nearly identical to the homeodomain of the mouse and Drosophila HMX (see Fig 1.5). However, it is not clear if MLS-2 can bind the mouse or Drosophila HMX binding motif. We could gain more confidence in MLS-2 binding to the mouse or Drosophila HMX binding motif if we could demonstrate rescue of the *mls-2* phenotype with mouse or Drosophila HMX. Having the MLS-2 binding motif from worms and the binding motifs of related family members, gives us sequence information to assist in finding novel MLS-2 candidate target genes.

MLS-2 and Ras cooperate to turn on *lin-48/Ovo* expression during duct morphogenesis (Chapter Three). However, we do not know if MLS-2 or Ras promote *lin-48* expression directly or indirectly. To test if MLS-2 might promote *lin-48* expression directly, I searched the ~5kb *lin-48* promoter (the same promoter region that drives *lin-48* expression in the duct) for the MLS-2 binding motif, and the mouse and Drosophila HMX motifs. I did not find the MLS-2 binding motif GCAAATGGG or the mouse binding motif CAATTAA in the *lin-48* promoter. However, I did find the shorter Drosophila HMX motif TAATTG three places in the *lin-48* promoter (Fig 6.3). It could be that the shorter Drosophila motif is more likely to appear at random because it is a 6-mer. However, a report from the Chamberlin lab suggests that at least one of the three sites (position 4756) may be important for *lin-48* expression. A deletion of only 200 base pairs in the *lin-48* promoter that deletes the Drosophila HMX site at position 4756, almost completely abolishes *lin-48* expression in the duct (Johnson et al., 2001)(Figure 6.3). If we can demonstrate that MLS-2 can bind to the Drosophila HMX motif, the data

from the Chamberlin lab may suggest that MLS-2 binding directly to *lin-48* may be necessary for its expression in the duct.

We set up a collaboration with Dr. Sridhar Hannenhalli to find MLS-2 target genes based on binding site motifs for the mouse HMX family (CAATTAA) and the mouse ETS family (A/G CCGGA A/T G T/C) (Berger et al., 2008; Wei et al., 2010). LIN-1, a downstream transcription factor in the Ras pathway is an ETS transcription factor (Jacobs et al., 1998). I hypothesized that MLS-2 and LIN-1 could potentially co-regulate target genes, such as *lin-48* (see Chapter Three). Dr. Hannenhalli searched the promoter (2 kb upstream) of all genes in *C.elegans* for presence of both the HMX and ETS motif, and he came up with a list of 447 genes. Sridhar performed the same analysis in a related nematode species *C.briggsae* and found 262 genes with an HMX and ETS site in their promoter. To eliminate potential false positives, he made a list of genes that had an HMX and ETS site in the promoter of a *C.elegans* gene and also the *C.briggsae* homologous gene. Dr. Hannenhalli's reduced, and potentially more specific list contained only 15 genes (Table 6.1). Most of the genes on the list are unnamed proteins with no reported functions. Analyzing mutants, performing RNAi, or making reporters with these genes are all ways to see if they could be potential MLS-2 and/or Ras target genes.

I am excited about a florescence activated cell sorting (FACS) based approach to find MLS-2 target genes. This FACS approach is a collaboration with Dr. John I. Murray in the Department of Genetics. The idea is to FACS sort the duct and pore cells from embryos, followed by RNA sequencing to get the profile of all transcripts expressed in the duct and pore. To sort the duct and pore we will use a strain bearing two reporters,

one green and one red. The reporters, ceh-6::GFP and hlh-16::mcherry, are both expressed in numerous lineages, but only overlap in the duct and pore (Fig. 6.4). Therefore, gaiting cells that are both green and red should only select the duct and pore. We will then perform the same strategy in an *mls-2* strain bearing ceh-6::GFP and hlh-16::mcherry to sort the duct and pore. I confirmed that hlh-16::mcherry is still expressed in the duct and pore in an *mls-2* background (data not shown), and I hypothesize that ceh-6::GFP is also still expressed in the duct and pore. After collecting the duct and pore cells from both wild type and *mls-2* mutants we will perform RNA sequencing on both strains. Genes that are differentially expressed in the duct and pore in an *mls-2* background will be candidate target genes. Members of the lab that continue this project could then perform further analysis including mutant assessment, making reporters, and potentially chromatin immuno-precipitation of potential candidate genes. In addition, we can look for preferred binding sites for MLS-2 and the HMX family in the promoters of the candidate targets to refine our list. This FACS approach should identify MLS-2 target genes that might explain how MLS-2 promotes cell shape acquisition.

Concluding Remarks

In my research, I have exploited the *C.elegans* excretory system in an attempt to learn more about tube formation in complex tubular organs. Although I have learned about the genetic requirements for Ras signaling in building a tube, key questions pertaining to how signaling controls these steps remain. I have described a homeodomain

transcription factor, MLS-2, that promotes cell elongation in the excretory system. I hypothesize that MLS-2 family members in higher organisms may have similar roles and/or targets as MLS-2 in the excretory system. Once functional targets of both MLS-2 and Ras are identified, understanding how these genes and pathways act to promote tubulogenesis will be clarified. With common human defects such as atherosclerosis and kidney disease being attributed to defects in tube architecture, these studies in the *C.elegans* excretory system should have broad implications in human health.

Materials and Methods

Strains and Alleles

N2 var. Bristol was the wild-type strain. Descriptions of each gene can be found at www.wormbase.org. *LGII: aff-1(tm2214)*(Sapir et al., 2007). *LGV: sos-1*(*cs41*) (Rocheleau et al., 2002). Transgenes used are: *jcIs1* (AJM-1::GFP) (Koppen et al., 2001a), *wgIs87* (ceh-6::GFP) (Murray lab), *stIs10544 (hlh-16::mcherry)* (Murray lab).

Marker analysis and imaging

Images were captured by differential interference contrast (DIC) and epifluorescence microscopy using a Zeiss Axioskop and Hamamatsu C5985 camera, or by confocal microscopy using a Leica SP5. Images were processed for brightness and contrast using Photoshop or ImageJ.

sos-1 temperature shifts

Newly hatched *sos-1; aff-1;* AJM-1::GFP worms were shifted from the permissive temperature (20ºC) to the non-permissive temperature (25ºC) between 1-7 hours after hatch. *aff-1* mutants do not lay eggs, but instead the embryos hatch within the moms (Sapir et al., 2007). To obtain 3-fold embryos, gravid *sos-1; aff-1;* AJM-1::GFP worms were bleach/NaOH treated, followed by hand-picking 3-fold embryos from the bleached moms. The 3-fold embryos were monitored every half hour until they hatched. Once the worms hatched they were transferred to the non-permissive temperature and scored 1-7 hours later.

Acknowledgements

I would like to thank Sridhar Hannenhalli, formerly of the Department of Genetics, for the collaboration using binding motifs to find MLS-2 target genes. I would also like to thank John I. Murray in the Department of Genetics for setting the FACS based collaboration to find novel MLS-2 target genes.

Figure Legends

Figure 6.1. In search of targets for Ras downstream effectors at each step of duct development. Timeline of excretory system development showing potential contributions of Ras downstream genes *lin-1, eor-1, sur-2*. *mls-2* acts in parallel to Ras potentially during morphogenesis.

Figure 6.2. Ras may affect the G1-to-G2 pore transition. A) Percentage of worms that were normal or had an abnormal junction pattern in the excretory system. Abnormal junction no shift versus 6-7 hour shift p=0.040l; abnormal junction 1-5 hour shift versus 6-7 hour shift p=0.0642. B-D) *sos-1; aff-1;* AJM-1::GFP worms scored 6-7 hours after shift. Junction phenotypes were associated with abnormal fluid accumulation. B) Large intercellular loop between the duct and pore cells. Asterisk marks the loop. C,D) Duct and pore disconnected from each other.

Figure 6.3. Drosophila HMX motif in lin-48 promoter may be necessary for duct expression. Figure taken and modified from (Johnson et al., 2001). *lin-48* promoter drives good expression in the duct cell, except with a specific 200bp deletion (bottom row). Not shown are the other two Drosophila HMX motifs in the *lin-48* promoter at positions 1052 and 3142, as they appear dispensable for *lin-48* duct expression.

Figure 6.4. ceh-6::GFP and hlh-16::mcherry expression overlap in the duct and pore lineages. A)Lineage tree with expression of a translational reporter ceh-6::GFP and a transcriptional reporter hlh-16::mcherry. Expression of these two reporters only overlaps in the duct and pore lineages. Expression patterns based on data from the Murray lab. B-D) Enclosure stage embryo expressing ceh-6::GFP and hlh-16::mcherry with overlap in the duct and pore.

Table 6.1. Potential MLS-2 and LIN-1 common target genes.15 genes that have an HMX and ETS motif in the promoter of a *C.elegans* gene, and an HMX and ETS motif in the homologous gene in *C.briggsae*.

Figure 6.1

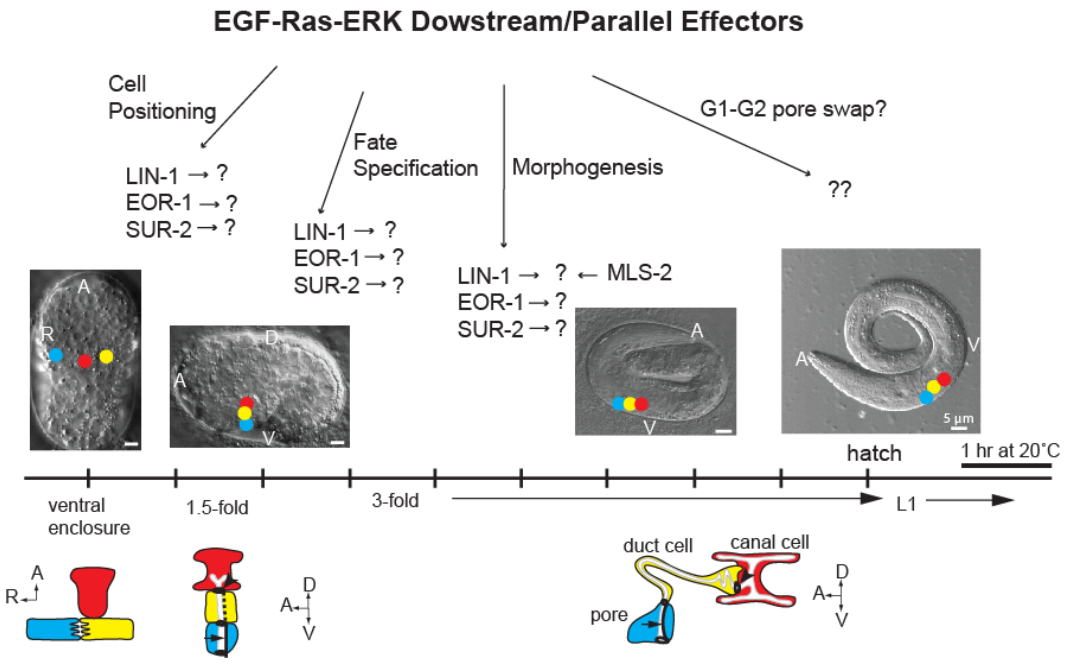
EGF-Ras-ERK Dowstream/Parallel Effectors
Cell Positioning
LIN-1 → ?
EOR-1 → ?
SUR-2 → ?
Fate Specification
LIN-1 → ?
EOR-1 → ?
SUR-2 → ?
Morphogenesis
LIN-1 → ? ← MLS-2
EOR-1 → ?
SUR-2 → ?
G1-G2 pore swap?
??
A
R
D
A
V
A
V
A
V
5 µm
hatch
1 hr at 20°C
ventral enclosure
1.5-fold
3-fold
L1
A
R
D
A
V
duct cell
canal cell
pore
D
A
V

Figure 6.2

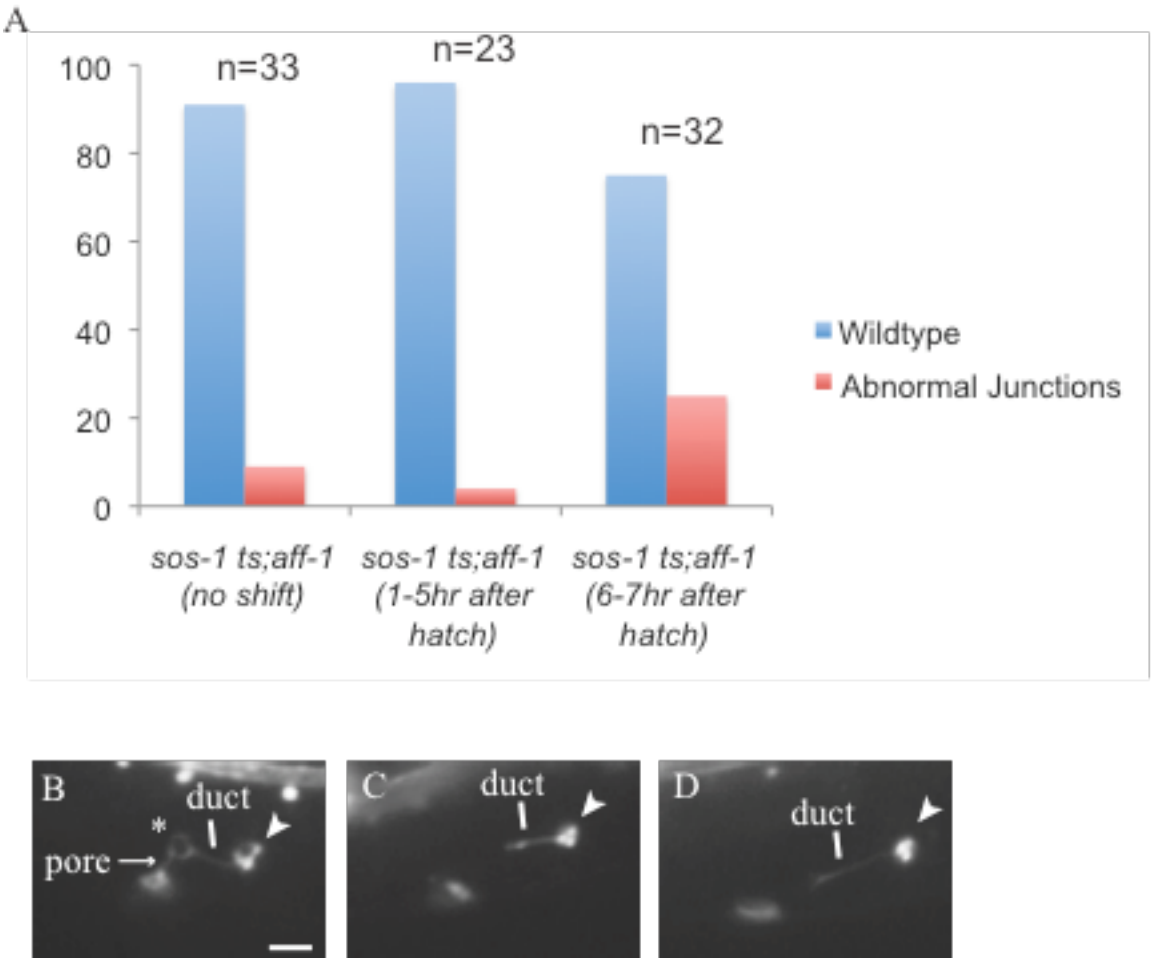
A
100
80
60
40
20
0
n=33
n=23
n=32
Wildtype
Abnormal Junctions
sos-1 ts;aff-1 (no shift)
sos-1 ts;aff-1 (1-5hr after hatch)
sos-1 ts;aff-1 (6-7hr after hatch)
B
duct
pore
C
duct
D
duct

Figure 6.3

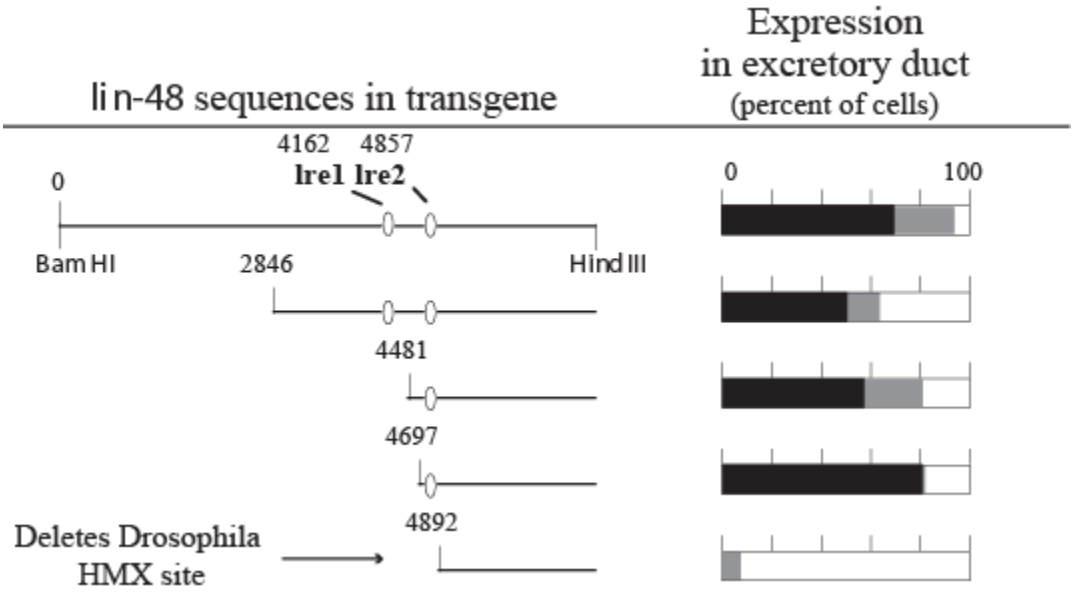
lin-48 sequences in transgene
Expression
in excretory duct
(percent of cells)
4162
4857
lre1
lre2
0
0
100
Bam HI
2846
Hind III
4481
4697
4892
Deletes Drosophila
HMX site

Figure 6.4

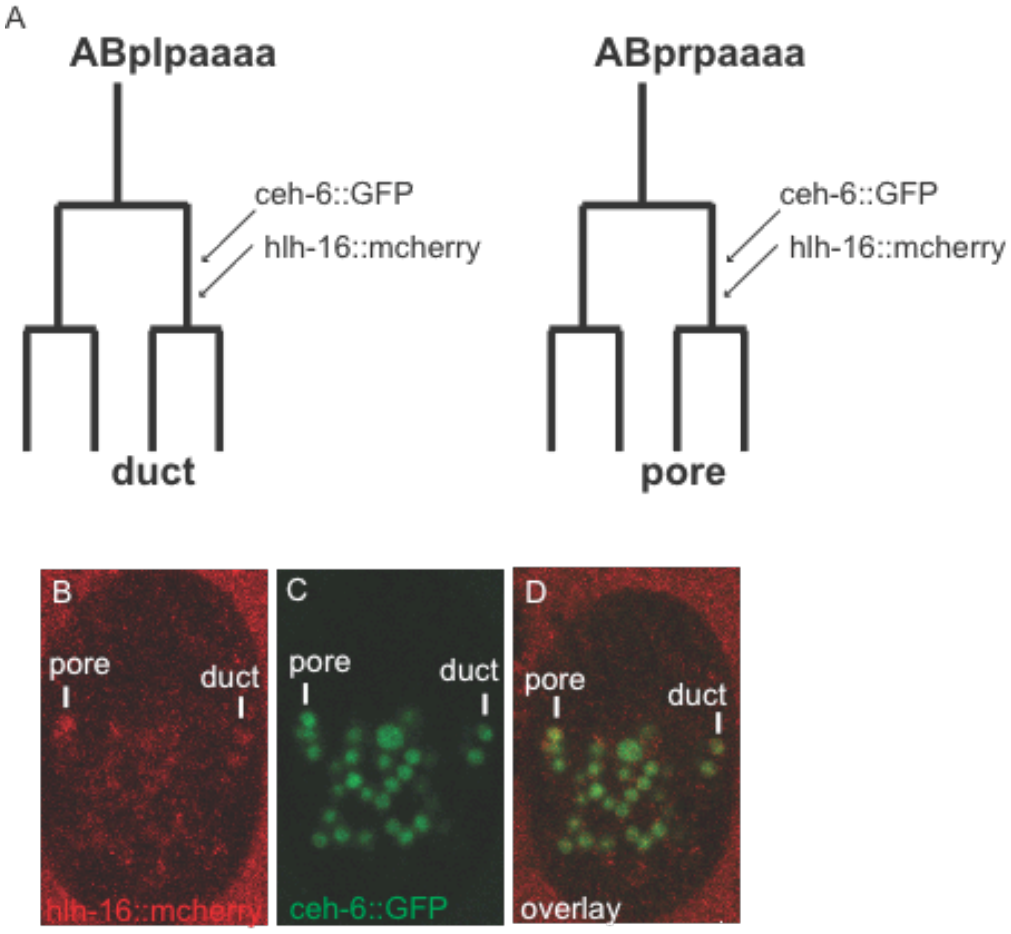
A
ABplpaaaa
ceh-6::GFP
hlh-16::mcherry
duct
ABprpaaaa
ceh-6::GFP
hlh-16::mcherry
pore
B
pore
duct
hlh-16::mcherry
C
pore
duct
ceh-6::GFP
D
pore
duct
overlay

Table 6.1

C.elegans gene	*C.briggsae* gene	Wormbase Annotation
C33G8.4	CBG19063	Uncharacterized protein
F57B9.8	CBG16480	Tyrosine protein kinase
Y43F11A.1	CBG10027	Unnamed protein
T10D4.1	CBG20893	Unnamed protein
M02G9.2	CBG02724	Unnamed protein
C15C8.1	CBG08573	Unnamed protein
T22B11.4	CBG01732	Unnamed protein
F26A1.8	CBG17976	Unnamed protein
Y32H12A.7	CBG05169	Predicted unusual protein kinase
T16H12.4	CBG09887	RNA Pol II subunit SSL1
C30G12.1	CBG13131	Unnamed protein
K07C11.8	CBG11323	Unnamed protein
W05B10.4	CBG08550	Unnamed protein
F15G9.2	CBG16046	Unnamed protein
H43IO7.3	CBG01437	Glycosyltransferase

Addendum:

A ROLE FOR THE RAL GEF RGL-1 IN EXCRETORY SYSTEM DEVELOPMENT

Introduction

The *C.elegans* 1° vulval fate is specified by activation of the canonical EGF-Ras-Erk signaling cascade (Sternberg, 2005). Recently, the Reiner lab demonstrated that in addition to Ras signaling through the Raf kinase, Ras can alternatively signal through the Ral guanine nucleotide exchange factor (GEF) RGL-1 to promote the 2° vulval fate (Zand et al., 2011). Thus, Ras signaling through RGL-1 antagonizes Ras signaling through Raf and the canonical pathway (Zand et al., 2011). The Reiner lab also made another observation with *rgl-1* mutants in the excretory system that is unpublished. Hyper-activating Ras leads to specification of multiple vulval cells (Beitel et al., 1990), and specification of two duct cells (Abdus-Saboor et al., 2011). Mutants where Ras is hyper-activated sometimes have a 'bump' protruding from the worm near the duct cell, and it is thought that the 'bump' corresponds to two-duct cells being specified. The Reiner lab noticed that when *rgl-1* mutants were put into a Ras hyperactive background, the frequency of the 'bumps' near the duct cell increased. This raised the hypothesis that Ras signaling thru *rgl-1* may antagonize Ras signaling through the canonical pathway, analogous to observations made in the vulva. We established a collaboration with the Reiner lab to this hypothesis.

Results and Discussion

Mutants with Ras hyperactivated *(n1046)* had the duct bump less than 20% of the time (Fig. A.1). However, when *n1046* was combined with two different *rgl-1* alleles, the percentage of duct bumps greatly increased (Fig A.1). We visualized the duct cell with

lin-48p::GFP in *n1046* mutants alone and in combination with *rgl-1* at L1, L4, and adult. *n1046* alone had a high percentage of 2-duct cell specification, thus *rgl-1* didn't have an effect on a phenotype that already reached its higher limit (Fig A.2). In addition, duct morphology was not altered in an *n1046* background alone versus in combination with *rgl-1* (data not shown). These data did show that the bumps corresponded to the duct protrusions, as the bumps were almost always positive for *lin-48* duct expression (data not shown). The question still remained as to why the *rgl-1* mutation was enhancing duct protrusion in a hyper-activated Ras background.

To investigate the *rgl-1* enhancement of duct protrusion in further detail we analyzed *n1046* alone and in combination with *rgl-1* with the AJM-1::GFP marker. Hyper-activating Ras leads to two-ducts being specified and no G1 pore specification (Abdus-Saboor et al., 2011) (Fig A.3A). However, most times the G2 pore still enters the excretory system in a two-duct background and wraps around the second duct that is positioned ventrally (Abdus-Saboor et al., 2011) (Fig. A.3B). Surprisingly, in *rgl-1;n1046* adults, the G2 ventral signal was almost always gone (Fig. A.3B-D). While we have not analyzed adult *n1046* mutants alone to make sure they do not lose the ventral G2 signal, the loss of the G2 signal in *n1046;rgl-1* is the only difference we have noticed that might provide insight into how *rgl-1* is causing increased duct protrusions.

Several hypotheses could explain how *rgl-1* is causing enhanced duct protrusions in an *n1046* background based on my limited observations. *rgl-1* may antagonize the canonical EGF-Ras pathway in the duct, leading to increased growth and elongation of the duct cell, which causes in enhancement of duct protrusions. Alternatively, *rgl-1* may

weaken the junction where the duct connects to the outside of the worm, resulting in the duct being able to break through the hypodermis. The loss of the G2 ventral signal in *rgl-1;n1046* does not distinguish between these two hypotheses. Thus, further tests need to be performed to determine if the same *rgl-1* alternative pathway utilized in the vulva, is also utilized in the excretory duct.

Materials and Methods

Strains and Alleles

N2 var. Bristol was the wild-type strain. Descriptions of each gene can be found at www.wormbase.org. *LGIV: let-60(n1046)* (Beitel et al., 1990). LGX: *rgl-1(ok1921)* (Knockout Consortium allele)*, rgl-1(tm2255)* (Knockout Consortium allele). Transgenes used are: *jcIs1* (AJM-1::GFP) (Koppen et al., 2001a), *saIs14* (*lin-48p*::GFP)(Johnson et al., 2001), *wIs78* (AJM-1::GFP) (Koh and Rothman, 2001).

Marker analysis and imaging

Images were captured by differential interference contrast (DIC) and epifluorescence microscopy using a Zeiss Axioskop and Hamamatsu C5985 camera. Images were processed for brightness and contrast using Photoshop.

Acknowledgements

I thank David Reiner for contacting Meera and I to setup this collaboration. All of the strains analyzed were made in the Reiner lab. I also thank Meera for helping me score and confirm the 'loss of G2 signal' phenotype.

Figure Legends

Figure A.1. *rgl-1* enhances *n1046* duct bump. A) Percentage of adult worms showing the excretory duct bump phenotype. n at least 20 for each genotype. B) Image of an adult *rgl-1;n1046* worm showing the duct bump phenotype. White line marks the bump.

Figure A.2. *rgl-1* does not affect *lin-48* expression of *n1046*. A) Bar graph showing percentage of *n1046* and *n1046;rgl-1* mutants with the 2 *lin-48* expressing duct cells. B) Representative image of *n1046* L4 with 2 *lin-48* positive duct cells. White lines show each *lin-48* expressing duct cell. Note: *n1046;rgl-1* was indistinguishable from *n1046*.

Figure A.3. *rgl-1;n1046* mutants lack ventral G2 pore signal. (A,B) Same dataset, different observations. A) Percentage of *n1046* and *n1046;rgl-1* mutants that have a pore auto-cellular junction (AJ) scored by AJM-1::GFP. B) Percentage of *n1046* and *n1046;rgl-1* mutants that have a ventral G2 signal scored by AJM-1::GFP. (C,D) DIC and corresponding florescence micrograph of *n1046;rgl-1* that lacks a ventral G2 signal. Asterisk marks region where G2 ventral signal would normally be located.

Figure A.1

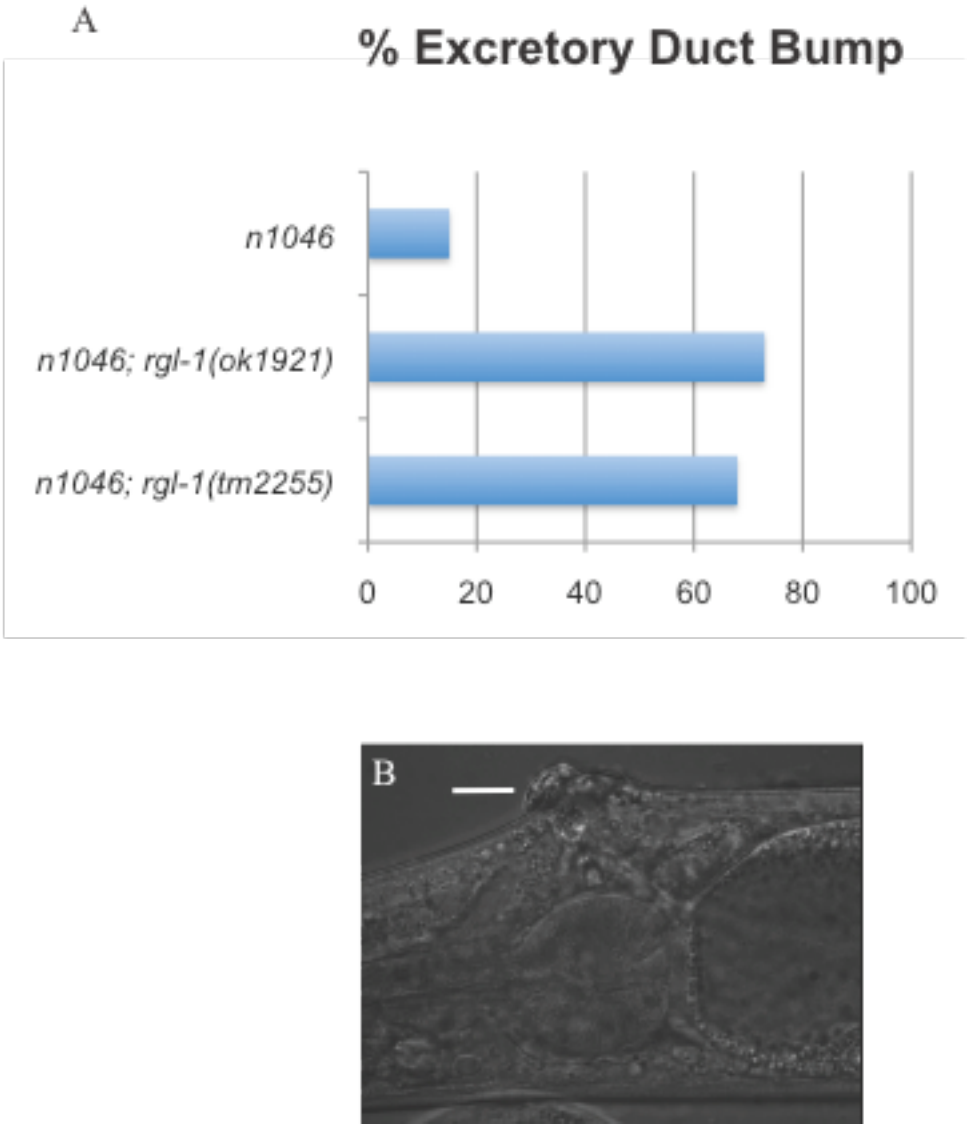
A
% Excretory Duct Bump
n1046
n1046; rgl-1(ok1921)
n1046; rgl-1(tm2255)
0
20
40
60
80
100
B

Figure A.2

A

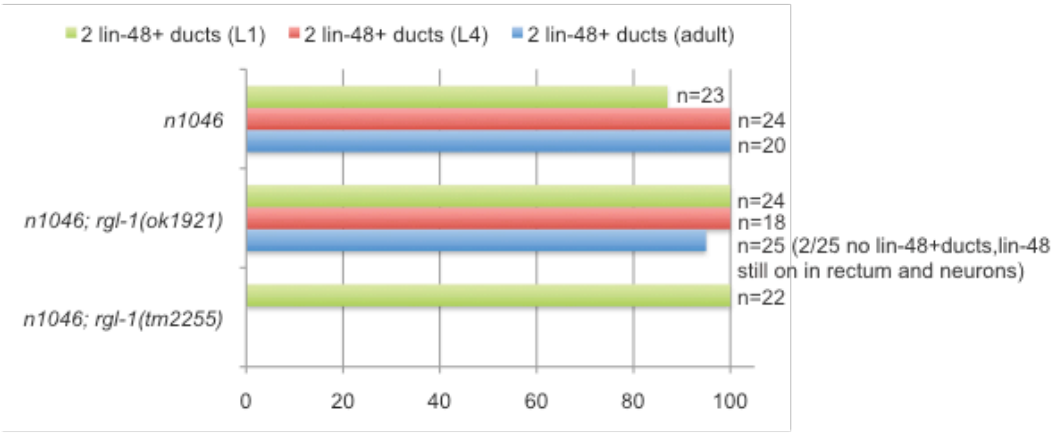
2 lin-48+ ducts (L1)
2 lin-48+ ducts (L4)
2 lin-48+ ducts (adult)
n1046
n1046; rgl-1(ok1921)
n1046; rgl-1(tm2255)
n=23
n=24
n=20
n=24
n=18
n=25 (2/25 no lin-48+ducts,lin-48 still on in rectum and neurons)
n=22
0
20
40
60
80
100

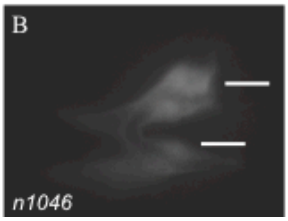
B
n1046

Figure A.3

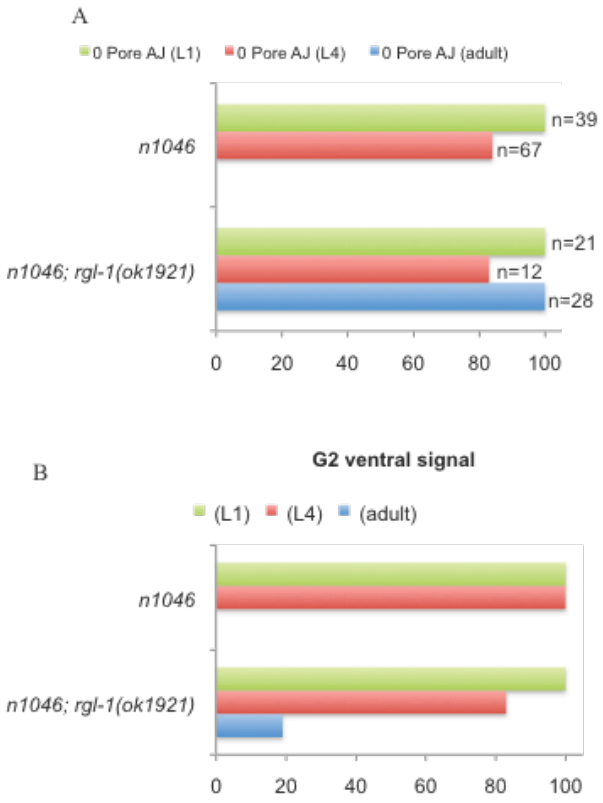
A
0 Pore AJ (L1)
0 Pore AJ (L4)
0 Pore AJ (adult)
n1046
n1046; rgl-1(ok1921)
n=39
n=67
n=21
n=12
n=28
0
20
40
60
80
100
B
G2 ventral signal
(L1)
(L4)
(adult)
n1046
n1046; rgl-1(ok1921)
0
20
40
60
80
100

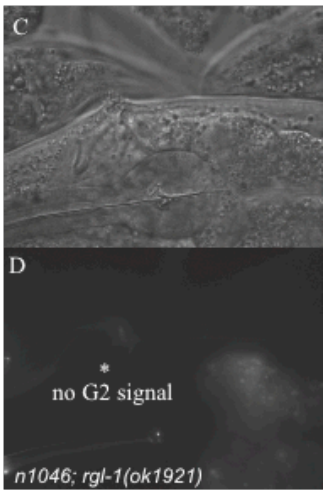
C
D
no G2 signal
n1046; rgl-1(ok1921)

References

Abdus-Saboor, I., Mancuso, V.P., Murray, J.I., Palozola, K., Norris, C., Hall, D.H., Howell, K., Huang, K., Sundaram, M.V., 2011. Notch and Ras promote sequential steps of excretory tube development in C. elegans. Development 138, 3545-3555.

Acloque, H., Adams, M.S., Fishwick, K., Bronner-Fraser, M., Nieto, M.A., 2009. Epithelial-mesenchymal transitions: the importance of changing cell state in development and disease. The Journal of clinical investigation 119, 1438-1449.

Adamska, M., Leger, S., Brand, M., Hadrys, T., Braun, T., Bober, E., 2000. Inner ear and lateral line expression of a zebrafish Nkx5-1 gene and its downregulation in the ears of FGF8 mutant, ace. Mech Develop 97, 161-165.

Adamska, M., Wolff, A., Kreusler, M., Wittbrodt, J., Braun, T., Bober, E., 2001. Five Nkx5 genes show differential expression patterns in anlagen of sensory organs in medaka: insight into the evolution of the gene family. Dev Genes Evol 211, 338-349.

Albertson, D.G., Thomson, J.N., 1976. The pharynx of Caenorhabditis elegans. Philosophical transactions of the Royal Society of London. Series B, Biological sciences 275, 299-325.

Andrew, D.J., Ewald, A.J., 2010. Morphogenesis of epithelial tubes: Insights into tube formation, elongation, and elaboration. Developmental biology 341, 34-55.

Avinoam, O., Fridman, K., Valansi, C., Abutbul, I., Zeev-Ben-Mordehai, T., Maurer, U.E., Sapir, A., Danino, D., Grunewald, K., White, J.M., Podbilewicz, B., 2011. Conserved eukaryotic fusogens can fuse viral envelopes to cells. Science 332, 589-592.

Bagnat, M., Cheung, I.D., Mostov, K.E., Stainier, D.Y., 2007. Genetic control of single lumen formation in the zebrafish gut. Nature cell biology 9, 954-960.

Bao, Z., Murray, J.I., Boyle, T., Ooi, S.L., Sandel, M.J., Waterston, R.H., 2006. Automated cell lineage tracing in Caenorhabditis elegans. Proc Natl Acad Sci U S A 103, 2707-2712.

Bar, T., Guldner, F.H., Wolff, J.R., 1984. "Seamless" endothelial cells of blood capillaries. Cell and tissue research 235, 99-106.

Baran, R., Castelblanco, L., Tang, G., Shapiro, I., Goncharov, A., Jin, Y., 2010. Motor neuron synapse and axon defects in a C. elegans alpha-tubulin mutant. PloS one 5, e9655.

Bargmann, C.I., Hartwieg, E., Horvitz, H.R., 1993. Odorant-selective genes and neurons mediate olfaction in C. elegans. Cell 74, 515-527.

Barr, M.M., 2003. Super models. Physiological genomics 13, 15-24.

Baum, B., Georgiou, M., 2011. Dynamics of adherens junctions in epithelial establishment, maintenance, and remodeling. The Journal of cell biology 192, 907-917.

Beitel, G.J., Clark, S.G., Horvitz, H.R., 1990. Caenorhabditis elegans ras gene let-60 acts as a switch in the pathway of vulval induction. Nature 348, 503-509.

Beitel, G.J., Tuck, S., Greenwald, I., Horvitz, H.R., 1995a. The *Caenorhabditis elegans* gene *lin-1* encodes an ETS-domain protein and defines a branch in the vulval induction pathway. Genes Dev. 9, 3149-3162.

Beitel, G.J., Tuck, S., Greenwald, I., Horvitz, H.R., 1995b. The Caenorhabditis elegans gene lin-1 encodes an ETS-domain protein and defines a branch of the vulval induction pathway. Genes Dev 9, 3149-3162.

Berger, M.F., Badis, G., Gehrke, A.R., Talukder, S., Philippakis, A.A., Pena-Castillo, L., Alleyne, T.M., Mnaimneh, S., Botvinnik, O.B., Chan, E.T., Khalid, F., Zhang, W., Newburger, D., Jaeger, S.A., Morris, Q.D., Bulyk, M.L., Hughes, T.R., 2008. Variation in homeodomain DNA binding revealed by high-resolution analysis of sequence preferences. Cell 133, 1266-1276.

Berrier, A.L., Yamada, K.M., 2007. Cell-matrix adhesion. J Cell Physiol 213, 565-573.

Blum, Y., Belting, H.G., Ellertsdottir, E., Herwig, L., Luders, F., Affolter, M., 2008. Complex cell rearrangements during intersegmental vessel sprouting and vessel fusion in the zebrafish embryo. Developmental biology 316, 312-322.

Blume-Jensen, P., Hunter, T., 2001. Oncogenic kinase signalling. Nature 411, 355-365.

Bober, E., Baum, C., Braun, T., Arnold, H.H., 1994. A Novel Nk-Related Mouse Homeobox Gene - Expression in Central and Peripheral Nervous Structures during Embryonic-Development. Developmental biology 162, 288-303.

Bobinnec, Y., Fukuda, M., Nishida, E., 2000. Identification and characterization of Caenorhabditis elegans gamma-tubulin in dividing cells and differentiated tissues. Journal of cell science 113 Pt 21, 3747-3759.

Bossinger, O., Klebes, A., Segbert, C., Theres, C., Knust, E., 2001. Zonula adherens formation in Caenorhabditis elegans requires dlg-1, the homologue of the Drosophila gene discs large. Dev Biol 230, 29-42.

Boyle, T.J., Bao, Z., Murray, J.I., Araya, C.L., Waterston, R.H., 2006. AceTree: a tool for visual analysis of Caenorhabditis elegans embryogenesis. BMC Bioinformatics 7, 275.

Brenner, S., 1974. The genetics of Caenorhabditis elegans. Genetics 77, 71-94.

Brodu, V., Casanova, J., 2006. The RhoGAP crossveinless-c links trachealess and EGFR signaling to cell shape remodeling in Drosophila tracheal invagination. Genes & development 20, 1817-1828.

Bryant, D.M., Mostov, K.E., 2008. From cells to organs: building polarized tissue. Nature reviews. Molecular cell biology 9, 887-901.

Buechner, M., 2002. Tubes and the single C. elegans excretory cell. Trends in cell biology 12, 479-484.

Buechner, M., Hall, D.H., Bhatt, H., Hedgecock, E.M., 1999. Cystic canal mutants in Caenorhabditis elegans are defective in the apical membrane domain of the renal (excretory) cell. Developmental biology 214, 227-241.

Burglin, T.R., Ruvkun, G., 2001. Regulation of ectodermal and excretory function by the C-elegans POU homeobox gene ceh-6. Development 128, 779-790.

Burrows, A.E., Smogorzewska, A., Elledge, S.J., 2010. Polybromo-associated BRG1-associated factor components BRD7 and BAF180 are critical regulators of p53 required for induction of replicative senescence. Proc Natl Acad Sci U S A 107, 14280-14285.

Calixto, A., Chelur, D., Topalidou, I., Chen, X., Chalfie, M., 2010. Enhanced neuronal RNAi in C. elegans using SID-1. Nature methods 7, 554-559.

Carmeliet, P., Ferreira, V., Breier, G., Pollefeyt, S., Kieckens, L., Gertsenstein, M., Fahrig, M., Vandenhoeck, A., Harpal, K., Eberhardt, C., Declercq, C., Pawling, J., Moons, L., Collen, D., Risau, W., Nagy, A., 1996. Abnormal blood vessel development and lethality in embryos lacking a single VEGF allele. Nature 380, 435-439.

Cartier, L., Laforge, T., Feki, A., Arnaudeau, S., Dubois-Dauphin, M., Krause, K.H., 2006. Pax6-induced alteration of cell fate: shape changes, expression of neuronal alpha tubulin, postmitotic phenotype, and cell migration. Journal of neurobiology 66, 421-436.

Cela, C., Llimargas, M., 2006. Egfr is essential for maintaining epithelial integrity during tracheal remodelling in Drosophila. Development 133, 3115-3125.

Chalfie, M., Thomson, J.N., 1982. Structural and functional diversity in the neuronal microtubules of Caenorhabditis elegans. The Journal of cell biology 93, 15-23.

Chang, C., Hsieh, Y.W., Lesch, B.J., Bargmann, C.I., Chuang, C.F., 2011. Microtubule-based localization of a synaptic calcium-signaling complex is required for left-right neuronal asymmetry in C. elegans. Development 138, 3509-3518.

Chang, L., Goldman, R.D., 2004. Intermediate filaments mediate cytoskeletal crosstalk. Nature reviews. Molecular cell biology 5, 601-613.

Chanut-Delalande, H., Fernandes, I., Roch, F., Payre, F., Plaza, S., 2006. Shavenbaby couples patterning to epidermal cell shape control. PLoS Biol 4, e290.

Chen, N., Greenwald, I., 2004. The lateral signal for LIN-12/Notch in *C. elegans* vulval development comprises redundant secreted and transmembrane DSL proteins. Dev. Cell 6, 183-192.

Chesarone, M.A., DuPage, A.G., Goode, B.L., 2010. Unleashing formins to remodel the actin and microtubule cytoskeletons. Nature reviews. Molecular cell biology 11, 62-74.

Chi, X., Michos, O., Shakya, R., Riccio, P., Enomoto, H., Licht, J.D., Asai, N., Takahashi, M., Ohgami, N., Kato, M., Mendelsohn, C., Costantini, F., 2009. Ret-dependent cell rearrangements in the Wolffian duct epithelium initiate ureteric bud morphogenesis. Developmental cell 17, 199-209.

Church, D., Guan, K.L., Lambie, E.J., 1995. Three genes of the MAP kinase cascade, *mek-2, mpk-1/sur-1* and *let-60 ras*, are required for meiotic cell cycle progression in *Caenorhabditis elegans*. Development 121, 2525-2535.

Costantini, F., 2010. GDNF/Ret signaling and renal branching morphogenesis: From mesenchymal signals to epithelial cell behaviors. Organogenesis 6, 252-262.

Costantini, F., Shakya, R., 2006. GDNF/Ret signaling and the development of the kidney. BioEssays : news and reviews in molecular, cellular and developmental biology 28, 117-127.

Dai, X., Schonbaum, C., Degenstein, L., Bai, W., Mahowald, A., Fuchs, E., 1998. The ovo gene required for cuticle formation and oogenesis in flies is involved in hair formation and spermatogenesis in mice. Genes & development 12, 3452-3463.

Deitcher, D.L., Fekete, D.M., Cepko, C.L., 1994. Asymmetric expression of a novel homeobox gene in vertebrate sensory organs. The Journal of neuroscience : the official journal of the Society for Neuroscience 14, 486-498.

Devine, W.P., Lubarsky, B., Shaw, K., Luschnig, S., Messina, L., Krasnow, M.A., 2005. Requirement for chitin biosynthesis in epithelial tube morphogenesis. Proc Natl Acad Sci U S A 102, 17014-17019.

DeVore, D.L., Horvitz, H.R., Stern, M.J., 1995. An FGF receptor signaling pathway is required for the normal cell migrations of the sex myoblasts in *C. elegans* hermaphrodites. Cell 83, 611-620.

DeWitt, N., 2005. Angiogenesis. Nature 438, 931-931.

Dressler, G.R., 2009. Advances in early kidney specification, development and patterning. Development 136, 3863-3874.

Driscoll, M., Dean, E., Reilly, E., Bergholz, E., Chalfie, M., 1989. Genetic and molecular analysis of a Caenorhabditis elegans beta-tubulin that conveys benzimidazole sensitivity. The Journal of cell biology 109, 2993-3003.

Duerr, J.S., Frisby, D.L., Gaskin, J., Duke, A., Asermely, K., Huddleston, D., Eiden, L.E., Rand, J.B., 1999. The cat-1 gene of Caenorhabditis elegans encodes a vesicular monoamine transporter required for specific monoamine-dependent behaviors. J Neurosci 19, 72-84.

Eilken, H.M., Adams, R.H., 2010. Dynamics of endothelial cell behavior in sprouting angiogenesis. Current opinion in cell biology 22, 617-625.

Ellis, G.C., Phillips, J.B., O'Rourke, S., Lyczak, R., Bowerman, B., 2004. Maternally expressed and partially redundant beta-tubulins in Caenorhabditis elegans are autoregulated. Journal of cell science 117, 457-464.

Fekete, D.M., 1999. Development of the vertebrate ear: insights from knockouts and mutants. Trends in neurosciences 22, 263-269.

Feng, Y., Xu, Q.L., 2010. Pivotal role of hmx2 and hmx3 in zebrafish inner ear and lateral line development. Developmental biology 339, 507-518.

Ferguson, E.L., Horvitz, H.R., 1985. Identification and characterization of 22 genes that affect the vulval cell lineages of the nematode *Caenorhabditis elegans*. Genetics 110, 17-72.

Ferrara, N., Gerber, H.P., LeCouter, J., 2003. The biology of VEGF and its receptors. Nat Med 9, 669-676.

Fire, A., Kondo, K., Waterston, R., 1990. Vectors for low copy transformation of C. elegans. Nucleic Acids Research 18, 4269-4270.

Folkman, J., Haudenschild, C., 1980. Angiogenesis by Capillary Endothelial-Cells in Culture. Transactions of the ophthalmological societies of the United Kingdom 100, 346-353.

Frankel, N., Davis, G.K., Vargas, D., Wang, S., Payre, F., Stern, D.L., 2010. Phenotypic robustness conferred by apparently redundant transcriptional enhancers. Nature 466, 490-493.

Frankel, N., Erezyilmaz, D.F., McGregor, A.P., Wang, S., Payre, F., Stern, D.L., 2011. Morphological evolution caused by many subtle-effect substitutions in regulatory DNA. Nature 474, 598-603.

Friedman, J.R., Kaestner, K.H., 2006. The Foxa family of transcription factors in development and metabolism. Cellular and molecular life sciences : CMLS 63, 2317-2328.

Fuchs, E., Karakesisoglou, I., 2001. Bridging cytoskeletal intersections. Genes & development 15, 1-14.

Fukushige, T., Yasuda, H., Siddiqui, S.S., 1995. Selective expression of the tba-1 alpha tubulin gene in a set of mechanosensory and motor neurons during the development of Caenorhabditis elegans. Biochim Biophys Acta 1261, 401-416.

Gehring, W.J., Ikeo, K., 1999. Pax 6: mastering eye morphogenesis and eye evolution. Trends in genetics : TIG 15, 371-377.

Gervais, L., Casanova, J., 2011. The Drosophila homologue of SRF acts as a boosting mechanism to sustain FGF-induced terminal branching in the tracheal system. Development 138, 1269-1274.

Ghabrial, A., Luschnig, S., Metzstein, M.M., Krasnow, M.A., 2003. Branching morphogenesis of the Drosophila tracheal system. Annu Rev Cell Dev Biol 19, 623-647.

Ghabrial, A.S., Krasnow, M.A., 2006. Social interactions among epithelial cells during tracheal branching morphogenesis. Nature 441, 746-749.

Ghabrial, A.S., Levi, B.P., Krasnow, M.A., 2011. A systematic screen for tube morphogenesis and branching genes in the Drosophila tracheal system. PLoS genetics 7, e1002087.

Goldman, R.D., Khuon, S., Chou, Y.H., Opal, P., Steinert, P.M., 1996. The function of intermediate filaments in cell shape and cytoskeletal integrity. The Journal of cell biology 134, 971-983.

Goldstein, B., Macara, I.G., 2007. The PAR proteins: fundamental players in animal cell polarization. Developmental cell 13, 609-622.

Gonczy, P., Schnabel, H., Kaletta, T., Amores, A.D., Hyman, T., Schnabel, R., 1999. Dissection of cell division processes in the one cell stage Caenorhabditis elegans embryo by mutational analysis. The Journal of cell biology 144, 927-946.

Gongal, P.A., March, L.D., Holly, V.L., Pillay, L.M., Berry-Wynne, K.M., Kagechika, H., Waskiewicz, A.J., 2011. Hmx4 regulates Sonic hedgehog signaling through control of retinoic acid synthesis during forebrain patterning. Developmental biology 355, 55-64.

Greenwald, I.S., Sternberg, P.W., Horvitz, H.R., 1983. The lin-12 locus specifies cell fates in Caenorhabditis elegans. Cell 34, 435-444.

Hannak, E., Oegema, K., Kirkham, M., Gonczy, P., Habermann, B., Hyman, A.A., 2002. The kinetically dominant assembly pathway for centrosomal asters in Caenorhabditis elegans is gamma-tubulin dependent. The Journal of cell biology 157, 591-602.

Hao, L., Thein, M., Brust-Mascher, I., Civelekoglu-Scholey, G., Lu, Y., Acar, S., Prevo, B., Shaham, S., Scholey, J.M., 2011. Intraflagellar transport delivers tubulin isotypes to sensory cilium middle and distal segments. Nature cell biology 13, 790-798.

Heiman, M.G., Shaham, S., 2009. DEX-1 and DYF-7 establish sensory dendrite length by anchoring dendritic tips during cell migration. Cell 137, 344-355.

Hellstrom, M., Phng, L.K., Hofmann, J.J., Wallgard, E., Coultas, L., Lindblom, P., Alva, J., Nilsson, A.K., Karlsson, L., Gaiano, N., Yoon, K., Rossant, J., Iruela-Arispe, M.L., Kalen, M., Gerhardt, H., Betsholtz, C., 2007. Dll4 signalling through Notch1 regulates formation of tip cells during angiogenesis. Nature 445, 776-780.

Herbrand, H., Guthrie, S., Hadrys, T., Hoffmann, S., Arnold, H.H., Rinkwitz-Brandt, S., Bober, E., 1998. Two regulatory genes, cNkx5-1 and cPax2, show different responses to local signals during otic placode and vesicle formation in the chick embryo. Development 125, 645-654.

Herrmann, H., Bar, H., Kreplak, L., Strelkov, S.V., Aebi, U., 2007. Intermediate filaments: from cell architecture to nanomechanics. Nature reviews. Molecular cell biology 8, 562-573.

Hill, R.J., Sternberg, P.W., 1992. The gene lin-3 encodes an inductive signal for vulval development in C. elegans [see comments]. Nature 358, 470-476.

Hogan, B.L., Kolodziej, P.A., 2002. Organogenesis: molecular mechanisms of tubulogenesis. Nat Rev Genet 3, 513-523.

Howard, R.M., Sundaram, M.V., 2002. C. elegans EOR-1/PLZF and EOR-2 positively regulate Ras and Wnt signaling and function redundantly with LIN-25 and the SUR-2 Mediator component. Genes & development 16, 1815-1827.

Howell, K., Arur, S., Schedl, T., Sundaram, M.V., 2010. EOR-2 is an obligate binding partner of the BTB-zinc finger protein EOR-1 in Caenorhabditis elegans. Genetics 184, 899-913.

Hurd, D.D., Miller, R.M., Nunez, L., Portman, D.S., 2010. Specific alpha- and beta-tubulin isotypes optimize the functions of sensory Cilia in Caenorhabditis elegans. Genetics 185, 883-896.

Hwang, B.J., Sternberg, P.W., 2004. A cell-specific enhancer that specifies lin-3 expression in the C. elegans anchor cell for vulval development. Development 131, 143-151.

Iruela-Arispe, M.L., Davis, G.E., 2009. Cellular and molecular mechanisms of vascular lumen formation. Developmental cell 16, 222-231.

Jacobs, D., Beitel, G.J., Clark, S.G., Horvitz, H.R., Kornfeld, K., 1998. Gain-of-function mutations in the Caenorhabditis elegans lin-1 ETS gene identify a C-terminal regulatory domain phosphorylated by ERK MAP kinase. Genetics 149, 1809-1822.

Jakobsson, L., Franco, C.A., Bentley, K., Collins, R.T., Ponsioen, B., Aspalter, I.M., Rosewell, I., Busse, M., Thurston, G., Medvinsky, A., Schulte-Merker, S., Gerhardt, H., 2010. Endothelial cells dynamically compete for the tip cell position during angiogenic sprouting. Nature cell biology 12, 943-953.

Jarriault, S., Schwab, Y., Greenwald, I., 2008. A Caenorhabditis elegans model for epithelial-neuronal transdifferentiation. Proc Natl Acad Sci U S A 105, 3790-3795.

Jiang, Y., Horner, V., Liu, J., 2005. The HMX homeodomain protein MLS-2 regulates cleavage orientation, cell proliferation and cell fate specification in the C. elegans postembryonic mesoderm. Development 132, 4119-4130.

Johnson, A.D., Fitzsimmons, D., Hagman, J., Chamberlin, H.M., 2001. EGL-38 Pax regulates the ovo-related gene lin-48 during Caenorhabditis elegans organ development. Development 128, 2857-2865.

Johnson, S.A., Hunter, T., 2005. Kinomics: methods for deciphering the kinome. Nature methods 2, 17-25.

Jurgens, G., Wieschaus, E., Nussleinvolhard, C., Kluding, H., 1984. Mutations Affecting the Pattern of the Larval Cuticle in Drosophila-Melanogaster .2. Zygotic Loci on the 3rd Chromosome. Roux Arch Dev Biol 193, 283-295.

Kalluri, R., Neilson, E.G., 2003. Epithelial-mesenchymal transition and its implications for fibrosis. J Clin Invest 112, 1776-1784.

Kalluri, R., Weinberg, R.A., 2009. The basics of epithelial-mesenchymal transition. The Journal of clinical investigation 119, 1420-1428.

Kamath, R.S., Fraser, A.G., Dong, Y., Poulin, G., Durbin, R., Gotta, M., Kanapin, A., Le Bot, N., Moreno, S., Sohrmann, M., Welchman, D.P., Zipperlen, P., Ahringer, J., 2003. Systematic functional analysis of the Caenorhabditis elegans genome using RNAi. Nature 421, 231-237.

Kamath, R.S., Martinez-Campos, M., Zipperlen, P., Fraser, A.G., Ahringer, J., 2001. Effectiveness of specific RNA-mediated interference through ingested double-stranded RNA in Caenorhabditis elegans. Genome biology 2, RESEARCH0002.

Kamei, M., Saunders, W.B., Bayless, K.J., Dye, L., Davis, G.E., Weinstein, B.M., 2006. Endothelial tubes assemble from intracellular vacuoles in vivo. Nature 442, 453-456.

Kanning, K.C., Kaplan, A., Henderson, C.E., 2010. Motor neuron diversity in development and disease. Annu Rev Neurosci 33, 409-440.

Kim, K., Kim, R., Sengupta, P., 2010. The HMX/NKX homeodomain protein MLS-2 specifies the identity of the AWC sensory neuron type via regulation of the ceh-36 Otx gene in C. elegans. Development 137, 963-974.

Klambt, C., Glazer, L., Shilo, B.Z., 1992. Breathless, a Drosophila Fgf Receptor Homolog, Is Essential for Migration of Tracheal and Specific Midline Glial-Cells. Genes & development 6, 1668-1678.

Koh, K., Rothman, J.H., 2001. ELT-5 and ELT-6 are required continuously to regulate epidermal seam cell differentiation and cell fusion in C. elegans. Development 128, 2867-2880.

Koppen, M., Simske, J.S., Sims, P.A., Firestein, B.L., Hall, D.H., Radice, A.D., Rongo, C., Hardin, J.D., 2001a. Cooperative regulation of AJM-1 controls junctional integrity in Caenorhabditis elegans epithelia. Nature cell biology 3, 983-991.

Koppen, M., Simske, J.S., Sims, P.A., Firestein, B.L., Hall, D.H., Radice, A.D., Rongo, C., Hardin, J.D., 2001b. Cooperative regulation of AJM-1 controls junctional integrity in *Caenorhabditis elegans* epithelia. Nature Cell Biol. 3, 983-991.

Kosako, H., Yamaguchi, N., Aranami, C., Ushiyama, M., Kose, S., Imamoto, N., Taniguchi, H., Nishida, E., Hattori, S., 2009. Phosphoproteomics reveals new ERK MAP kinase targets and links ERK to nucleoporin-mediated nuclear transport. Nature structural & molecular biology 16, 1026-1035.

Kuure, S., Cebrian, C., Machingo, Q., Lu, B.C., Chi, X.A., Hyink, D., D'Agati, V., Gurniak, C., Witke, W., Costantini, F., 2010a. Actin Depolymerizing Factors Cofilin1 and Destrin Are Required for Ureteric Bud Branching Morphogenesis. PLoS genetics 6.

Kuure, S., Chi, X., Lu, B., Costantini, F., 2010b. The transcription factors Etv4 and Etv5 mediate formation of the ureteric bud tip domain during kidney development. Development 137, 1975-1979.

Kwon, C.S., Wagner, D., 2007. Unwinding chromatin for development and growth: a few genes at a time. Trends in genetics : TIG 23, 403-412.

Lambie, E.J., Kimble, J., 1991a. Two homologous regulatory genes, *lin-12* and *glp-1*, have overlapping functions. Development 112, 231-240.

Lambie, E.J., Kimble, J., 1991b. Two homologous regulatory genes, lin-12 and glp-1, have overlapping functions. Development 112, 231-240.

Lanjuin, A., VanHoven, M.K., Bargmann, C.I., Thompson, J.K., Sengupta, P., 2003. Otx/otd homeobox genes specify distinct sensory neuron identities in C. elegans. Developmental cell 5, 621-633.

Lee, H., Van Vactor, D., 2003. Neurons take shape. Current biology : CB 13, R152-161.

Lee, T., Hacohen, N., Krasnow, M., Montell, D.J., 1996. Regulated Breathless receptor tyrosine kinase activity required to pattern cell migration area branching in the Drosophila tracheal system. Genes & development 10, 2912-2921.

Lehner, B., Crombie, C., Tischler, J., Fortunato, A., Fraser, A.G., 2006. Systematic mapping of genetic interactions in Caenorhabditis elegans identifies common modifiers of diverse signaling pathways. Nature genetics 38, 896-903.

Leung, C.L., Green, K.J., Liem, R.K., 2002. Plakins: a family of versatile cytolinker proteins. Trends in cell biology 12, 37-45.

Levitan, D., Greenwald, I., 1998. LIN-12 protein expression and localization during vulval development in C. elegans. Development 125, 3101-3109.

Lewis, T.S., Hunt, J.B., Aveline, L.D., Jonscher, K.R., Louie, D.F., Yeh, J.M., Nahreini, T.S., Resing, K.A., Ahn, N.G., 2000. Identification of novel MAP kinase pathway signaling targets by functional proteomics and mass spectrometry. Molecular cell 6, 1343-1354.

Liegeois, S., Benedetto, A., Michaux, G., Belliard, G., Labouesse, M., 2007. Genes required for osmoregulation and apical secretion in Caenorhabditis elegans. Genetics 175, 709-724.

Lloyd, C., Chan, J., 2004. Microtubules and the shape of plants to come. Nature reviews. Molecular cell biology 5, 13-22.

Lu, B.C., Cebrian, C., Chi, X., Kuure, S., Kuo, R., Bates, C.M., Arber, S., Hassell, J., MacNeil, L., Hoshi, M., Jain, S., Asai, N., Takahashi, M., Schmidt-Ott, K.M., Barasch, J., D'Agati, V., Costantini, F., 2009. Etv4 and Etv5 are required downstream of GDNF and Ret for kidney branching morphogenesis. Nature genetics 41, 1295-1302.

Lu, C., Mains, P.E., 2005. Mutations of a redundant alpha-tubulin gene affect Caenorhabditis elegans early embryonic cleavage via MEI-1/katanin-dependent and -independent pathways. Genetics 170, 115-126.

Lu, C., Srayko, M., Mains, P.E., 2004. The Caenorhabditis elegans microtubule-severing complex MEI-1/MEI-2 katanin interacts differently with two superficially redundant beta-tubulin isotypes. Molecular biology of the cell 15, 142-150.

Lubarsky, B., Krasnow, M.A., 2003. Tube morphogenesis: making and shaping biological tubes. Cell 112, 19-28.

Maloof, J.N., Kenyon, C., 1998. The Hox gene lin-39 is required during C. elegans vulval induction to select the outcome of Ras signaling. Development 125, 181-190.

Mancuso, V.P., Parry, J.M., Storer, L., Poggioli, C., Nguyen, K.C., Hall, D.H., Sundaram, M.V., 2012. Extracellular leucine-rich repeat proteins are required to organize the apical extracellular matrix and maintain epithelial junction integrity in C. elegans. Development.

Mango, S.E., 2009. The molecular basis of organ formation: insights from the C. elegans foregut. Annu Rev Cell Dev Biol 25, 597-628.

Mani, S.A., Guo, W., Liao, M.J., Eaton, E.N., Ayyanan, A., Zhou, A.Y., Brooks, M., Reinhard, F., Zhang, C.C., Shipitsin, M., Campbell, L.L., Polyak, K., Brisken, C., Yang, J., Weinberg, R.A., 2008. The epithelial-mesenchymal transition generates cells with properties of stem cells. Cell 133, 704-715.

Marin, O., Valdeolmillos, M., Moya, F., 2006. Neurons in motion: same principles for different shapes? Trends in neurosciences 29, 655-661.

Martinez, P., Davidson, E.H., 1997. SpHmx, a sea urchin homeobox gene expressed in embryonic pigment cells. Developmental biology 181, 213-222.

Mason, C.A., Edmondson, J.C., Hatten, M.E., 1988. The extending astroglial process: development of glial cell shape, the growing tip, and interactions with neurons. The Journal of neuroscience : the official journal of the Society for Neuroscience 8, 3124-3134.

Mattingly, B.C., Buechner, M., 2011. The FGD homologue EXC-5 regulates apical trafficking in C. elegans tubules. Developmental biology 359, 59-72.

McKean, P.G., Vaughan, S., Gull, K., 2001. The extended tubulin superfamily. Journal of cell science 114, 2723-2733.

McLean, J., Xiao, S., Miyazaki, K., Robertson, J., 2008. A novel peripherin isoform generated by alternative translation is required for normal filament network formation. Journal of neurochemistry 104, 1663-1673.

Meinertzhagen, I.A., Takemura, S.Y., Lu, Z., Huang, S., Gao, S., Ting, C.Y., Lee, C.H., 2009. From form to function: the ways to know a neuron. Journal of neurogenetics 23, 68-77.

Melki, R., Carlier, M.F., Pantaloni, D., Timasheff, S.N., 1989. Cold depolymerization of microtubules to double rings: geometric stabilization of assemblies. Biochemistry 28, 9143-9152.

Metzger, R.J., Krasnow, M.A., 1999. Genetic control of branching morphogenesis. Science 284, 1635-1639.

Michos, O., Cebrian, C., Hyink, D., Grieshammer, U., Williams, L., D'Agati, V., Licht, J.D., Martin, G.R., Costantini, F., 2010. Kidney development in the absence of Gdnf and Spry1 requires Fgf10. PLoS genetics 6, e1000809.

Moore, M.W., Klein, R.D., Farinas, I., Sauer, H., Armanini, M., Phillips, H., Reichardt, L.F., Ryan, A.M., Carver-Moore, K., Rosenthal, A., 1996. Renal and neuronal abnormalities in mice lacking GDNF. Nature 382, 76-79.

Moskowitz, I.P., Rothman, J.H., 1996. lin-12 and glp-1 are required zygotically for early embryonic cellular interactions and are regulated by maternal GLP-1 signaling in Caenorhabditis elegans. Development 122, 4105-4117.

Munroe, R.J., Prabhu, V., Acland, G.M., Johnson, K.R., Harris, B.S., O'Brien, T.P., Welsh, I.C., Noden, D.M., Schimenti, J.C., 2009. Mouse H6 Homeobox 1 (Hmx 1) mutations cause cranial abnormalities and reduced body mass. Bmc Developmental Biology 9.

Murray, J.I., Bao, Z., Boyle, T.J., Waterston, R.H., 2006. The lineaging of fluorescently-labeled Caenorhabditis elegans embryos with StarryNite and AceTree. Nat Protoc 1, 1468-1476.

Myat, M.M., Lightfoot, H., Wang, P., Andrew, D.J., 2005. A molecular link between FGF and Dpp signaling in branch-specific migration of the Drosophila trachea. Developmental biology 281, 38-52.

Nelson, F.K., Albert, P.S., Riddle, D.L., 1983. Fine structure of the Caenorhabditis elegans secretory-excretory system. J Ultrastruct Res 82, 156-171.

Nelson, F.K., Riddle, D.L., 1984. Functional study of the Caenorhabditis elegans secretory-excretory system using laser microsurgery. J Exp Zool 231, 45-56.

Neves, A., Priess, J.R., 2005. The REF-1 family of bHLH transcription factors pattern C. elegans embryos through Notch-dependent and Notch-independent pathways. Dev Cell 8, 867-879.

Nishimura, M., Inoue, Y., Hayashi, S., 2007. A wave of EGFR signaling determines cell alignment and intercalation in the Drosophila tracheal placode. Development 134, 4273-4282.

Noyes, M.B., Christensen, R.G., Wakabayashi, A., Stormo, G.D., Brodsky, M.H., Wolfe, S.A., 2008. Analysis of homeodomain specificities allows the family-wide prediction of preferred recognition sites. Cell 133, 1277-1289.

Ohmachi, M., Rocheleau, C.E., Church, D., Lambie, E., Schedl, T., Sundaram, M.V., 2002. C. elegans ksr-1 and ksr-2 have both unique and redundant functions and are required for MPK-1 ERK phosphorylation. Current biology : CB 12, 427-433.

Oikonomou, G., Shaham, S., 2011. The glia of Caenorhabditis elegans. Glia 59, 1253-1263.

Oka, T., Yamamoto, R., Futai, M., 1997. Three vha genes encode proteolipids of Caenorhabditis elegans vacuolar-type ATPase. Gene structures and preferential expression in an H-shaped excretory cell and rectal cells. Journal of Biological Chemistry 272, 24387-24392.

Otani, T., Oshima, K., Onishi, S., Takeda, M., Shinmyozu, K., Yonemura, S., Hayashi, S., 2011. IKKepsilon regulates cell elongation through recycling endosome shuttling. Developmental cell 20, 219-232.

Payre, F., Vincent, A., Carreno, S., 1999. ovo/svb integrates Wingless and DER pathways to control epidermis differentiation. Nature 400, 271-275.

Peinado, H., Olmeda, D., Cano, A., 2007. Snail, Zeb and bHLH factors in tumour progression: an alliance against the epithelial phenotype? Nature reviews. Cancer 7, 415-428.

Phillips, J.B., Lyczak, R., Ellis, G.C., Bowerman, B., 2004. Roles for two partially redundant alpha-tubulins during mitosis in early Caenorhabditis elegans embryos. Cell motility and the cytoskeleton 58, 112-126.

Phng, L.K., Gerhardt, H., 2009. Angiogenesis: a team effort coordinated by notch. Dev Cell 16, 196-208.

Plaza, S., Chanut-Delalande, H., Fernandes, I., Wassarman, P.M., Payre, F., 2010. From A to Z: apical structures and zona pellucida-domain proteins. Trends in cell biology 20, 524-532.

Plenefisch, J.D., Zhu, X., Hedgecock, E.M., 2000. Fragile skeletal muscle attachments in dystrophic mutants of Caenorhabditis elegans: isolation and characterization of the mua genes. Development 127, 1197-1207.

Podbilewicz, B., Leikina, E., Sapir, A., Valansi, C., Suissa, M., Shemer, G., Chernomordik, L.V., 2006. The C. elegans developmental fusogen EFF-1 mediates homotypic fusion in heterologous cells and in vivo. Developmental cell 11, 471-481.

Pohl, C., Bao, Z., 2010. Chiral forces organize left-right patterning in C. elegans by uncoupling midline and anteroposterior axis. Dev Cell 19, 402-412.

Pollack, A.L., Runyan, R.B., Mostov, K.E., 1998. Morphogenetic mechanisms of epithelial tubulogenesis: MDCK cell polarity is transiently rearranged without loss of cell-cell contact during scatter factor hepatocyte growth factor-induced tubulogenesis. Developmental biology 204, 64-79.

Pollard, T.D., Cooper, J.A., 2009. Actin, a central player in cell shape and movement. Science 326, 1208-1212.

Portman, D.S., Emmons, S.W., 2004. Identification of C. elegans sensory ray genes using whole-genome expression profiling. Developmental biology 270, 499-512.

Potempa, S., Ridley, A.J., 1998. Activation of both MAP kinase and phosphatidylinositide 3-kinase by Ras is required for hepatocyte growth factor/scatter factor-induced adherens junction disassembly. Molecular biology of the cell 9, 2185-2200.

Qian, L., Wythe, J.D., Liu, J., Cartry, J., Vogler, G., Mohapatra, B., Otway, R.T., Huang, Y., King, I.N., Maillet, M., Zheng, Y., Crawley, T., Taghli-Lamallem, O., Semsarian, C., Dunwoodie, S., Winlaw, D., Harvey, R.P., Fatkin, D., Towbin, J.A., Molkentin, J.D., Srivastava, D., Ocorr, K., Bruneau, B.G., Bodmer, R., 2011. Tinman/Nkx2-5 acts via miR-1 and upstream of Cdc42 to regulate heart function across species. The Journal of cell biology 193, 1181-1196.

Rasmussen, J.P., English, K., Tenlen, J.R., Priess, J.R., 2008. Notch signaling and morphogenesis of single-cell tubes in the C. elegans digestive tract. Developmental cell 14, 559-569.

Red-Horse, K., Ueno, H., Weissman, I.L., Krasnow, M.A., 2010. Coronary arteries form by developmental reprogramming of venous cells. Nature 464, 549-553.

Reece-Hoyes, J.S., Deplancke, B., Shingles, J., Grove, C.A., Hope, I.A., Walhout, A.J., 2005. A compendium of Caenorhabditis elegans regulatory transcription factors: a resource for mapping transcription regulatory networks. Genome biology 6, R110.

Reginensi, A., Clarkson, M., Neirijnck, Y., Lu, B.S., Ohyama, T., Groves, A.K., Sock, E., Wegner, M., Costantini, F., Chaboissier, M.C., Schedl, A., 2011. SOX9 controls epithelial branching by activating RET effector genes during kidney development. Hum Mol Genet 20, 1143-1153.

Riddle, D.L., Blumenthal, T., Meyer, B.J., Priess, J.R., 1997. C.elegans II, Monograph series. Cold Spring Harbour laboratory Press, Plainview, NY, p. 1222.

Ridley, A.J., Comoglio, P.M., Hall, A., 1995. Regulation of scatter factor/hepatocyte growth factor responses by Ras, Rac, and Rho in MDCK cells. Molecular and cellular biology 15, 1110-1122.

Rink, J.C., Vu, H.T., Sanchez Alvarado, A., 2011. The maintenance and regeneration of the planarian excretory system are regulated by EGFR signaling. Development 138, 3769-3780.

Rinkwitzbrandt, S., Justus, M., Oldenettel, I., Arnold, H.H., Bober, E., 1995. Distinct Temporal Expression of Mouse Nkx-5.1 and Nkx-5.2 Homeobox Genes during Brain and Ear Development. Mech Develop 52, 371-381.

Rocheleau, C.E., Cullison, K., Huang, K., Bernstein, Y., Spilker, A.C., Sundaram, M.V., 2008. The Caenorhabditis elegans ekl (enhancer of ksr-1 lethality) genes include putative components of a germline small RNA pathway. Genetics 178, 1431-1443.

Rocheleau, C.E., Howard, R.M., Goldman, A.P., Volk, M.L., Girard, L.J., Sundaram, M.V., 2002. A lin-45 raf enhancer screen identifies eor-1, eor-2 and unusual alleles of Ras pathway genes in Caenorhabditis elegans. Genetics 161, 121-131.

Roubin, R., Naert, K., Popovici, C., Vatcher, G., Coulier, F., Thierry-Mieg, J., Pontarotti, P., Birnbaum, D., Baillie, D., Thierry-Mieg, D., 1999. let-756, a C. elegans fgf essential for worm development. Oncogene 18, 6741-6747.

Samakovlis, C., Manning, G., Steneberg, P., Hacohen, N., Cantera, R., Krasnow, M.A., 1996. Genetic control of epithelial tube fusion during Drosophila tracheal development. Development 122, 3531-3536.

Santella, A., Du, Z., Nowotschin, S., Hadjantonakis, A.-K., Bao, Z., 2010. A hybrid blob-slice model for accurate and efficient detection of fluorescence labeled nuclei in 3D. BMC Bioinformatics 11, 580.

Sapir, A., Choi, J., Leikina, E., Avinoam, O., Valansi, C., Chernomordik, L.V., Newman, A.P., Podbilewicz, B., 2007. AFF-1, a FOS-1-regulated fusogen, mediates fusion of the anchor cell in C. elegans. Developmental cell 12, 683-698.

Sawyer, J.M., Harrell, J.R., Shemer, G., Sullivan-Brown, J., Roh-Johnson, M., Goldstein, B., 2010. Apical constriction: a cell shape change that can drive morphogenesis. Developmental biology 341, 5-19.

Schlessinger, J., 2000. Cell signaling by receptor tyrosine kinases. Cell 103, 211-225.

Schoenwolf, G.C., 1984. Histological and Ultrastructural Studies of Secondary Neurulation in Mouse Embryos. Am J Anat 169, 361-376.

Schoenwolf, G.C., Delongo, J., 1980. Ultrastructure of Secondary Neurulation in the Chick-Embryo. Am J Anat 158, 43-63.

Schoenwolf, G.C., Smith, J.L., 1990. Mechanisms of neurulation: traditional viewpoint and recent advances. Development 109, 243-270.

Schorderet, D.F., Nichini, O., Boisset, G., Polok, B., Tiab, L., Mayeur, H., Raji, B., de la Houssaye, G., Abitbol, M.M., Munier, F.L., 2008. Mutation in the human homeobox gene NKX5-3 causes an oculo-auricular syndrome. Am J Hum Genet 82, 1178-1184.

Schottenfeld, J., Song, Y., Ghabrial, A.S., 2010. Tube continued: morphogenesis of the Drosophila tracheal system. Current opinion in cell biology 22, 633-639.

Schuchardt, A., D'Agati, V., Larsson-Blomberg, L., Costantini, F., Pachnis, V., 1994. Defects in the kidney and enteric nervous system of mice lacking the tyrosine kinase receptor Ret. Nature 367, 380-383.

Segbert, C., Johnson, K., Theres, C., van Furden, D., Bossinger, O., 2004. Molecular and functional analysis of apical junction formation in the gut epithelium of Caenorhabditis elegans. Developmental biology 266, 17-26.

Shakya, R., Jho, E.H., Kotka, P., Wu, Z., Kholodilov, N., Burke, R., D'Agati, V., Costantini, F., 2005a. The role of GDNF in patterning the excretory system. Developmental biology 283, 70-84.

Shakya, R., Watanabe, T., Costantini, F., 2005b. The role of GDNF/Ret signaling in ureteric bud cell fate and branching morphogenesis. Dev Cell 8, 65-74.

Shaw, P.A., Zhang, X., Russo, A.F., Amendt, B.A., Henderson, S., Williams, V., 2003. Homeobox protein, Hmx3, in postnatally developing rat submandibular glands. J Histochem Cytochem 51, 385-396.

Shibata, Y., Uchida, M., Takeshita, H., Nishiwaki, K., Sawa, H., 2012. Multiple functions of PBRM-1/Polybromo- and LET-526/Osa-containing chromatin remodeling complexes in C. elegans development. Developmental biology 361, 349-357.

Shishido, E., Higashijima, S., Emori, Y., Saigo, K., 1993. 2 Fgf-Receptor Homologs of Drosophila - One Is Expressed in Mesodermal Primordium in Early Embryos. Development 117, 751-761.

Simske, J.S., Kaech, S.M., Harp, S.A., Kim, S.K., 1996. LET-23 receptor localization by the cell junction protein LIN-7 during *C. elegans* vulval induction. Cell 85, 195-204.

Smith, D.H., 2009. Stretch growth of integrated axon tracts: extremes and exploitations. Progress in neurobiology 89, 231-239.

Song, R., Yosypiv, I.V., 2011. Genetics of congenital anomalies of the kidney and urinary tract. Pediatr Nephrol 26, 353-364.

St Johnston, D., Sanson, B., 2011. Epithelial polarity and morphogenesis. Current opinion in cell biology.

Stadler, H.S., Murray, J.C., Leysens, N.J., Goodfellow, P.J., Solursh, M., 1995. Phylogenetic Conservation and Physical Mapping of Members of the H6 Homeobox Gene Family. Mamm Genome 6, 383-388.

Stadler, H.S., Padanilam, B.J., Buetow, K., Murray, J.C., Solursh, M., 1992. Identification and Genetic-Mapping of a Homeobox Gene to the 4p16.1 Region of Human Chromosome-4. P Natl Acad Sci USA 89, 11579-11583.

Stadler, H.S., Solursh, M., 1994. Characterization of the Homeobox-Containing Gene Gh6 Identifies Novel Regions of Homeobox Gene-Expression in the Developing Chick-Embryo. Developmental biology 161, 251-262.

Sternberg, P.W., 2005. Vulval development. WormBook : the online review of C. elegans biology, 1-28.

Stiess, M., Bradke, F., 2010. Neuronal polarization: the cytoskeleton leads the way. Dev Neurobiol 71, 430-444.

Stone, C.E., Hall, D.H., Sundaram, M.V., 2009. Lipocalin signaling controls unicellular tube development in the Caenorhabditis elegans excretory system. Developmental biology 329, 201-211.

Struhl, G., Fitzgerald, K., Greenwald, I., 1993. Intrinsic activity of the Lin-12 and Notch intracellular domains in vivo. Cell 74, 331-345.

Suchting, S., Freitas, C., le Noble, F., Benedito, R., Breant, C., Duarte, A., Eichmann, A., 2007. The Notch ligand Delta-like 4 negatively regulates endothelial tip cell formation and vessel branching. P Natl Acad Sci USA 104, 3225-3230.

Sulston, J.E., Horvitz, H.R., 1977. Post-embryonic cell lineages of the nematode *Caenorhabditis elegans*. Dev. Biol. 56, 110-156.

Sulston, J.E., Scheirenberg, E., White, J.G., Thomson, J.N., 1983. The embryonic cell lineage of the nematode *Caenorhabditis elegans*. Dev. Biol. 100, 64-119.

Sundaram, M., Han, M., 1995. The C. elegans ksr-1 gene encodes a novel Raf-related kinase involved in Ras-mediated signal transduction. Cell 83, 889-901.

Sundaram, M.V., 2005. The love-hate relationship between Ras and Notch. Genes & Development 19, 1825-1839.

Sundaram, M.V., 2006. RTK/Ras/MAPK signaling. WormBook, 1-19.

Sutherland, D., Samakovlis, C., Krasnow, M.A., 1996. Branchless encodes a Drosophila FGF homolog that controls tracheal cell migration and the pattern of branching. Cell 87, 1091-1101.

Tammela, T., Zarkada, G., Wallgard, E., Murtomaki, A., Suchting, S., Wirzenius, M., Waltari, M., Hellstrom, M., Schomber, T., Peltonen, R., Freitas, C., Duarte, A., Isoniemi, H., Laakkonen, P., Christofori, G., Yla-Herttuala, S., Shibuya, M., Pytowski, B., Eichmann, A., Betsholtz, C., Alitalo, K., 2008. Blocking VEGFR-3 suppresses angiogenic sprouting and vascular network formation. Nature 454, 656-U668.

Tavernarakis, N., Wang, S.L., Dorovkov, M., Ryazanov, A., Driscoll, M., 2000. Heritable and inducible genetic interference by double-stranded RNA encoded by transgenes. Nature genetics 24, 180-183.

Thompson, M., 2009. Polybromo-1: the chromatin targeting subunit of the PBAF complex. Biochimie 91, 309-319.

Totong, R., Achilleos, A., Nance, J., 2007. PAR-6 is required for junction formation but not apicobasal polarization in C. elegans embryonic epithelial cells. Development 134, 1259-1268.

Tseng, A.S., Tapon, N., Kanda, H., Cigizoglu, S., Edelmann, L., Pellock, B., White, K., Hariharan, I.K., 2007. Capicua regulates cell proliferation downstream of the receptor tyrosine kinase/ras signaling pathway. Current biology : CB 17, 728-733.

Wagmaister, J.A., Miley, G.R., Morris, C.A., Gleason, J.E., Miller, L.M., Kornfeld, K., Eisenmann, D.M., 2006. Identification of cis-regulatory elements from the C. elegans Hox gene lin-39

required for embryonic expression and for regulation by the transcription factors LIN-1, LIN-31 and LIN-39. Developmental biology 297, 550-565.

Wang, G.V., Dolecki, G.J., Carlos, R., Humphreys, T., 1990. Characterization and expression of two sea urchin homeobox gene sequences. Developmental genetics 11, 77-87.

Wang, W., Grimmer, J.F., Van De Water, T.R., Lufkin, T., 2004. Hmx2 and Hmx3 homeobox genes direct development of the murine inner ear and hypothalamus and can be functionally replaced by Drosophila Hmx. Developmental cell 7, 439-453.

Wang, W., Lo, P., Frasch, M., Lufkin, T., 2000. Hmx: an evolutionary conserved homeobox gene family expressed in the developing nervous system in mice and Drosophila. Mech Dev 99, 123-137.

Wang, W., Lufkin, T., 2005. Hmx homeobox gene function in inner ear and nervous system cell-type specification and development. Experimental cell research 306, 373-379.

Wang, W.D., Van de Water, T., Lufkin, T., 1998. Inner ear and maternal reproductive defects in mice lacking the Hmx3 homeobox gene. Development 125, 621-634.

Wang, X., Chamberlin, H.M., 2002. Multiple regulatory changes contribute to the evolution of the Caenorhabditis lin-48 ovo gene. Genes & development 16, 2345-2349.

Ward, S., Thomson, N., White, J.G., Brenner, S., 1975. Electron microscopical reconstruction of the anterior sensory anatomy of the nematode Caenorhabditis elegans.?2UU. The Journal of comparative neurology 160, 313-337.

Weaver, M., Krasnow, M.A., 2008. Dual origin of tissue-specific progenitor cells in Drosophila tracheal remodeling. Science 321, 1496-1499.

Wei, G.H., Badis, G., Berger, M.F., Kivioja, T., Palin, K., Enge, M., Bonke, M., Jolma, A., Varjosalo, M., Gehrke, A.R., Yan, J., Talukder, S., Turunen, M., Taipale, M., Stunnenberg, H.G., Ukkonen, E., Hughes, T.R., Bulyk, M.L., Taipale, J., 2010. Genome-wide analysis of ETS-family DNA-binding in vitro and in vivo. The EMBO journal 29, 2147-2160.

Willis, J.H., Munro, E., Lyczak, R., Bowerman, B., 2006. Conditional dominant mutations in the Caenorhabditis elegans gene act-2 identify cytoplasmic and muscle roles for a redundant actin isoform. Molecular biology of the cell 17, 1051-1064.

Winston, W.M., Molodowitch, C., Hunter, C.P., 2002. Systemic RNAi in C. elegans requires the putative transmembrane protein SID-1. Science 295, 2456-2459.

Wright, A.J., Hunter, C.P., 2003. Mutations in a beta-tubulin disrupt spindle orientation and microtubule dynamics in the early Caenorhabditis elegans embryo. Molecular biology of the cell 14, 4512-4525.

Wu, Y., Han, M., 1994. Suppression of activated Let-60 Ras defines a role of *Caenorhabditis elegans sur-1* MAP kinase in vulval differentiation. Genes Dev. 8, 147-159.

Yochem, J., Sundaram, M., Han, M., 1997. Ras is required for a limited number of cell fates and not for general proliferation in Caenorhabditis elegans. Molecular and cellular biology 17, 2716-2722.

Yoshimura, S., Murray, J.I., Lu, Y., Waterston, R.H., Shaham, S., 2008. mls-2 and vab-3 Control glia development, hlh-17/Olig expression and glia-dependent neurite extension in C. elegans. Development 135, 2263-2275.

Yoshiura, K., Leysens, N.J., Reiter, R.S., Murray, J.C., 1998. Cloning, characterization, and mapping of the mouse homeobox gene Hmx1. Genomics 50, 61-68.

Zand, T.P., Reiner, D.J., Der, C.J., 2011. Ras effector switching promotes divergent cell fates in C. elegans vulval patterning. Developmental cell 20, 84-96.

Zeisberg, E.M., Tarnavski, O., Zeisberg, M., Dorfman, A.L., McMullen, J.R., Gustafsson, E., Chandraker, A., Yuan, X., Pu, W.T., Roberts, A.B., Neilson, E.G., Sayegh, M.H., Izumo, S., Kalluri, R., 2007. Endothelial-to-mesenchymal transition contributes to cardiac fibrosis. Nat Med 13, 952-961.

Zhang, X., Greenwald, I., 2011. Spatial regulation of lag-2 transcription during vulval precursor cell fate patterning in Caenorhabditis elegans. Genetics 188, 847-858.